National Library
of Canada

Canadian Theses Service

Ottawa, Canada
K1A 0N4

Bibliothèque nationale
du Canada

Service des thèses canadiennes

NOTICE

The quality of this microform is heavily dependent upon the quality of the original thesis submitted for microfilming. Every effort has been made to ensure the highest quality of reproduction possible.

If pages are missing, contact the university which granted the degree.

Some pages may have indistinct print especially if the original pages were typed with a poor typewriter ribbon or if the university sent us an inferior photocopy.

Previously copyrighted materials (journal articles, published tests, etc.) are not filmed.

Reproduction in full or in part of this microform is governed by the Canadian Copyright Act, R.S.C. 1970, c. C-30.

AVIS

La qualité de cette microforme dépend grandement de la qualité de la thèse soumise au microfilmage. Nous avons tout fait pour assurer une qualité supérieure de reproduction.

S'il manque des pages, veuillez communiquer avec l'université qui a conféré le grade.

La qualité d'impression de certaines pages peut laisser à désirer, surtout si les pages originales ont été dactylographiées à l'aide d'un ruban usé ou si l'université nous a fait parvenir une photocopie de qualité inférieure.

Les documents qui font déjà l'objet d'un droit d'auteur (articles de revue, tests publiés, etc.) ne sont pas microfilmés.

La reproduction, même partielle, de cette microforme est soumise à la Loi canadienne sur le droit d'auteur, SRC 1970, c. C-30.

NL-339 (r. 88/04)

Canada

THE UNIVERSITY OF ALBERTA

THE GENESIS OF SPELEOTHEMIC CALCITE DEPOSITS ON GRAND CAYMAN ISLAND, BRITISH WEST INDIES.

by

©

DUNCAN STUART SMITH

A THESIS

SUBMITTED TO THE FACULTY OF GRADUATE STUDIES AND RESEARCH

IN PARTIAL FULFILMENT OF THE REQUIREMENTS FOR THE DEGREE

OF MASTER OF SCIENCE

DEPARTMENT OF GEOLOGY

EDMONTON, ALBERTA

FALL, 1987

Permission has been granted to the National Library of Canada to microfilm this thesis and to lend or sell copies of the film.

L'autorisation a été accordée à la Bibliothèque nationale du Canada de microfilmer cette thèse et de prêter ou de vendre des exemplaires du film.

The author (copyright owner) has reserved other publication rights, and neither the thesis nor extensive extracts from it may be printed or otherwise reproduced without his/her written permission.

L'auteur (titulaire du droit d'auteur) se réserve les autres droits de publication; ni la thèse ni de longs extraits de celle-ci ne doivent être imprimés ou autrement reproduits sans son autorisation écrite.

ISBN 0-315-41009-4

THE UNIVERSITY OF ALBERTA

RELEASE FORM

NAME OF AUTHOR DUNCAN STUART SMITH

TITLE OF THESIS THE GENESIS OF SPELEOTHEMIC CALCITE DEPOSITS ON GRAND CAYMAN ISLAND, BRITISH WEST INDIES.

DEGREE FOR WHICH THESIS WAS PRESENTED MASTER OF SCIENCE

YEAR THIS DEGREE GRANTED FALL, 1987

Permission is hereby granted to THE UNIVERSITY OF ALBERTA LIBRARY to reproduce single copies of this thesis and to lend or sell such copies for private, scholarly or scientific research purposes only.

The author reserves other publication rights, and neither the thesis nor extensive extracts from it may be printed or otherwise reproduced without the author's written permission.

(SIGNED) Duncan Smith

PERMANENT ADDRESS:

'Willow Barn, Stonehouse Farm
Dusthouse lane, Finstall, Bromsgrove
Worcestershire, ENGLAND

DATED July 8th 1987

THE UNIVERSITY OF ALBERTA

FACULTY OF GRADUATE STUDIES AND RESEARCH

The undersigned certify that they have read, and recommend to the Faculty of Graduate Studies and Research, for acceptance, a thesis entitled THE GENESIS OF SPELEOTHEMIC CALCITE DEPOSITS ON GRAND CAYMAN ISLAND, BRITISH WEST INDIES. submitted by DUNCAN STUART SMITH in partial fulfilment of the requirements for the degree of MASTER OF SCIENCE.

....

Supervisor

....

....

....

Date.....July 3rd 1987.....

DEDICATION

To my parents - the debt is great.

ABSTRACT

The Oligocene-Miocene Bluff Formation of Grand Cayman Island is characterized by numerous solution cavities, joints and skeletal molds which developed as a result of karst processes. Later precipitation of calcite has occurred in many of these voids, creating a remarkable series of flow banded calcite deposits. Where these banded calcites occur in the larger (spelean) solution cavities, their volumetric abundance and morphological diversity *eg*. stalagmites, stalactites and rimstone is spectacular.

The formation and spatial distribution of the spelean environment can be related to the geochemistry of the groundwater. The zone of active dissolution, which occurs at the transition between the marine and meteoric phreatic zones, exerts a positive control on the areal extent of cave formation. Since the chemically aggressive hydrological zone is intrinsically linked to eustasy and/or vertical tectonic movements, these larger regional events ultimately control speleogenesis on Grand Cayman Island.

The original crystal morphology of the Caymanian speleothemic calcite is commonly preserved in the form of inclusion rich growth bands. The variable morphology of these growth bands, indicates that crystal morphology changed throughout the ontogeny of the crystal in response to the fluctuating physical and chemical conditions of the pore water. The common occurrence of algae, fungi, bacteria and amorphous organic material in the speleothemic calcite, indicates that these speleothems are not totally abiogenic. The common association of organic material with (1) the nucleation of large calcite spherulites, (2) the unusual predominance of length slow crystals at disconformity surfaces, and (3) marked changes in crystallite morphology, indicates that biological activity and organic material is an important controlling factor of crystal morphology. The presence of organic material is also considered an important factor in the pigmentation of the banded flowstone, as indicated by the lack of correlation between trace element content and colour.

Caymanian speleothemic calcite in general exhibits a weak cathodoluminescence, major exceptions, however, being the occurrence of bright orange luminescence in, (1) speleothemic calcite in the presence of organic material, and (2) late stage porosity occluding cements. The former indicates that important activator and sensitizer trace elements may be preferentially hosted in the organic material, while the latter indicates that the trace element concentration may be the result of the influx of a chemically distinct water (alloenrichment).

Stable isotope geochemistry shows that speleothemic calcite was precipitated in the meteoric diagenetic realm. The $\delta^{18}O$ and $\delta^{13}C$ ratios of individual calcite layers varied by up to + 2.3‰ SMOW and + 5.5‰ PDB, respectively. This is indicative of the involvement of a dynamic pore water system, the geochemistry of which fluctuated in response to climatic, lithologic, hydrodynamic and pedologic factors.

ACKNOWLEDGEMENTS

I am indebted to my supervisor Dr. Brian Jones for his guidance, support and tutelage. I am certain that were it not for his his uncompromising "red pen", this thesis would never have attained such clarity or depth.

Most gratefully acknowledged are George Braybrook for his invaluable assistance and expertise with the scanning electron microscope; Dr. Fred Longstaffe for the use of his isotope facilities; Diane Caird for her assistance with the isotopic analyses and Alex Stelmach for his assistance with the atomic absorption spectrophotometric analyses.

Many thanks to my fellow graduate students, Elsie Tsang and especially Suzanne Pleydell, who have encouraged and supported me over the last two years. I shall always be indebted to Leni Honsaker for a "Home away from Home".

This thesis was made possible by financial support provided by the Natural Sciences and Engineering Research Council of Canada (Grant No. A6090 awarded to Dr. Brian Jones) and the logistical support of Richard Beswick, Director of The Water Authority, Cayman Islands.

TABLE OF CONTENTS

I. INTRODUCTION 1

A. AREA OF STUDY 1

B. CLIMATE 3

II. OBJECTIVES 4

III. METHODS OF STUDY 5

IV. GENERAL GEOLOGY AND TECTONICS 8

A. PREVIOUS STUDIES 8

B. TECTONICS 11

The origin of the Cayman Islands 13

V. SPELEOLOGY OF GRAND CAYMAN ISLAND 15

A. PRECIPITATION FEATURES (Speleothems) 15

Dripstone 16

Rimstone 18

Flowstone 19

B. DISSOLUTION FEATURES (Speleogens) 21

Phreatic speleogens 22

Vadose speleogens 22

C. SPELEOTHEM DATING 23

Radiogenic Isotopes 23

Growth Rates 24

Field Relationships 25

D. A SPELEOGENETIC MODEL FOR GRAND CAYMAN ISLAND 27

Carbonate Dissolution Geochemistry 29

Developing the speleogenetic model 35

VI. PETROGRAPHY OF CAYMANIAN SPELEOTHEMS.......................... 40
  A. INTRODUCTION.. 40
  B. NOMENCLATURE.. 41
  C. ABIOGENIC CALCITE... 44
    Inclusion Patterns and Growth Banding................................ 44
    Asymmetrical Crystals.. 47
    Crystal Junctions.. 49
    Trigonal Crystals.. 51
  B. INTERNAL SEDIMENT... 54
  D. DISCUSSION OF ABIOGENIC DATA.. 56
  E. BIOGENIC ASSOCIATIONS... 59
    Calcite 'Rafts'.. 61
    Uncalcified and Calcified filaments.................................. 62
    Microborings... 63
    Calcified Spherical Bodies... 63
  F. DISCUSSION OF BIOGENIC DATA... 63
    Microorganisms and their criteria for recognition.................... 64
    Micro-organisms In Caymanian Speleothems............................. 65
VII. COLOUR BANDING.. 69
VIII. CATHODOLUMINESCENCE... 72
  A. INTRODUCTION.. 72
  B. THEORETICAL CONSIDERATIONS.. 73
  C. RESULTS... 74
  D. DISCUSSION OF DATA.. 76
    Dolostone Luminescence... 76
    Organics - Their Influence On Luminescent Properties................. 76
    Changes In The Redox Potential....................................... 78

The Significance of REE's 83

D. SYNOPSIS 84

IX. STABLE ISOTOPE GEOCHEMISTRY 85

A. INTRODUCTION 85

B. SPELEOTHEMIC ISOTOPE DATA 85

D. DISCUSSION OF DATA 103

E. SYNOPSIS 107

X. CONCLUSIONS 109

XI. PHOTOGRAPHIC PLATES 111

XII. REFERENCES 151

LIST OF FIGURES

Figure 1. The location of the Cayman Islands and sampling localities 2

Figure 2. General geology of Grand Cayman Island 9

Figure 3. Geological cross section of Grand Cayman Island 10

Figure 4. The Cayman Islands in relation to Caribbean tectonics 12

Figure 5. Genesis of an unusual flowstone body from Pirate Caves 20

Figure 6. Dissolution rates of dolomite as a function of the saturation index....... 31

Figure 7. The theory of Mischungskorrosion 32

Figure 8. Changes in the saturation index of calcite as a function of varying pH and percent seawater 34

Figure 9. Summary diagram to illustrate the regional speleogenetic controls on Grand Cayman Island 37

Figure 10. Growth asymmetry and the resulting curvature of the crystals leads to the development of a characteristic 'mottled' optical extinction pattern 48

Figure 11. Growth of asymmetrical crystals 49

Figure 12. Orientation of the overgrowth crystallites is strongly dependant on the crystallographic lattice information derived from the 'parent' (or substrate) 50

Figure 13. Trigonal crystal development 53

Figure 14. Schematic illustration of a screw dislocation 58

Figure 15. Origin of calcite 'rafts' in the Caymanian speleothems 67

Figure 16. Eh-pH diagram of the stability fields of iron and manganese compounds at 25 °C and 1 atmosphere 81

Figure 17. Stable isotopic geochemistry of all speleothems selected for analysis 88

Figure 18. Evolution of the isotopic geochemistry of the pore waters responsible for the precipitation of sample EEQ 728 89

Figure 19. The isotopic mixing of Caribbean sea water and fresh water from Grand Cayman Island.. 92

Figure 20. Diagenetic temperatures assessed from the $\delta^{18}O$ ratios of sample EEQ 278 93

Figure 21. Speleothemic isotope data in relation to the isotopic data of the Bluff Formation and associated sediments.. 97

Figure 22. Evolution of the isotope geochemistry of pore waters responsible for the precipitation of sample EEQ 727 99

Figure 23. Evolution of the isotope geochemistry of pore waters responsible for the precipitation of sample EEQ 726.. 100

Figure 24. Evolution of the isotope geochemistry of pore waters responsible for the precipitation of sample CIQ 1250 101

Figure 25. Evolution of the isotope geochemistry of pore waters responsible for the precipitation of sample BH 730.. 102

Figure 26. Evolution of the isotope geochemistry of pore waters responsible for the precipitation of sample EEQ 1219.. 102

Figure 27. Summary diagram of the isotopic geochemistry of the Caymanian speleothems.. 104

Figure 28. Suggested evolution of the $\delta^{13}C$ ratios of the Caymanian groundwater in relation to the isotopic geochemistry of the speleothemic calcite.. 106

LIST OF TABLES

Table 1. Summary of commonly used descriptive terms for calcite crystal morphologies 42

Table 2. Growth bands (types I to V) as classified by Kendall and Broughton (1978) 45

Table 3. Results of the atomic absorption spectrophotometry on three flowstone samples of varied colour 71

Table 4. Some of the more common impurity ions which are involved as activators, sensitizers and quenchers in luminescence of calcite 77

Table 5. $\delta^{18}O$ and $\delta^{13}C$ values for all the speleothems sampled 86

Table 6. $\delta^{18}O$ ratios for selected water samples taken from diverse hydrological environments on Grand Cayman Island 87

I. INTRODUCTION

The Oligocene-Miocene Bluff Formation of Grand Cayman Island is characterized by a well developed karst terrain. Solution widened joints, shafts, rills, and a well developed moldic porosity are some of the more abundant karst forms. Subsurface karst forms are also well developed on Grand Cayman Island, including deep phreatic caves, and more accessible vadose cave systems. An important addition to many of these karst features, is the presence of a later phase of calcite precipitation. In general, these calcites can be described as speleothems (Moore, 1952), having formed as a secondary mineral phase in a cave or cavity environment. They commonly posses marked colour banding, and a convolute morphology.

The morphology, composition and stable isotope geochemistry of the speleothemic calcite, will be a reflection of the physiochemical and biochemical conditions present in the cavity at the time of precipitation. These variables will be controlled by factors of varying regional and local significance *eg*. Climate, tectonism, eustasy, lithology, and biological activity. The documentation and interpretation of these deposits, and the environments in which they formed, will provide vital evidence with which to unravel the post emergent diagenetic history of Grand Cayman Island.

A. AREA OF STUDY

The Cayman Islands, consisting of Grand Cayman , Little Cayman and Cayman Brac, are located in the Caribbean Sea (Fig.1). Grand Cayman Island, the largest of the three islands, is approximately 35 km long and between 8 km and 16 km wide. Located 257 km WNW of Jamaica, and approximately 240 km SW of the Isla de Pinas (Cuba), Grand Cayman Island is separated from the other two Cayman Islands by approximately 97 km of open sea. The combined area of all the Cayman Islands is 264 km^2.

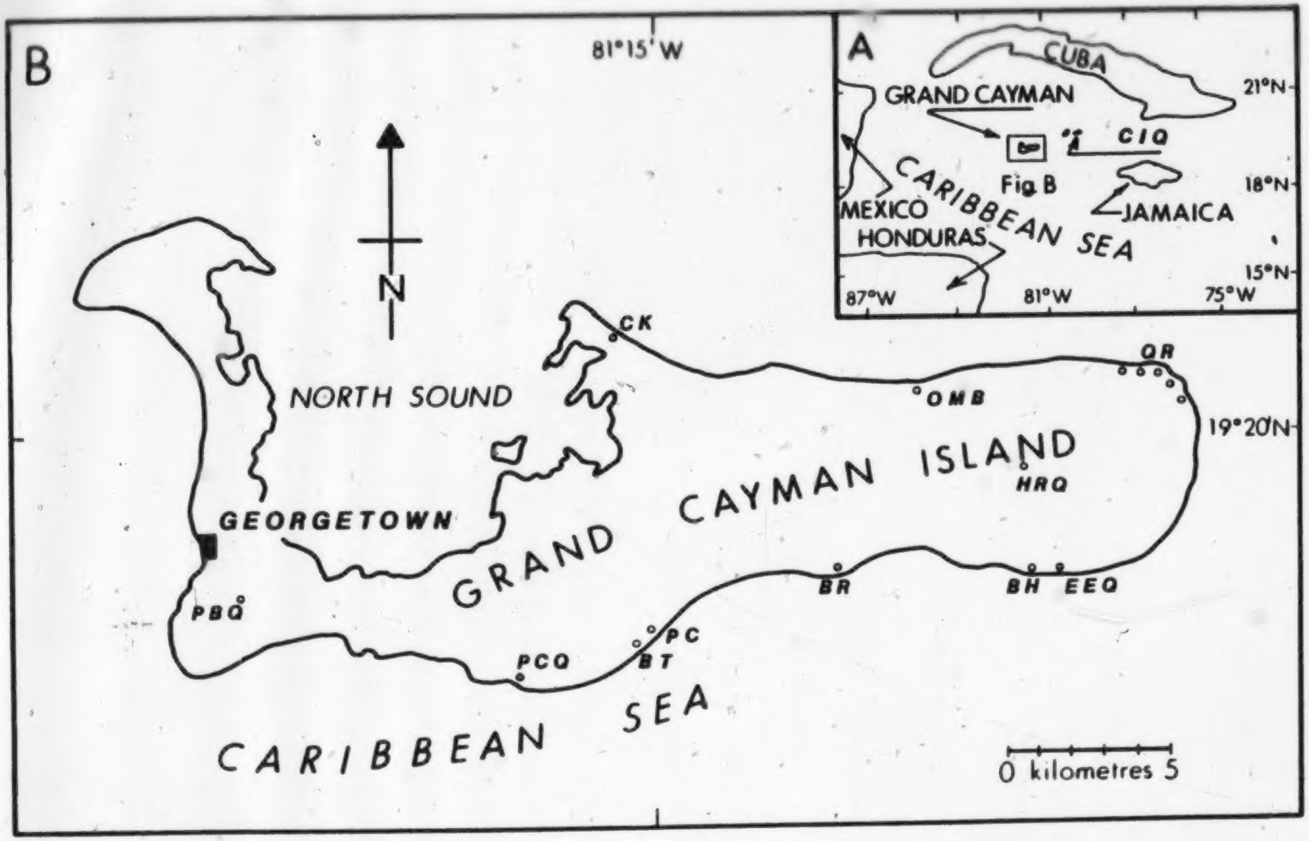
B
81°15'W
N
NORTH SOUND
GEORGETOWN
GRAND CAYMAN ISLAND
CK
OMB
QR
19°20'N
HRQ
PBQ
PCQ
PC
BT
BR
BH
EEQ
CARIBBEAN SEA
0 kilometres 5
A
CUBA
GRAND CAYMAN
CIQ
21°N
Fig B
18°N
MEXICO
CARIBBEAN SEA
JAMAICA
HONDURAS
15°N
87°W
81°W
75°W

Figure 1: A - The Cayman Islands and their location in the Caribbean Sea. (CIQ) is the Cross Island Road sampling locality on Cayman Brac. B - Sampling localities on Grand Cayman Isalnd, (PBQ) = Paul Bodden Quarry, (PCQ) = Pedro Castle Quarry, (BT) = Boddentown, (PC) = Pirate Caves, (BR) = Breakers, (BH) = Blowholes, (EEQ) = East End Quarry, (QR) = Queens Road, (OMB) = Old Man Bay Village Caves, (CK) = Cayman Kai.

The subaerial relief of the Cayman Islands in general is small, being on average less than 20m above sea level. The maximum elevation occurs on Cayman Brac, where the Bluff Formation rises some 40 m above sea level. By contrast, the submarine relief of the area is quite vast, falling rapidly away in the south to abyssal depths of 6000 m or more.

The majority of samples collected for this study came from Grand Cayman Island. Each sample collected is given a unique catalogue number which can be related directly to the sample locality on the island (Fig. 1).

B. CLIMATE

The sub-tropical climate of Grand Cayman Island is subject to distinct seasonal variation. Throughout the West Indies, the general equability of the climate is modified by variation in elevation and exposure to the prevailing winds. Grand Cayman Island, with its low relief and open exposure to the ocean, has a diurnal temperature variation of only 8 °C, and average winter and summer temperatures of 24 °C and 28 °C respectively (Sauer, 1982).

Rainfall at Georgetown averages 1740 mm per year (Hsü *et al.*, 1972), with a distinct dry season from December to April when rainfall averages less than 80 mm per month. An increase in rainfall from 12 mm per month, to 25 mm per month during the period of May through November, constitutes a distinct 'rainy season'. In spite of its low relief, Grand Cayman Island has a considerable variation in rainfall distribution . Rainfall is distinctly greater within a NE / SW trending belt which runs from the Old Man Bay area on the North shore, to the Georgetown district. The region to the South of this belt, including Bodden Town and Old Isaacs, is conspicuously dry. To the North and NorthWest, the islands considerable disruption of the Trade Winds passage often results in heavy tropical convectional downpours.

II. OBJECTIVES

The speleogenesis and speleothems of Grand Cayman Island provide a record of the post emergent history of the Island. The genesis of the speleothems, and the environments in which they formed, can provide a more thorough understanding of this period in the Islands history. Accordingly, the objectives of this study were :

1. to study the caves presently found on Grand Cayman Island, with particular reference to any diagnostic morphological features (Bretz, 1942) which might aid in the interpretation of their mode of formation, and hence their relevance to the geological history of the Cayman Islands.
2. to determine the morphology and origin of calcite crystal morphologies which occur in the speleothemic deposits of the Grand Cayman Island.
3. to describe and interpret cathodoluminescent zonation present in the calcite crystals, with particular reference to the documentation of cathodoluminescent 'signatures' in the speleothemic calcite (Meyers, 1974).
4. to determine (a) the origin of the diagenetic fluids responsible for the precipitation of the speleothems, and (b) what the controls of the stable isotopic geochemistry of the precipitated calcite were.

III. METHODS OF STUDY

A complete documentation and interpretation of the speleothemic calcite which has formed on Grand Cayman Island requires a multifaceted approach which goes beyond a simple description of the megascopic features. A detailed knowledge of the microscopic characteristics and stable isotopic geochemistry of the speleothems will enable a significant contribution to be made towards a more complete understanding of the these deposits. In order to gain as much data as possible in the limited time available, the following methods of study were employed.

1. documentation of the megascopic speleologic features and their relationship to the host dolomitic formation.
2. study of 40 petrographic thin sections on both a conventional petrographic and a Jenamed™ fluorescent microscope.
3. examination of cement micro-morphology using a 'Cambridge stereoscan 250™' Scanning Electron Microscope (SEM). Both fractured samples and polished thin sections were studied, the thin sections were first etched in dilute HCl to enhance the relief of the section. All samples were prepared with a gold conductive coating. Qualitative elemental analyses were obtained through the use of the 'Kevex' X-ray dispersive system attached to the SEM.
4. The cathodoluminescent zonation was examined with the aid of a Technosyn™ cold cathode luminesence microscope (Model 8200 MarkII). Operating procedures were kept as constant as possible throughout this study, the following being typical operating parameters, a) Voltage 15-20 Kv, b) Gun current 350-550 µA, and c) Operating vacuum 0.05-0.1 Torr. Polished thin sections were used predominantly for this study, although un-polished thin sections performed adequately. For the purpose of comparison with other published data, extreme caution is advised when

making qualitative comparisons of luminescent colour and intensity. These parameters may vary independently of the material being studied, being a function of the amperage and accelerating voltage of the cathode 'gun', and the photographic procedures employed.

5. Trace element analysis of colour banded speleothemic calcite, was obtained by atomic absorption spectrophotometry (AAS). A 1gm sample of speleothemic calcite was put into an acid (HCl) solution, and then analyzed in the AA unit. The results obtained from the speleothemic calcite were calibrated with University of Alberta laboratory standards, all results being reported in the standard parts per million (ppm) notation.
6. The stable isotopic geochemistry of the speleothems was assessed in the following way. Calcium carbonate samples (30mg to 50mg) were extracted from polished rock slabs (Plate 17A) using a small electric hand drill, in a manner similar to that described by Prezbindowski (1980). After sieving, the < 44 µm fraction was reacted in anhydrous phosphoric acid, using the procedure described by Walters *et al.* (1972), and modified after McCrea (1950). Isotopic analysis of the evolved CO_2 was carried out on a VG Micromass 602D mass spectrometer, using standard techniques (Craig, 1957). Unless otherwise stated, results are reported in the normal δ permill notation, relative to the Chicago PDB standard (Craig, 1957).

Considering the dolomitic nature of the host Bluff Formation, care was taken to avoid dolomite contamination of the calcite samples. To ensure that no contamination had occurred, the mineralogy of each sample was determined by X-ray diffraction. Operating conditions were kept constant throughout, (Radiation: Co $K_{alpha\ 1}$, Scaler: 1.10^3, Multiplier: x1, Scan Speed: 1° 2θ per min., Slit Width: 1°, Scan Range: $2\theta = 25°-52°$).

In order to calculate d-spacing offset due to Ca/Mg solid solution (Goldsmith and Graf, 1960), each sample was 'spiked' with pure quartz (Internal standard, D-Quartz), producing a strong reference point (3.343 Å) close to the major calcite and dolomite peaks. If dolomite was found to be present in any of the samples, then its percentage of the total sample was calculated using the method described in Royse *et al.* (1971) . Final isotopic enrichment was established by a 602D micromass mass spectrometer. The limits of experimental error for $\delta^{18}O$ and $\delta^{13}C$ in this study are ±0.2 ‰.

IV. GENERAL GEOLOGY AND TECTONICS.

A. PREVIOUS STUDIES

The Cayman Islands, in particular Grand Cayman Island, have been studied by numerous researchers. The first geological description of the Cayman Islands, was by Savage English (1912), who described Grand Cayman Island as, "...just a flat coral covered summit of the submarine ridge...so that its surface geology is of the simplest ".

Hydrick (1917), produced a brief geological report of the formations occurring on the Cayman Islands. It was not until 1926, however, that Matley formally named two formations. His observation of the geology on Cayman Brac, led to the introduction of the terms 'Bluff Formation' for the fine grained coralline 'limestone' of the island, and 'Ironshore Formation', for the less consolidated Pleistocene rocks which lie unconformably above the Bluff Formation.

The Bluff 'Limestone' is in fact a cream to tan coloured, dense, porcelaneous dolomitic unit (Folk *et al.*, 1973; Jones *et al.*, 1984) with well developed moldic porosity. Geographically, this formation dominates much of the east end of the Island (Fig. 2). Corals from the Bluff Formation were originally dated as Miocene in age (Vaughan 1926), with later foraminiferal studies yielding Oligocene-Miocene ages.

The Ironshore Formation is formed of poorly consolidated reef limestone which is characteristically "case hardened". Brunt *et al.* (1973), has divided the Ironshore Formation into five distinct facies based upon the lithology and biota. The contact between the Bluff Formation and the Ironshore Formation represents a 'buried landscape' unconformity (Brunt *et al.*, 1973), which is most pronounced in the south-west of the Island (Fig. 3).

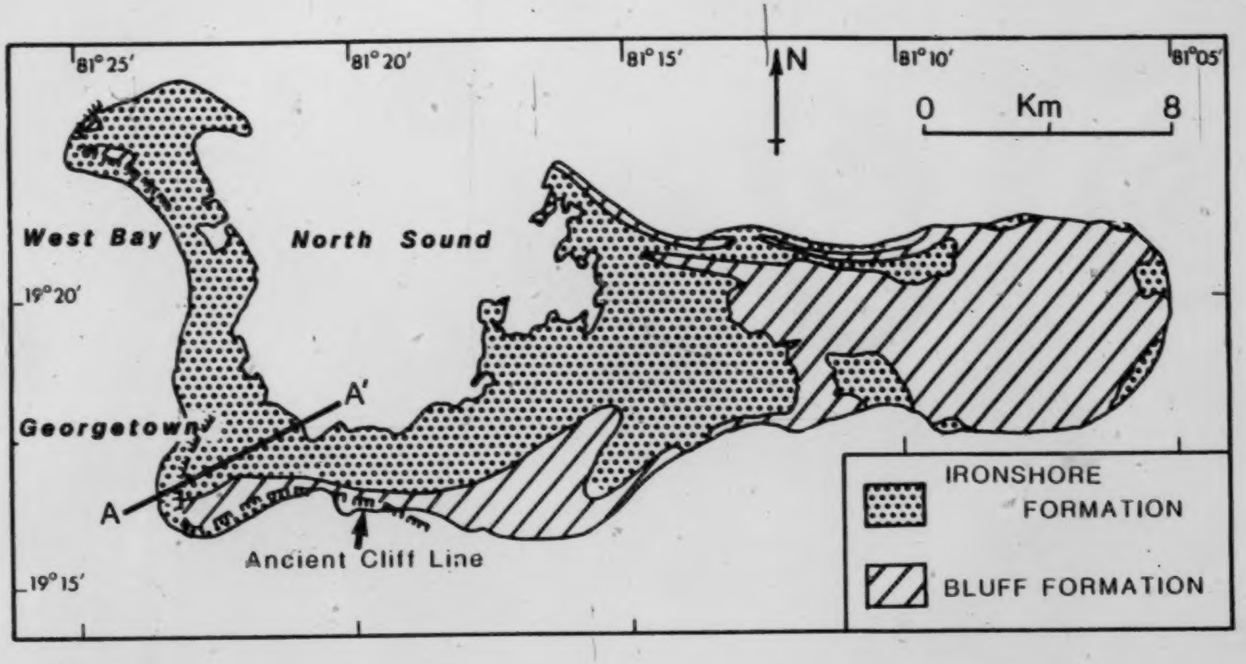
81° 25′
81° 20′
81° 15′
N
81° 10′
81°05′
0 Km 8
West Bay
North Sound
19° 20′
Georgetown
A′
A
Ancient Cliff Line
19° 15′
IRONSHORE FORMATION
BLUFF FORMATION

Figure 2: General Geology of Grand Cayman Island. After Brunt *et al.* 1973.

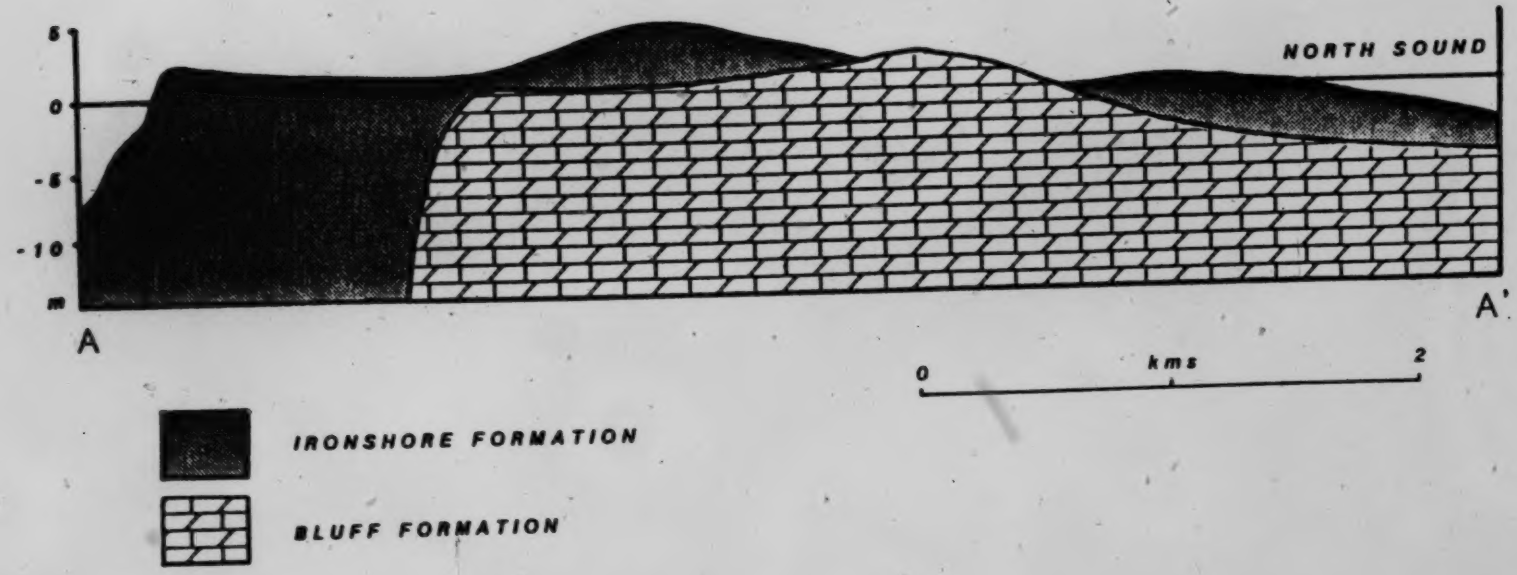
5
0
-5
-10
m
A
A'
NORTH SOUND
0
kms
2
IRONSHORE FORMATION
BLUFF FORMATION

Figure 3: Geological cross section of south western Grand Cayman Island. After Brunt *et al.* 1973.

Structurally, the Bluff Formation appears as a massive, poorly stratified unit, with a near horizontal attitude. Little evidence for faulting has been found on Grand Cayman Island, although a series of parallel joint systems (Rigby and Roberts, 1976) is clear evidence of some form of tectonic stress.

B. TECTONICS

The tectonic control of relative sea level may have greatly influenced the Tertiary depositional environment of the Cayman Islands. Any change in sea level, could have a profound effect upon the composition of the diagenetic fluid in the Bluff Formation. Thus the processes of speleogenesis and subsequent speleothem deposition, must be viewed in light of the tectonic controls of this region.

Historically, the Caribbean area has been extensively traversed with bathymetric and geophysical devices (Bowin, 1968; Molnar and Sykes, 1969; Erickson *et al.*, 1972; McDonald and Holcombe, 1978). The conclusion of these, and many other related works, is the conception of a complex 'microplate tectonic' scenario for the Caribbean region (Fig. 4). This scenario places the present day Cayman Islands very close to the major active boundary between the North American and the Caribbean plate.

The region is dominated by the Cayman Trench, formerly the Bartlett trench, which extends 1600 km from the Windward passage to the Gulf of Honduras. It is a steep sided, graben like-structure, approximately 150 km wide and up to 6000 m deep. It is bounded on the north by the Cayman Ridge and to the south by the Nicaraguan plateau.

The Cayman Ridge, upon which the Cayman Islands lie, extends from the Sierra Maestra of Cuba to within 100 km of the British Honduras continental slope. The southern margin of the ridge, a precipitous fault orientated wall, shows both increased heat flow (Erickson *et al.*, 1972) and seismic activity, the result of left lateral motion along the Orient fault zone.

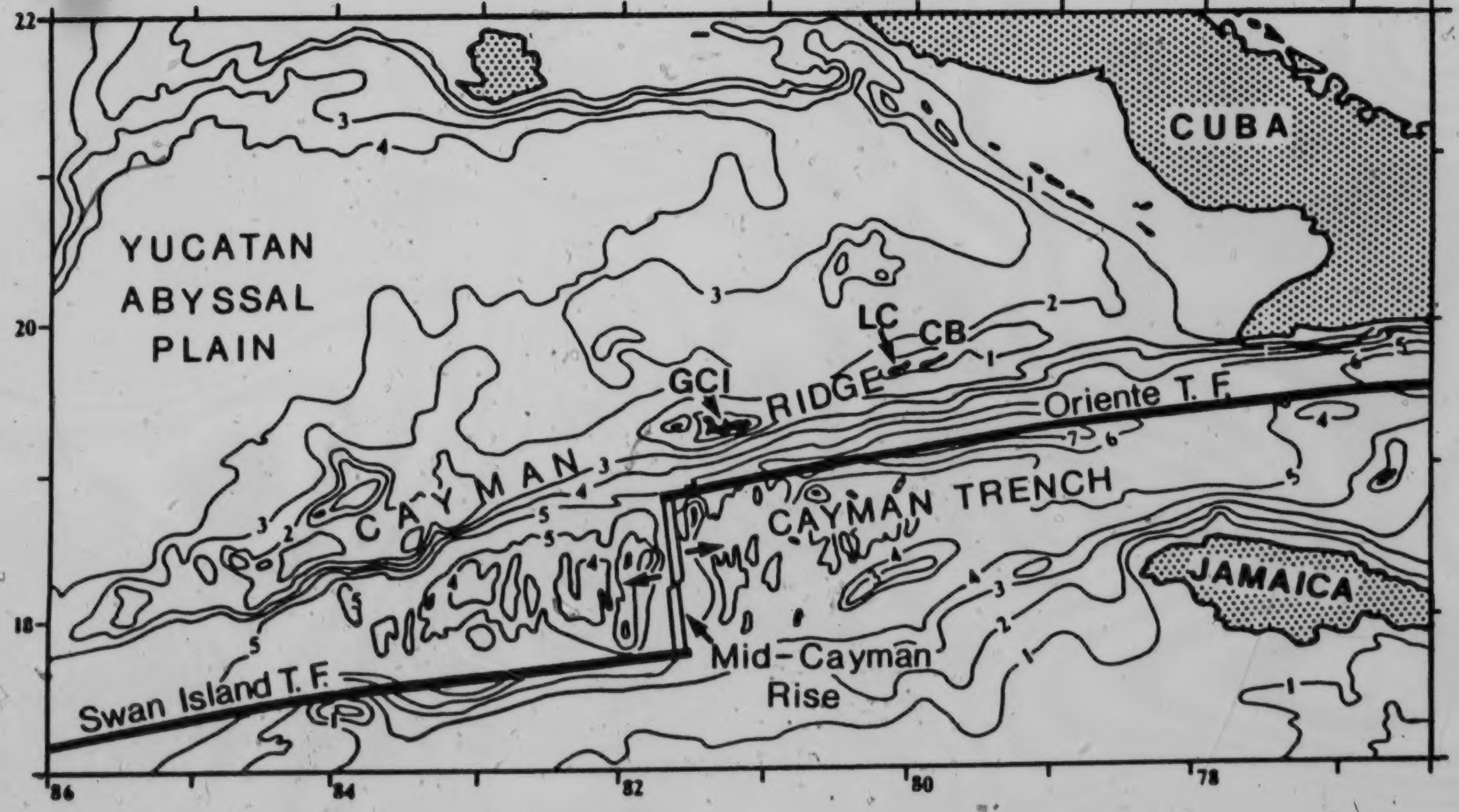
CUBA
YUCATAN
ABYSSAL
PLAIN
JAMAICA
CAYMAN RIDGE
CAYMAN TRENCH
GCI
LC
CB
Oriente T. F.
Swan Island T. F.
Mid-Cayman
Rise
22
20
18
86
84
82
80
78
1
2
3
4
5
6
7

Figure 4. The Cayman Islands, (GCI) Grand Cayman Island, (CB) Cayman Brac, and (LC) Little Cayman in a Caribbean tectonic setting.

The Nicaraguan Plateau extends from Honduras and Nicaragua to Haiti, its southern margin dipping gently towards the Columbia Basin, while the northern margin forms the steep southern wall of the Cayman Trench. Heat flow and seismic activity are now concentrated around the Bonacca Ridge and the Swan Island Fault Zone (Fig. 4)

The central region of the trench, marked by elevated and jagged relief which trends in a N/S manner, forms the Mid Cayman Rise. There, increased heat flow (Erickson, 1972) and increased seismic activity (Molnar and Sykes, 1969) are the direct consequence of active oceanic plate accretion.

The origin of the Cayman Islands

A late Cretaceous change in the 'poles of rotation', caused the South American plate to rotate clockwise with respect to the North American plate (Ladd, 1976). The resulting compressional regime, was resolved by a southerly dipping subduction zone beneath the present Central Caribbean region (Perfit and Heezen, 1978). Partial melting of the North American plate resulted in a chain of volcanic islands, surrounded by shallow water carbonates and clastics. These form the Cretaceous 'basement' of Southern Cuba, Haiti, Jamaica, the Cayman Ridge and the Nicaraguan Plateau.

By the early Tertiary, the South American plate had begun to move eastwards with respect to the North American Plate, imposing an extensional regime upon the central Caribbean region . A series of left lateral transverse faults developed, separating the Orient Province and the Cayman Ridge, from the Nicaraguan Plateau and Jamaica. During its post Eocene development, oceanic crust 'leaked' into the Cayman Trench rift zone, forming an active spreading ridge at the Mid Cayman Rise.

The Cayman Ridge was predominantly a shallow carbonate bank during the early Oligocene, but by the end of the Oligocene, deposition of deep water limestone is indicative of extensive vertical tectonics. The shallow water Oligocene-Miocene Bluff Formation of the Cayman Islands attests to the fact that these were isolated pinnacles on the ridge, in an area that was subsiding at rates up to 6 cm per year (Ladd, 1976).

Finally, post middle Miocene uplift elevated the Cayman Islands, subaerially exposing the Bluff Formation.

V. SPELEOLOGY OF GRAND CAYMAN ISLAND

Speleogenesis encompasses all processes which affect the creation and development of natural underground cavities (Moore and Nicholas, 1964; Bögli, 1980). This includes such diverse elements as climate, tectonics, lithology, groundwater composition and flow mechanics, all of which may in some way affect the creation or development of subterranean cavities via corrosion or erosion. While speleogenesis *sensu stricto* does not include the deposition clastic, organic and chemical cave sediments, these speleothems are nevertheless an integral part of the speleologic environment.

Large cave systems are common on Grand Cayman Island. Although access to some is restricted, Pirate Caves, located at Boddentown on the south coast of the island, and the Old Man Bay Village Caves located on the north east side of the island are easy to reach (Fig. 1). In the Cayman Islands, interface and subsurface karst development is the result of, (1) dissolution due to the downward percolation of meteoric waters, and (2) dissolution of the bedrock in the marine or mixing zone phreatic realm. The passage of these 'aggressive' waters through the vadose and phreatic realms, created numerous shallow and deep cave environments on Grand Cayman Island and Cayman Brac. The presence of deep cave environments, has been interpreted on the basis of both groundwater recharge and drill pressure data (Ng, 1985).

A. PRECIPITATION FEATURES (Speleothems)

Secondary mineral precipitates, formed in the cave environment, have been termed *speleothems* by Moore (1952). With the exception of a few tiny water droplets on isolated stalactite tips (Plate 1B), the active formation of speleothems in both the Pirate Caves and Old Man Bay Village Caves is presently negligible. It is possible that these caves are still active, with speleothem deposition occurring during periods of increased meteoric influx, a rain storm for example. However, the incredible diversity and density of speleothems at the Old Man Bay Village Caves (Plates 1 and 2), cannot be reconciled in this manner.

In comparison with the Pirate Caves system, the density of speleothems in the Old Man Bay Village Caves is striking. These speleothems must have been produced at some time in the past, when the caves were under the influence of vastly increased rates of meteoric influx.

The distinction between the Old Man Bay Village Caves and Pirate Caves may be related to their differing depths below the surface, and the effects that this can have upon the geochemistry of the vadose fluids. Passages which contain speleothems in the Old Man Bay Village Caves, begin at approximately 5 m below the surface and continue to much greater depths. This is significantly deeper than Pirate Caves, which rarely exceed 3 m below the surface. This difference in depths may have a marked effect upon the saturation state of the fluid entering the cave systems. As meteoric percolates through the overlying strata, dissolution of the bedrock will occur, and the fluid will eventually become saturated or oversaturated with respect to calcite. Fluids entering the Pirate Caves probably remained undersaturated with respect to calcite, while those entering the Old Man Bay Village Caves become saturated with respect to calcite. Upon entering the Old Man Bay Village Caves, the meteoric fluid with a higher PCO_2 will degass, and the precipitation of speleothems will follow.

The speleothems of any cave can be subdivided by their mode of formation into dripstone, rimstone and rimstone pool deposits, and flowstone.

Dripstone

The Old Man Bay Village Caves contain abundant dripstones (Plate 1C), many of the cave passages being practically impassable by virtue of the density of stalactites, stalagmites and stalacto-stalagmites (columns). The stalactites are locally so dense that the roof of the cavity cannot be seen, and many of the individual stalactites have coalesced to form composite features with interconnecting drapes (Plate 2B). There are abundant type

II stalactites (Bögli, 1980) in these caves, many of which display distinctive concentric laminae and a characteristic central 'soda straw' (Plate 1D). Type I stalactites, which also occur in the Old Man Bay Village Caves, are recognized by the lack of a 'soda straw', and a 'drape' or 'flag' which commonly accompanies them (Plate 1B). One particular stalactite at Old Man Bay Village Caves (Plate 1B) shows a small water droplet forming at the tip, this individual stalactite is indicative of the presently subdued rate of speleothem precipitation in the cave as a whole.

The fractured surface of many stalactites (Plate 1B), shows that their longitudinal section commonly produces a near planar set of laminae. Consequently, when viewed as a fragmentary particle, care must be taken not to confuse a vertical speleothem fragment as part of a horizontal speleothem or flowstone. This point is especially pertinent, in view of the fact that 'clastic' deposits of fragmentary stalactites occur in these caves (Plate 3A). Such a deposit, the result of delicate stalactites being stripped from the ceiling and later deposited as a coarse stalactite conglomerate, may be the result of natural causes, *i.e.* a catastrophic influx of water (hurricane 'surge'), or anthropogenic causes, *i.e.* vandals.

In addition to the smooth forms of stalactite, many of the stalactites and accompanying flags at that locality posses a highly serrated morphology (Plate 1A and 2E). The formation of a serrated edge, or the crenulated surface of a flag, can be related to increased CO_2 degassing as water flows over surface protuberances (Bögli, 1980). The initial growth of the surface protuberances on a smooth surface may be the result of turbulence in the fluid flowing over the speleothem. Water droplets collect at the drape or stalactite margin, where subsequent CO_2 degassing of the droplet eventually causes precipitation of a 'tooth'. When the droplet reaches a critical size, it will flow to the next 'saw tooth', and continue the process until its size causes it to move on again. The continued process will eventually lead to the beautiful serrated morphology.

The macroscopic distinction between stalactites and stalagmites in the rock record is aided by their markedly dissimilar internal and external morphologies. A comparison of the fractured surface of the stalactite (Plate 1D) with that of a stalagmite (Plate 2A), shows that unlike the former, they do not possess a central "soda straw". Furthermore, while the constructive laminae of the stalactite are concentric, the laminae of the stalagmite are distinctly disharmonic. The overall external morphology of most stalagmites in the Old Man Bay Village caves show distinctly rounded terminations (Plate 1C). This is indicative of a relatively short fall for the water droplet; had the distance of fall been greater, then a distinctive 'splash cup' would have developed (Franke, 1965).

'Eccentrics', or vertical speleothems which appear to defy natural gravitational control, are rare on Grand Cayman Island. The delicate helictites and heligmites of Moore (1954), were not found in either the Old Man Bay Village Caves, or the Pirate Caves. There was, however, one large stalactite in the Old Man Bay Village Caves with a clearly eccentric form (Plate 1C). This stalactite, over 1.5 m in length, displays a marked growth asymmetry towards its termination. The causes of asymmetrical growth are both varied and disputed (Bögli, 1980). For the more delicate helictites, capiliarity is the generally accepted controlling factor. For this larger feature however, a process whereby oversaturated fluids crystallize in the central canal, and hinder or obstruct the water circulation (McGrain, 1942), is more plausible. This process diverts the flow of saturated fluids, resulting in the uneven precipitation of calcite.

Rimstone

As water, saturated with respect to calcite flows in a thin layer over an irregular surface, the point at which it flows over the irregularity will be an area of increased CO_2 degassing. The loss of CO_2 causes the precipitation of calcite which over a period of time constructs a calcite ledge, behind which water is dammed. In certain passages of the Old Man Bay Village Caves, tens of square metres are covered by massive rimstone deposits (Plate 4A). Where the water has cascaded down a steeper gradient, the rimstone terraces become small crescentic cups (Plate 2F), demonstrating the morphological control exerted by the fluid flow dynamics. Where the gradient approaches 1:1, there is a clear transition from rimstone (flowstone) to dripstone forms. This combination of horizontal and vertical speleothems (Plate 4A), forms what is commonly described as a 'Meduse-dripstone' (Bögli, 1980).

Flowstone

Near horizontal, smooth, banded deposits are rare in the Old Man Bay Village Caves. Most of these deposits have developed calc-sinter bars and are more correctly described as a rimstone deposit. One area of this cave does posses a near vertical flowstone deposit, in the form of a sinter band (Plate 4D), the result of water flowing at a steep gradient along the cave wall. This particular speleothem has been damaged, fortunately in this instance, for it provides a view of the colour variation which occurs throughout this speleothem.

The best examples of *in situ* horizontal flowstone are located in the Pirate Caves (Plate 3G, H and 4B). There, well stratified flowstone fills former solution cut channels, which are now exposed in the cave wall. The dominant controlling influence upon the morphology of these bodies was probably the surface topography on which the flowstone developed. Where the flowstone has filled a former solution conduit, near horizontal bands of flowstone have developed which abut against the conduit margin (Plate 4B). Other flowstone deposits are distinctly curved (Plate 3G), possibly the result of saturated fluids flowing over a topographic mound, coating it in a thick flowstone deposit (Fig. 5). Ponding of fluids may have occurred, which precipitated horizontal flowstone around the mound. This, accompanied with the growth of small vertical speleothems from the roof of the cavity, may account for the deposit exposed in the wall of the Pirate caves system (Plate 3G).

In addition to the two large cave systems at Boddentown and Old Man Bay village, much of the studied flowstone occurs in association with numerous joints, fissures and small karst solution features (Plate 2D). Small exposures of vertical and horizontal flowstone occur on the walls of prominent joint systems at widely spaced localities, including Pedro Castle Quarry, Queen's Road, Cayman Kai and Blowholes (Fig. 1).

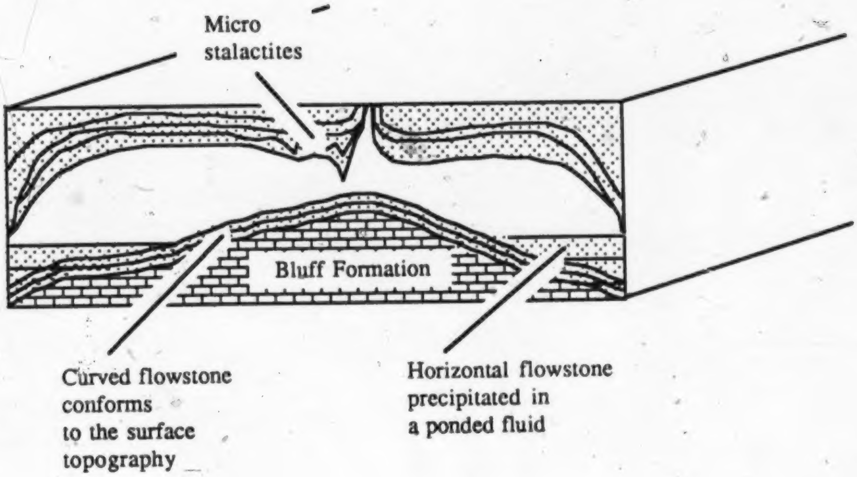
Micro stalactites
Bluff Formation
Curved flowstone conforms to the surface topography
Horizontal flowstone precipitated in a ponded fluid

Figure 5. Genesis of an unusual flowstone body from Pirate Caves, which highlights the morphological control exerted by the topograpy of the host dolostone.

Flowstone is rare at High Rock Quarry, although there was one boulder at this locality which contained well preserved stalactites (Plate 2C). Despite minor differences in spatial distribution and abundance, the associations between flowstone and the Bluff Formation were the same at each locality. Flowstone appears as a deposit on the joint surface, forming vertical or highly inclined layers of colour banded calcite approximately 1 cm to 1.5 cm thick, or as completely filled 'pockets' of flowstone (Plate 2D). The common occurrence of flowstone on the joint surfaces, indicates that these joints probably acted as interface or subsurface conduits for the passage of groundwater moving through the vadose zone, under gravitational control.

The presently 'pitted' and irregular morphology of these flowstones, indicates that they are now in a phase of dissolution. Thus, where the joints once acted as conduits for a fluid oversaturated with respect to calcite, they are now under the influence of fluids undersaturated with respect to calcite. The fact that these flowstones are found in environments where active dissolution of calcite is occurring, indicates that at least one major change in the pore water chemistry, or 'diagenetic environment', must have taken place.

B. DISSOLUTION FEATURES (Speleogens)

Of the two cave systems studied, Pirate Caves (Fig. 1) contains the greatest abundance of speleogens. The explanation for this lies in the fact that speleogenesis is essentially a two phase process involving, (1) the formation of the cave system through dissolution or collapse processes, and (2) the formation of speleothems through precipitation. At Pirate Caves, speleothems are limited to horizontal flowstone filling solutional cavities, leaving a cave system that is essentially devoid of stalactites, stalagmites, drapes or any other vertical speleothems. The original dissolution features are therefore present to this day. Precipitation of speleothems at the Old Man Bay Village caves, however, has been so great that the initial dissolution features have been totally masked by later precipitates.

The speleomorphology of the Pirate Caves, suggests that this is a "two cycle" cave system (Davis, 1930; Swinnerton, 1932; Bögli, 1980 Figs. 14.10. and 14.5 b), involving at least one phase of phreatic and one phase of vadose dissolution. The prominent 'keyhole' profile of the main cave passage (Plate 3B), is clear evidence of a vadose phase of dissolution following a period of phreatic dissolution. The upper tubular portion represents the phreatic phase, while the lower notch represents downcutting under the influence of gravitational forces in the vadose zone. Being a two cycle cave system, the speleogens present can be categorized into those which have either a vadose or phreatic origin.

Phreatic speleogens

Throughout the cave system, there are numerous 'ceiling solution pits' or 'inverse solution pockets' (Plate 3C, D), and 'solution scallops' (Plate 3B). The origin of the large inverse solution pockets (Plate 3C), is made clear by the lack of vertical solution grooves on the inside of the pocket. Had there been such grooves then this may have been a "vadose solution pocket" of Franke (1963); their absence, however, indicates that this feature formed through either, (1) the physical erosion of a strong eddying current, or (2) Mischungskorrosion (Bögli, 1964). Both of these mechanisms require that the passage be in the phreatic zone at some point in its development. The solution scallops which contour the ceiling of this cave system (Plates 15B, F), provide corroborative evidence towards a period of phreatic development.

The shape of the phreatic tube is controlled by the fluid pressure gradient, and the fabric of the substrate through which it cuts (Bögli, 1980). If the host carbonate is homogeneous, then the tube morphology will be controlled solely by the fluid pressure gradient. If the substrate possesses any weakness, however, then these will be exploited and the morphology of the tube altered accordingly. Bedding planes or fault planes are common sites of preferred erosion, and can thus control the morphology of the phreatic tube. The effects of bedding plane control are not marked on Grand Cayman Island, since the host carbonate, the Bluff Formation, forms a massive poorly bedded unit. However, the phreatic tubes from Pirate Caves do show an elliptical form which may indicate a poorly defined, sub-horizontal bedding plane attitude (Plate 3F).

Vadose speleogens

The vadose incision of the Pirate Caves phreatic tube has left a marked down cut notch, or 'key hole' structure (Plate 3B, F), which is perhaps the most prominent vadose feature. At present, the downcut notch is approximately 1.5 m in depth, however, a later fill of this notch through either natural or man made influences, may mask the true depth of this feature. The distinctive stepped appearance of the incision (Plate 3B, F) indicates that the water table did not fall in one continuous motion, but that there was probably at least two phases of decline.

A large vertical solution shaft (Plate 4C), is also a prominent vadose speleogen of the Pirate Caves. This shaft, approximately 2.5 m in length and 70 cm wide, is formed by chemically aggressive meteoric water entering through the ceiling of the cave. This is a "vadose flow feature" of Thrailkill (1968), demonstrating strong gravitational control upon the morphology. The prominent enlarged bowl at the base of the shaft probably resulted from enhanced dissolution due to the mixing of chemically dissimilar waters.

An indication of the fluctuating water table in this system, is given by the presence of a shaft which has been created between two cave levels during the development of the lower passage (Plate 4E). Now that the system is inactive, the exact origin of the shaft is unknown. Depending upon the movement of the water table, either a swallow shaft, a spring shaft or a piezometric shaft could have formed. Solution scallops which can be used to identify the dominant water flow direction in the shaft, were not present. The simplest explanation, is that water from an upper cave level has cut down to a lower cave level, in response to a falling water table (*i.e.* a swallow shaft)

C. SPELEOTHEM DATING

An important aspect of this study was to try and determine if a specific period of speleothem deposition occurred, or if this has been a continual process since the emergence of Grand Cayman Island. It was therefore necessary to try to date the speleothem formations. Three possibilities existed which might be able to date the speleothems, (1) radiogenic isotopes, (2) growth rates, and (3) field relationships.

Radiogenic Isotopes

Gascoyne *et al.* (1978) suggested that , "For precise, reproducible results, by the ^{230}Th/^{234}U method, only impervious speleothems free of detritus and containing > 0.05 ppm Uranium can be used." They also suggested that the primary source of Uranium and

Thorium in the geochemical cycle is the weathering of felsic igneous rocks. The distinct lack of felsic igneous rocks on, or around Grand Cayman Island, leads to a scarcity of Uranium in the geochemical cycle. These facts are in agreement with Woodroffe *et al.* (1983), whose attempts to obtain an absolute date from the speleothems via radiogenic isotopes, were unsuccessful due to a lack of Uranium in the samples.

Growth Rates

The establishment of a speleothems age from a comparison of its thickness and rate of growth has proved successful in the past (Dreybrodt, 1979; Bögli, 1980). Dreybrodt (1979) has provided the theoretical details of speleothem growth in sufficient detail to enable a good approximation of active speleothem age to be made. From this theory, it is apparent that stalagmite growth rates (and by analogy, flowstone growth rates) are dependant upon (1) the Ca^{2+} concentration of the source water, (2) the rate of supply (or drip rate), and (3) the temperature. Unfortunately, none of the above factors can be measured in an inactive cave system, therefore, if growth rates are going to be employed as a method of dating these speleothems, the following general assumptions must be made:

(1) from the high degree of permeability observed in the Bluff Formation, the rate of supply (the drip rate) will be high (< 250 seconds).

(2) as part of a tropical karst system, the molar concentration of Ca^{2+} is expected to be high (Atkinson and Smith, 1976).

(3) for ease of calculation, a temperature of 25 °C is assumed, which corresponds well with the measured water temperatures in the Old Man Bay Village Caves of between 25 °C and 23 °C.

Combining the theory of Dreybrodt (1979, Figures 5, 6, and 7, p.101), the assumptions made above, and the fact that some of the largest stalagmites in the Old Man Bay Village Caves are approximately 1 m in height , a period of growth of approximately 8,000 years is required. Unfortunately, this figure is very limited in terms of absolute dating on Grand Cayman Island, for it is not known when speleothem growth ceased. At the two extremes, this figure could place this particular speleothem of middle Miocene age (shortly after island emergence occurred), or as recent as 8,000 BP.

When all of the variables between differing localities are considered, including 'drip rate', Ca^{2+} concentration, and the time of the host cavity formation, the use of growth rates to establish a 'time frame' for the speleothems is severely restricted.

Field Relationships

An examination of the flowstones in relation to the surrounding geology, may prove to be the most informative in terms of acquiring an absolute date for the formation of the flowstones.

On Grand Cayman Island, the following important flowstone associations were observed:

(1) at East End Quarry and Breakers (Fig.1), flowstone is commonly interbedded with ooid and pisoid grainstones.

(2) some of the pisoid grainstones at East End Quarry, contain small (< 1.5 cm) angular clasts of laminated flowstone.

(3) at Blowholes, flowstone is common in the prominent joint system. These flowstones are nearly always followed by a distinct generation of breccia.

(4) although the Bluff Formation has been completely dolomitzed, the original calcite mineralogy of the speleothems remains intact.

The importance of the first two points becomes apparent in light of the fact that the presence of pisoids or ooids, has only been documented from the Pleistocene era of Grand Cayman Island (Brunt *et al.*, 1983). To date, neither the earlier Oligocene-Miocene Bluff Formation, nor the recent sediments of the Grand Cayman lagoons, have shown any presence of ooids. Consequently, the presence of interbedded flowstone and ooids, suggests that a dominant phase of flowstone precipitation occurred during the Pleistocene.

The presence of flowstone clasts in the ooid fills, further suggests that the flowstone was present prior to the onset of ooid formation.

At Blowholes, flowstone commonly appears as the first deposit on the joint surface, forming layers approximately 1 cm to 5 cm in thickness. These are followed by multiple generations of breccia, including an angular dolostone breccia with a red terra rosa matrix, and a breccia containing clasts of flowstone. The latter clearly post-dates at least one phase of flowstone formation, but its relation with the dolostone breccia is unknown. Many of the joint fill breccias are only semi-lithified, and are assumed to be of very recent formation. This complex pattern of cavity and joint fills is thought to be the result of continued erosion and brecciation via the process of wave activity. As erosion of the wave cut platform continues, pockets of flowstone or flowstone deposited on the wall of the joints become uncovered. The flowstone is then brecciated in the on-going process and deposited in the prominent joint sets. The association of flowstone with these breccias, indicates that the active formation of flowstone has now ceased at this locality, and is now in a destructive phase.

The precipitation of the speleothems can also be placed in a relative time frame alongside the process of dolomitization. The fact that all of the speleothems retain a calcite mineralogy, whereas the host carbonate has been completely dolomitized, indicates that speleothem precipitation was a post-dolomitization event. Pleydell (1987) suggested that dolomitization on Grand Cayman Island occurred as a 'mixing zone phenomena', either contemporaneous with, or shortly after island emergence. The theory of early dolomitization does not significantly reduce the time span during which the speleothems could have been precipitated. Consequently, as a method of absolute dating, the relationship between dolomitization and speleothem precipitation provides poor resolution.

In summary, the field relationships do not provide an absolute age for any of the speleothems on Grand Cayman Island. They do, however, suggest that a productive phase of flowstone deposition occurred during the Pleistocene period, one which has not been continued through to the present day.

D. A SPELEOGENETIC MODEL FOR GRAND CAYMAN ISLAND

Howard (1963), stated that, "...a universaly applicable origin of caves is impossible, unless one speaks in the vaguest and most inconsequential terms." When restricted to a limited geographical area however, an understanding of some of the basic principles involved and the controls that they exert upon dissolution and precipitation, can provide a foundation upon which to build an acceptable model of speleogenesis. Heeding the words of Howard (1963), a speleogenetic model for the Cayman Islands is proposed, keeping in mind the problems inherent with broad genetic speleological classifications.

The features present in the Pirate Caves system forms the basis of the argument for the overiding speleogenetic control on Grand Cayman Island. The assumption that the mode of formation for this cave system is applicable to the whole island, is valid since:

(1) the limited geographical area of the island and the separation of the cave systems, is small enough in comparison with the proposed sea level fluctuations as to be negligible.

(2) there is no evidence to suggest that the island has undergone differential tectonic activity, which might alter the water table position on different parts of the island.

After initial cave formation, which was probably in the phreatic zone, the Pirate Caves system began a phase of development in the vadose zone, where horizontal layers of flowstone began to fill the cave passages (Plates 3G, 3H and 4B). An important feature in deciphering the evolution of this cave system is the presence of this flowstone exposed in the walls of the Pirate Caves (Plate 4B). These exposures demonstrate how the present cave passage has cut a pre-existing passage in which flowstone had already been precipitated. A prominent phase of dissolution must therefore have followed a phase of precipitation. The similar occurrence of exposed and eroded flowstone in an inverse solution pocket (Plate 3C), further indicates that this later phase of dissolution must have been in the phreatic zone at some point. In summary, it appears that the Pirate Caves system, has undergone speleogenesis of a cyclical nature, with both vadose and phreatic features apparently overprinting each other.

Palmer (1984) noted that a common flaw in the analysis of cave origins is the misinterpretation of the effects of seasonal or short term fluctuations of groundwater flow. Many cave systems record the passage of ephemeral phreatic events, where for example during periods of high 'run-off', vadose passages become temporary phreatic tubes developing all the associated speleogens. In view of this, an alternative theory is advanced to explain the presence of phreatic speleogens in the Pirate Caves. These speleogens may be the result of fluctuations in the influx of meteoric water, which , during periods of 'flood' may fill the solution cavities, producing an ephemeral phreatic regime. This mode of formation suggests that the speleogens are in no way related to the permanent position of the water table. The applicability of this theory to the Pirate Caves system can be discounted, since the main phreatic tube would require a minimum of 650 cubic metres of water simply to fill it. Based upon rainfall data for Grand Cayman Island (Hsü *et al.*, 1972), the hydrological catchment area is not capable of supplying such a quantity of water. If the present meteorological data are a reflection of conditions in the past, then it is suggested that phreatic conditions were not due to ephemeral meteoric fluctuations, but to a rise in relative sea level, which raised the water table to such an extent that the Pirate Caves became part of a permanent marine, or 'mixed water' phreatic zone.

Independent evidence for global fluctuations in sea level during this period is presented in Vail and Hardenbol (1979) and Hallam (1984), while more specific evidence for a fluctuations in sea level on Grand Cayman Island, is presented in the form of numerous marine erosional terraces above and below present day sea level (Rigby and Roberts, 1976; Emery, 1981; Woodroffe *et al.*, 1983). Emery (1981) suggested that six marine terraces could be recognized on the south side of Grand Cayman Island, close to the location of Pirate Caves, at 2, 4, 6, 8, 11 and 15 metres above sea level. While the validity of the higher two terraces is debatable (Woodroffe *et al.*, 1983), the presence of a wave cut notch (Plate 4E), at approximately 6 m above present day sea level is clear evidence of a considerable rise in relative sea level in the past. Two wave cut notches are also found at 20 metres and 150 metres below the present day sea level (B. Jones pers. comm., 1987), suggesting that some of the caves on Grand Cayman Island may once have been 20 or 150 metres above sea level. It is interesting to speculate on the effects this could have had on the climate of the Island. One argument might be that such a substantial relief could have created an increase in orographic rainfall, which eventually led to the precipitation of the speleothems. Although this provides an answer to many questions, an increase in orographic rainfall is unlikely considering the limited areal extent of Grand Cayman Island.

Fluctuations in sea level could have profound implications upon the speleogenesis of Pirate Caves, and for Grand Cayman Island in general. As the sea level rises, the 'aggressive' transition zone which exists between the meteoric and marine bodies of water, will rise accordingly. It has been well documented, that the mixing of chemically dissimilar bodies of water, which occurs in the mixing zone, can lead to the extensive dissolution of carbonates (*eg*. Runnels, 1969; Plummer, 1975; Plummer *et al.*, 1976, 1979; Bögli, 1980; Hanshaw and Back, 1980a, 1980b; Palmer, 1984; Back *et al.*, 1986). The theoretical details of the dissolution geochemistry are dealt with at the outset, so as to provide a foundation upon which to further advance the Cayman speleogenetic model.

Carbonate Dissolution Geochemistry

In any carbonate terrain, the process of speleogenesis and the presence of speleothems is dependant upon a series of complex dissolution and precipitation reactions (Krauskopf, 1967; Stumm and Morgan, 1970; Bögli, 1980). To demonstrate these reactions, and the controls they exert upon speleogenesis, the simplest of carbonate systems ($CaCO_3$ - H_2O - CO_2) is considered first.

Calcium carbonate dissolution and precipitation is summarized by;

$$CO_2 + H_2O + CaCO_3 \leftrightarrow Ca^{2+} + 2\,HCO_3^- \qquad (1.0)$$

This equation (1.0) is in fact five separate equilibrium reactions, all of which can be treated as a separate entity, but never in total isolation from one another.

$$CO_{2(g)} \leftrightarrow CO_{2(aq)} \qquad (1.1)$$

$$CO_{2(aq)} + H_2O \leftrightarrow H_2CO_3 \qquad (1.2)$$

$$H_2CO_3 \leftrightarrow H^+ + HCO_3^- \qquad (1.3)$$

$$HCO_3^- \leftrightarrow H^+ + CO_3^{2-} \qquad (1.4)$$

$$CaCO_3 \leftrightarrow Ca^{2+} + CO_3^{2-} \qquad (1.5)$$

Five equilibrium constants determine the rate at which these reactions proceed, each constant being dependant upon temperature and pressure (Bathurst, 1975).

PCO_2 is a very important variable (1.1), which determines the rate at which reaction (1.0) proceeds. The amount of dissolved CO_2 ($CO_{2(aq)}$) will be dependant upon the initial CO_2 concentration of the water and the extent to which this CO_2 can be replenished by exchange with the gas phase ($CO_{2(g)}$). A system which is unable to exchange with the gas phase is said to be "closed", and the amount of $CaCO_3$ that can be dissolved is limited by a finite source of CO_2. If the system can exchange with the gas phase, then PCO_2 will remain constant, resulting in a greater amount of $CaCO_3$ dissolved.

The vadose speleogenetic processes on Grand Cayman Island will have occurred in an open system. For the phreatic speleogenetic processes, it would be natural to assume a closed system, this, however, may prove to be incorrect. Holland *et al.* (1964), Back *et al.* (1970), and Langmuir (1971) demonstrated that despite being confined, many limestone aquifers maintain CO_2 exchange with the atmosphere for considerable distances. Active dissolution can therefore occur in the phreatic zone, allowing speleogenesis to continue below the water table.

The natural system: The assumption that karst terrain and associated caves on Grand Cayman Island are developing in the system ($CaCO_3$ - H_2O - CO_2) is, however, far too simplistic. First, the host carbonate the Bluff Formation is not a limestone but a dolostone. Although the dissolution of dolomite is analogous to that of calcite (Drever, 1982) the rates are much slower. White (1984) made a comparative study of karst denudation rates in both limestone and dolostone terrains. An important conclusion of his study, based on research by Busenberg and Plummer (1982), was that as groundwater approaches saturation with respect to dolomite, the dissolution rate becomes immeasurably small. Consequently, meteoric waters can infiltrate into a dolostone terrain, and travel extensive distances through the fracture system before attaining equilibrium. The rapid decline in the dissolution rate as the saturation index approaches -2 (Fig. 6), will slow down the rate of karst denudation on Grand Cayman Island.

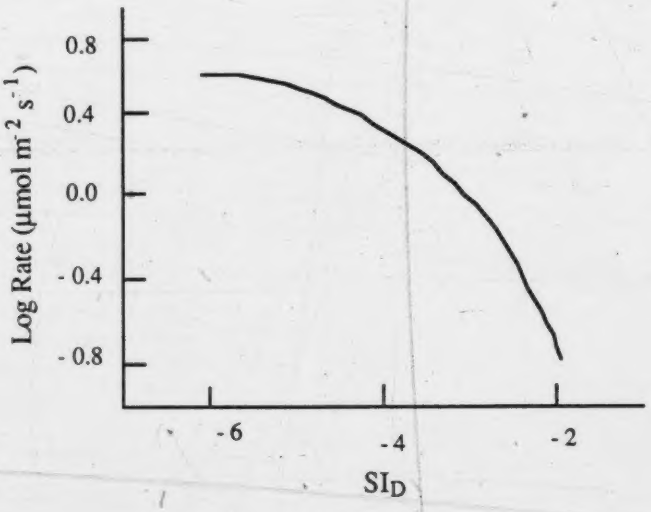

Figure 6. Dissolution rates of dolomite as a function of the saturation index (SI_D). After White (1984).

Second, it is unreasonable to assume that the composition of the groundwater remains constant. The small groundwater system on Grand Cayman Island is in a constant state of dynamic equilibrium with underlying marine waters, causing many of the groundwaters characteristics *eg*. ionic strength and PCO_2 ,to vary on a diurnal basis (Ng, 1985). Bögli (1964) in developing his theory of Mischungskorrosion, recognized the importance of the mixing of two dissimilar bodies of water. He demonstrated that when two bodies ~~of~~ water of dissimilar PCO_2 are mixed, the resulting fluid (Fig. 7) is commonly one which is undersaturated with respect to calcite (*i.e*. an "aggressive" water) .

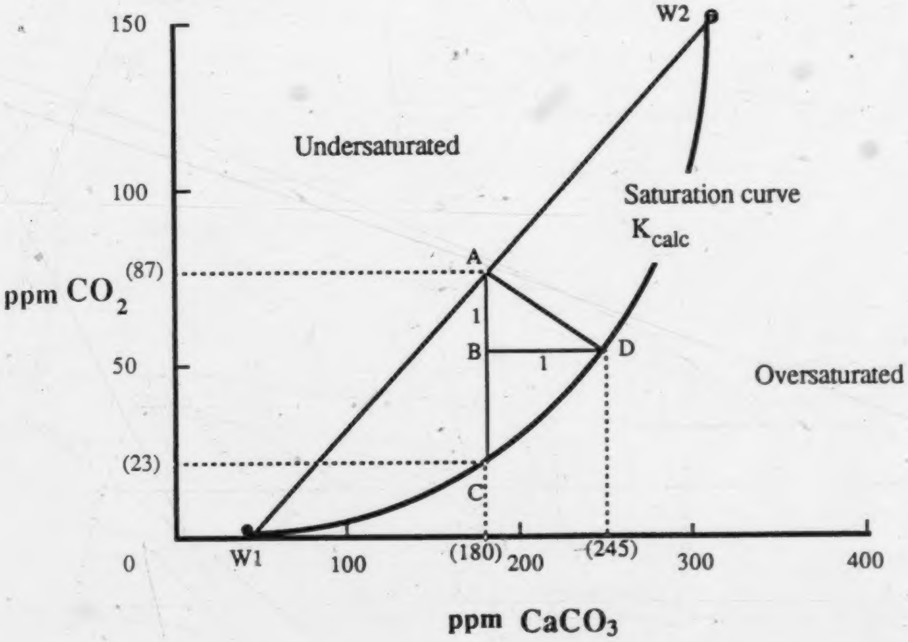

Figure 7. The theory of Mischungskorrosion: When two dissimilar bodies of water (W1, W2), saturated with respect to calcite are mixed to a ratio of 1:1, the resulting water (A) will be undersaturated with respect to calcite. Water 'A' requires only 23 ppm CO_2 at equilibrium, therefore, there is an excess CO_2 (A-C). The excess CO_2 will result in the additional dissolution of 65 ppm calcite. After Bögli (1980).

The theory of Mischungskorrosion can be expanded beyond simply CO_2 considerations, to include the effects of many independent variables. Runnels (1969), suggested that, "... the solubility of rock forming minerals is a non-linear function of such independent variables as salinity, partial pressure of gases, temperature..." Thus, the system "PCO_2 - $CaCO_3$" is only one in which the non-linear function of the solubility curve allows Mischungskorrosion to occur. An equally viable scenario for mixing corrosion results in the mixing of two bodies of water, where it is not the differing PCO_2, but the differing salinities which is the critical factor (Plummer, 1975).

The effect of mixing two bodies of water of differing salinities, is best illustrated if the groundwater composition is first reduced to a very simple chemical composition, H_2O - Ca^{2+} - CO_3^{2-}. If this groundwater were mixed with a fluid of similar composition, then the increased Ca^{2+} and CO_3^{2-} ion concentration product will drive reaction (1.0) toward the precipitation of calcite. If, on the other hand, an 'uncommon ion' is supplied as for example with the influx of sea water (Na^+, Cl^-), then the "Shielding Effect" (Picknett, 1977) will cause an increase in solubility, driving reaction (1.0) to dissolution. Shielding is the result of each ion attracting a cluster of opposingly charged ions. The resulting electrochemical shield is enough to prevent the Ca^{2+} and CO_3^{2-} ions coming together and forming the precipitate $CaCO_3$; the solution is effectively undersaturated. This apparent increase in the solubility is approximately proportional to the concentration of the electrolyte added (Krauskopf, 1967).

The molar concentration of ionic species, or the Ion Concentration Product (ICP), provides a good approximation of the solubility of the solution, but does not take into account the important effect of the charge of the ionic species in solution. The abundance of mutivalent ions in sea water can have a profound effect upon the dissolution and precipitation rates, the rate of change of mineral solubility being a function of the change in ionic strength (Plummer, 1975). This effect can be given a quantitative value by measuring the ionic strength of the solution, and the activity of a specific ion or ion pair.

The activity of an ion can be thought of as its *effective concentration* in solution. The activity of an ion is determined by the following relationship (Drever, 1982):

$$a_i = m_i \cdot \gamma_i \qquad (2.0)$$

Where: a_i = Activity of an ion

m_i = Molar concentration of an ion

γ_i = Activity coefficient of an ion

As the molar concentration of dissolved ionic species approaches zero, the activity coefficient will approach one. Consequently, in groundwater with a low molar concentration of dissolved ionic species, the apparent and actual concentration of ions is very similar. If, however, sea water is mixed with the groundwater, then γ_i will become less than one (Plummer, 1975). The effective concentration of Ca^{2+} and CO_3^{2-} is now reduced, leading to an apparent undersaturation (Fig. 8), and the dissolution of limestone.

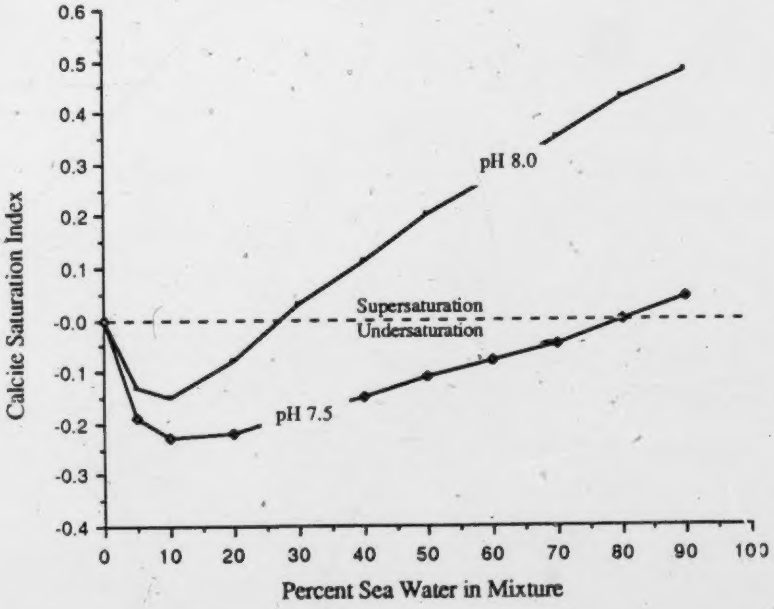

Figure 8. Changes in the saturation index of calcite as a function of varying pH and percent seawater, as demonstrated by the mixing of seawater with a carbonate grounwater. After Plummer (1975).

The degree of undersaturation can be very large, for example, at ionic strengths as low as 0.005 the effective concentration of $Ca^{2+}$and CO_3^{2-} is reduced to 74 % of their actual concentration (Krauskopf, 1967). The net result is the rapid dissolution of limestone in the 'mixing zone', which could greatly enhance the process of speleogenesis.

Plummer (1975) expanded these basic principles and concluded that the amount of undersaturation which occurs as a result of the mixing of seawater and carbonate groundwater, is a function of Pco_2, temperature, ionic strength, saturation index (Ω), and the pH of the end member solutions prior to mixing. Calculation based upon the mixing of both artificial and natural solutions from Florida and the Yucatan Peninsula, indicate that the mixing of high ionic strength, low PCO_2 saline waters with near saturated, low temperature, high Pco_2 carbonate groundwater, favours the formation of increased porosity and permeability. Succinctly, the mixing of marine and carbonate groundwaters will commonly lead to the formation of a geochemical environment which favours the formation of deep coastal phreatic caves.

Developing the speleogenetic model

The development of phreatic solution conduits on Grand Cayman Island, is probably the direct result of increased chemically aggressive water occurring at the interface between a fresh water lens and a relative highstand in saline water (Fig. 9). Fresh water migrates from the interior of the island to its margins, where it mixes with saline fluids creating an 'aggressive' zone of active dissolution in the phreatic regime. The presence of some of the phreatic conduits above the present day water table (*eg*. Pirate Caves), may be related to a similar situation recorded by Mylroie (1984) on the Bahamas. He documented the presence of many abandoned solution cavities exposed at approximately 6 m above present day sea level, and described these caves as, "... classic phreatic tubular conduits that exhibit later vadose incision features." The Bahaman examples contain relatively few collapse features, as do the Pirate Caves, and both contain well developed speleogens, including ceiling pockets.

Palmer (1986), noted the significance of the halocline, or the transition zone between the freshwater lens and the underlying sea water, as a mechanism for controlling the speleogenesis beneath Andros island. Palmer (1984) also suggested that this zone of aggressive water might be responsible for the predominance of fossil lens based caves, which, "...presumably represent Pleistocene eustatic still stands..." on the island of North Andros.

A similar scenario was probably responsible for the regional pattern of speleogenesis on the Cayman Islands. Mixing corrosion, which occurs at the base of a fresh water lens, in the transition zone between the marine phreatic and the meteoric phreatic zones, produced a series of lens base phreatic tubes (Fig. 9). In response to eustatic changes, vertical tectonic movement, or a combination of both, large scale movements of this transition zone occurred. In effect, as sea level rose so the lens base and the transition zone rose, and a new series of phreatic tubes developed stratigraphically higher in the formation, leaving the former cavities as deep coastal phreatic caves. Pirate Caves is one example of a phreatic system developed during a sea level 'high stand', producing caves which are now above the present day sea level. Finally, as the cycle completes itself, the sea level declines and phreatic cave systems are left 'perched' in the meteoric phreatic and the meteoric vadose zones. It is in these perched cave systems that the cyclical development of phreatic speleogens overprinted by vadose speleogens, and vice-versa, commonly occurs. In this manner, eustasy, and/or tectonic activity can be seen to control the regional pattern of speleogenesis on Grand Cayman Island.

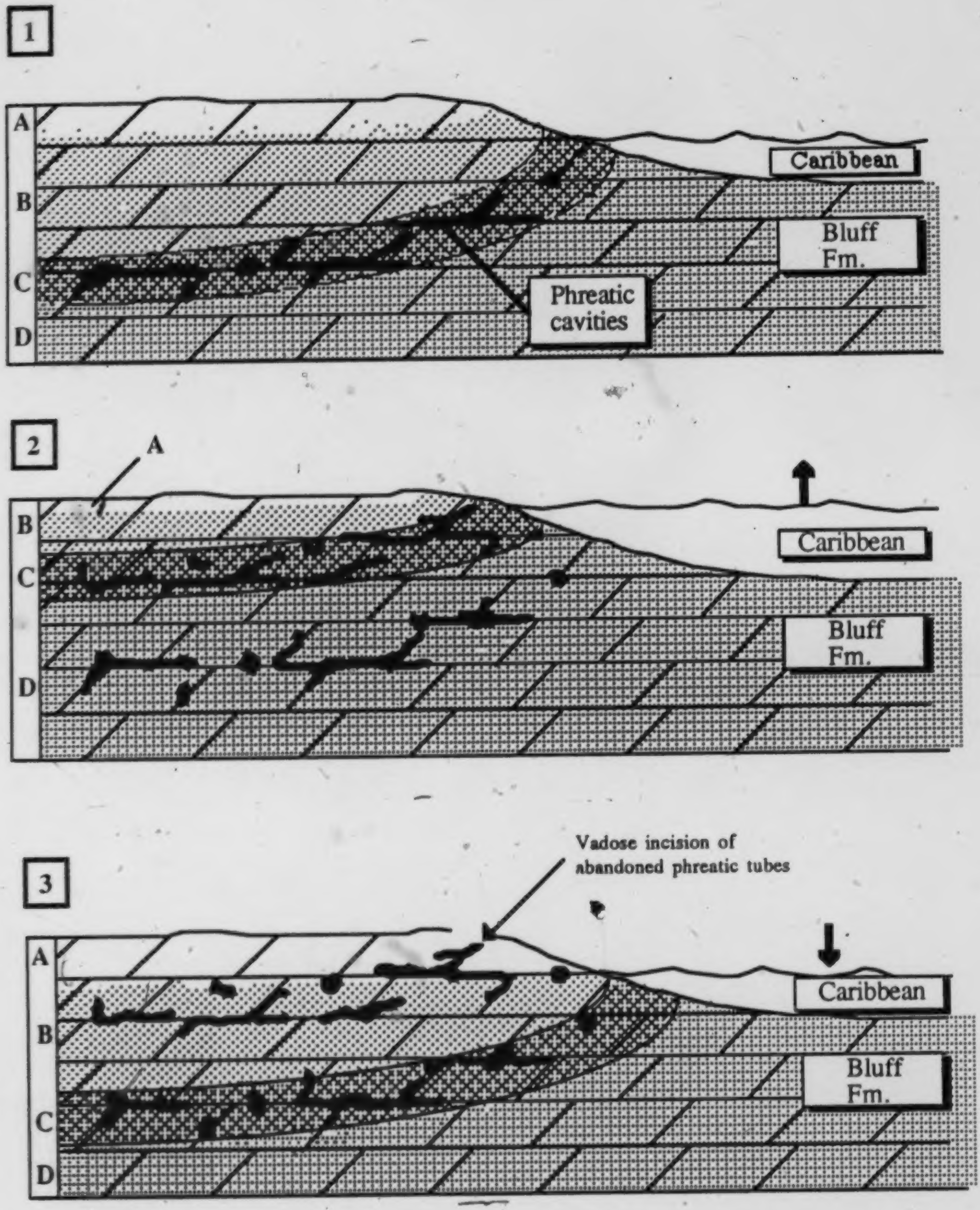
1
A
B
C
D
Caribbean
Bluff Fm.
Phreatic cavities
2
A
B
C
D
Caribbean
Bluff Fm.
Vadose incision of abandoned phreatic tubes
3
A
B
C
D
Caribbean
Bluff Fm.

Figure 9. Summary diagram to illustrate the regional speleogenetic controls on Grand Cayman Island. The three diagrams represent a chronological sequence, during which the Caribbean sea level rises (2), and then falls (3). Four hydrological zones are represented on each diagram, A = Meteoric vadose, B = Meteoric phreatic, C = Mixed water phreatic, and D = Marine phreatic.

E. DISCUSSION

The model proposed for the regional speleogenetic control on Grand Cayman Island appears to correlate well with the observed cave localities. Locally, however, there appear to be more subtle controls acting upon speleogenesis and in particular on the formation of speleothems. The abundance of speleothems in the Old Man Bay Village Caves, and the paucity of speleothems in the Pirate Caves, raises the question of (1) what is the source of the calcite saturated fluid which precipitated the speleothems at the Old Man Bay Village Caves, and secondly, why do the Pirate Caves not posses the same density of speleothems. It is possible that a local lithological control may be superimposed upon the larger regional model for speleogenesis.

Source of the $CaCO_3$: There are a number of equally viable possibilities to account for the presence of the oversaturated groundwater in the Old Man Bay Village Caves. A lack of evidence from the presently inactive cave system does not permit any individual cause to be singled out, the possibilities are nevertheless explored.

In the Old Man Bay Cave system, most of the easily accessible caverns with a dense speleothem growth, are no more than 5 m below the present surface. Consequently, all of the necessary Ca^{2+} and CO_3^{2-} ions, have to come from the dissolution of no more than 5 m of overlying dolostone.

To calculate the density of speleothems, and relate this to the amount of dolostone dissolution and its potential for providing the necessary $Ca^{2+}$and CO_3^{2-} is not a realistic proposition. Such a calculation could easily be an order of magnitude in error, and would serve only to confuse rather than clarify. If there is any uncertainty as to the ability of the present overlying dolostone to create the necessary oversaturated fluid, then it is feasible to suggest that the thickness of the Bluff Formation above the caves, was greater at the time of speleothem deposition. This is quite possible, since from the time of emergence (middle Miocene), an indeterminate amount of the Bluff Formation will have been removed through erosion.

There is an alternative scenario which involves the Pleistocene Ironshore Formation. This formation, which unconformably overlies the Bluff Formation (Fig. 3), is essentially a limestone containing much unstable biogenic $CaCO_3$, which could have acted as a 'source rock' for the necessary Ca^{2+} and CO_3^{2-} ions. It is quite possible that Pleistocene sea level fluctuations were such that the Ironshore Formation was deposited above the Old Man Bay Village Caves. In this situation, percolating meteoric waters would first have to pass through the Ironshore Formation, where much of the metastable aragonite and high magnesium calcite would be placed into solution. This fluid, which rapidly became oversaturated with respect to calcite, then precipitated the speleothems in the cave system already developed below.

Unfortunately, neither the increased thickness of the Bluff Formation, nor the presence of the overlying Ironshore Formation, could be expected to be locality specific. Therefore, a further explanation for the dichotomy observed between the Old Man Bay Village Caves and the Pirate Caves is sought. Perhaps the regional speleogenetic control of sea level fluctuation, has created the dissimilarities between the two cave systems. The evidence in the Pirate Caves is quite clear, in that a phreatic phase of dissolution, followed a period of speleothem precipitation in the vadose zone. This phase of dissolution, the result of a rise in sea level, may have removed all of the vertical and many of the horizontal speleothems in the Pirate Caves. If this later phase of dissolution did not extend to the Old Man Bay Village Caves, which are at a higher elevation, then it is conceivable that the Pirate Caves may at one time have been very similar to the Old Man Bay Village Caves.

VI. PETROGRAPHY OF CAYMANIAN SPELEOTHEMS

A. INTRODUCTION

The speleothemic calcite of Grand Cayman Island includes a complex array of megascopic and microscopic morphologies (Plates 5 and 6), the result of an equally complex interaction between physical, chemical and biological factors. Accordingly, the petrography of the Caymanian speleothems is approached from two viewpoints, (1) speleothemic features which are of an abiogenic origin, and which have been controlled by physical and chemical parameters, and (2) speleothemic features which are related in some manner to biogenic processes.

The precipitation of calcite speleothems is typically regarded as an abiogenic process, involving cave waters oversaturated with respect to calcite (Moore, 1962; Thrailkill, 1976; Kendall and Broughton, 1978). Variation in the morphology of constituent calcite crystals, is commonly attributed solely to the fluctuation of chemical and physical parameters (Katz, 1973; Folk, 1974; Lahann, 1978; Dreybrodt, 1979; Mucci and Morse, 1983; Given and Wilkinson, 1985). However, the presence of algae, fungi and bacteria in many caves, indicates that the speleologic environment is not abiogenic (Claus, 1955; Caumartin, 1963; Mason-Williams, 1969; Lefeure and Laporte, 1969; Cox, 1977; Draganov, 1977). The role that such microorganisms might play in determining the crystalline structure of speleothems, has been highlighted by recent studies which demonstrate the role that bacteria play in the formation of travertines (Chafetz and Meredith, 1983; Chafetz and Folk, 1984; Folk *et al.*, 1985; Chafetz, 1986). Similarly, Jones and Motyka (1987) have demonstrated how the distinct morphology and composition of some Caymanian stalactites may be attributed to the presence of algae and bacteria.

B. NOMENCLATURE

Calcite crystals, as seen in petrographic thin section, are commonly described as being bladed, acicular, columnar, palisade, needles and fibrous (Folk, 1965; Friedman, 1965; Kendall and Broughton, 1978; Braithwaite, 1979). Unfortunately, these terms have commonly been used synonymously, and without reference to any specific dimensions.

Some of the crystallographic and morphologic descriptions applied to calcite crystals have been sufficiently well defined such that reference to the original description provides ample morphologic and crystallographic information. For example, with careful petrography, 'fasicular-optic' (Kendall, 1977), 'radial-fibrous' and 'radiaxial-fibrous' (Bathurst, 1959, 1975; Kendall and Tucker, 1973) should be readily identifiable. These terms, however, apply to crystals with very distinct crystallographic features. Commonly, a crystal will not fit into such a 'pigeon hole' classification, at which point a more fundamental building block of description is required.

Friedman (1965) suggested that the description of the single crystal should be based upon terminology founded in igneous petrology. Crystallization textures are assigned the familiar terms of anhedral, subhedral and euhedral. While this classification is useful, it commonly requires further enhancement to fully convey an image of the crystal being described.

Folk (1965), established a four fold classification based upon the crystals origin, shape, size and foundation. He stated that "...seen in thin section there are two endpoints; either the calcite is equidimensional or it is fibrous." An intermediate group he named bladed "...for lack of a better word." To delineate these three end members he assigned each a specific length:width ratio (Table 1).

Kendall and Broughton (1978) established a rigid set of criteria for the terms columnar and acicular. They defined columnar crystals as being, "...elongate but wider than 10 μm...", and acicular as "...(markedly elongate and pointed) crystals that are less than 10 μm wide." (Table 1). Their use of the term columnar to describe crystals observed

NAME	DIMENSIONS	AUTHOR(S)	DESCRIPTION	DIAGRAM
EQUANT	Length:Width ratio ≤ 1.5:1	Folk (1965)	Equidimensional crystals, as seen in thin section	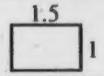
FIBROUS	Length:Width ratio ≥ 6:1	Folk (1965)	Fibrous crystals, as seen in thin section	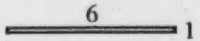
BLADED	Length:Width ratio between both the above	Folk (1965)	Bladed crystals, as seen in thin section	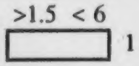
ACICULAR	Width < 10 microns	Kendall and Broughton (1978)	Markedly elongate crystals, that are < 10 microns wide, and pointed. No conception of packing is involved in this term.	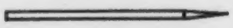
FIBROUS	(Fabric)	Kendall and Broughton (1978)	Closely packed acicular.	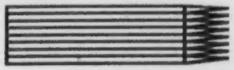
SPHERULITIC	(Fabric)	Kendall and Broughton (1978)	Radiating, closely packed acicular.	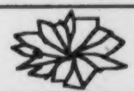
COLUMNAR	Width > 10 microns	Kendall and Broughton (1978)	Elongate crystals that are wider than 10 microns. The termination of the crystal is not implicit in the description.	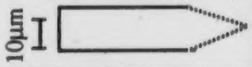
PALISADE	(Fabric)	Kendall and Broughton (1978)	A fabric composed of closely packed columnar crystals, the result of lateral coalescence of crystallites ?	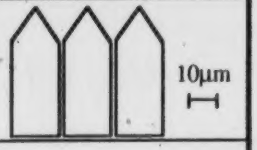
PRISMATIC	Not defined	Braithwaite (1979)	Example used has dimensions of 1000 microns by 100-200 microns, this is not part of a formal description however.	

Table 1: Summary of commonly used descriptive terms for calcite crystal morphologies and associated fabrics.

in two dimensions is somewhat misleading, as three dimensions are implicit in the term. Consequently, observation of these crystals on the SEM can lead to some misunderstanding.

Kendall and Broughton (1978) separated the terms fibrous, spherulitic and palisade from the unit crystal descriptions, suggesting that they be used only as fabric descriptions. Their use of the term fabric, to describe the mutual relationships which exists between more than one crystal, is consistent with that of Friedman (1965), who referred to these as *crystallization fabrics*. The terms fibrous, spherulitic and palisade should **always** be employed as fabric descriptions, where (1) fibrous describes closely packed acicular crystals, (2) spherulitic describes radiating closely packed acicular crystals (if the crystals in the spherule are > 10 µm wide, the fabric is termed radiating columnar), and (3) palisade describes a group of closely spaced, elongate crystals > 10 µm wide, that are aligned parallel to each other.

Descriptions of the unit crystal morphology, are commonly based on the appearance of the crystal in cross polarized light. For example, planar faces, crystal width and crystal terminations are all more readily identifiable in this way. This method, however, relies on the assumption that each distinct zone of extinction represents a unit crystal. This assumption is commonly invalid, for in many crystals the presence of unusual or uniform extinction patterns is due to the presence of subcrystals which result from crystal subdivision.

In relation to speleothemic calcite, a subcrystal can be created by (1) the emplacement of a lattice discordance in the growing crystal, or (2) through the deposition of material on the growing crystal surface, such that growth of discrete crystallite faces occurs. Following Kendall and Broughton (1978), the term subcrystal is employed for the former, while the latter is described as a syntaxial overgrowth crystallite.

In addition to the more commonly observed crystal habits, calcite crystals in the Caymanian speleothems also displayed either a trigonal or an asymmetrical morphology.

Trigonal calcite crystals have previously been documented from (1) fresh water lacustrine environments (Binkley *et al.*, 1980), (2) spelean environments (Kendall and Broughton, 1978), (3) surface springs (Braithwaite, 19798; Schreiber *et al.*, 1981), (4) pedologic zones (Chafetz *et al.*, 1985), and (5) shallow marine environments (Given and Wilkinson, 1984). Asymmetrical crystal morphology has not received a great deal of attention, although Kendall (1985) has briefly discussed their genesis.

C. ABIOGENIC CALCITE

Inclusion Patterns and Growth Banding

A very common feature throughout the speleothems of Grand Cayman Island, are bands of inclusion and organic rich calcite (Plate 7C, D, E, F, G). These distinct bands of calcite range from 150 μm wide (Plate 7D) to 5 μm wide (Plate 7 G, H). Characteristically, they will define former crystal faces, presenting a lasting record of how the morphology of the crystal has changed over time (Plate 8C). In view of this, the inclusion patterns are commonly referred to as growth banding.

To simplify the description of the Caymanian growth bands, the classification system defined by Kendall and Broughton (1978) is used. This classification system (Table 2) defines six types of growth banding (Type VI is omitted from the table, being inclusion free calcite), based upon whether or not (1) the growth band defines a former crystal face, and (2) the individual inclusions can be resolved with the petrographic microscope.

Sample 728c displays a series of growth bands (Plate 7C) developed in small crystallites which have coalesced to form a large (2 mm) crystal (Plate 7C). Close examination of the growth bands (Plate 7E), shows that most of the constituent inclusions are too small to be resolved. According to Kendall and Broughton (1978), this type of growth banding is described as being a "type II".

	INCLUSION PATTERN	SHAPE	COMPOSITION
I	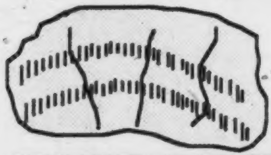	Smooth Rings	Linear inclusions
II	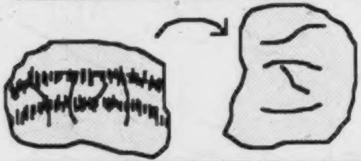	Smooth Rings	Pseudopleochroic calcite
III	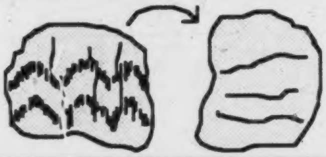	Defines former calcite crystal faces	Pseudopleochroic calcite
IV	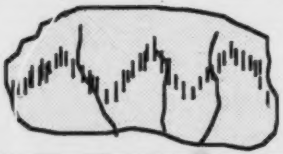	Defines former calcite crystal faces	Linear inclusions
V	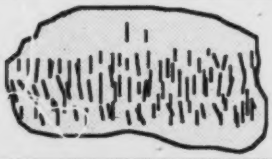	Thich, inclusion rich growth layers	

Table 2. Growth bands (types I to V) as classified by Kendall and Broughton (1978), can be recognized by their overall shape and the nature of the constituent inclusions

Sample EEQ 726, a stalactite, shows an unusual pattern of type II growth bands (Plate 9B) in which the growth of sucessive layers of calcite appear to form in different orientations. This distinctive fabric is probably the result of varying fluid flow rates over the exterior of the stalactite. These growth bands have a pseudo-pleochroic colour scheme, varying from brown to light brown, depending on the orientation of the thin section. This pseudo-pleochroic nature may be due to the wide separation of the two refractive indices in the constituent calcite.

The morphology of growth banding does not always remain constant throughout a single growth phase. Transitions from rhombohedral to rounded (Plate 8C), and flat to rhombohedral (Plate 9C) growth bands are common. The flat growth bands, which develop at right angles to the crystal c-axis, contain inclusion which can be resolved. Although not strictly a type IV growth band, it is a modification of this form, herein termed a "linear type 4 growth band".

In sample EEQ 728c there is the type V growth band, which is in effect a broad zone of inclusion rich calcite. This zone of type V inclusion rich calcite (approximately 1mm wide), is juxtaposed with a zone of type VI inclusion free calcite. The transition from inclusion poor to inclusion rich can be very abrupt. Inclusion rich calcite may follow a crystal growth disconformity (Plate 7A), or it may succeed well developed, inclusion free palisade calcite (Plate 7B).

Inclusions: The constituent elements of a growth band are the inclusions in the calcite. Individual inclusions can be resolved in type I, IV and V growth bands with the petrographic microscope. In the Caymanian speleothems these inclusions are commonly inclined at a slight angle to the former crystal faces which are defined by type III growth bands (Plate 7G, H). The orientation of these inclusions appears to be parallel to the principal growth direction (c-axis) of the host crystal. Examination of the inclusions on the SEM, shows that many of the inclusions are needle or spindle-like in shape (Plate 8D), approximately 50 µm long and 5 µm to 10 µm wide. Many have a distinctive elliptical opening about half way along their length (Plate 8D).

SEM examination shows that the lack of inclusions observed in type II and type 3 growth bands, is not a question of being able to resolve these features. A considerable amount of growth banding is the result of detrital organics and sub-micron sized calcite crystals being deposited upon crystallographic faces (Plate 8F, G). Commonly, etching in dilute HCl prior to SEM examination removes the organic material and many of the growth bands then appear as voids defining former crystal faces (Plate 8H).

Interpretation: Growth of a crystal begins with the 'seeding' of numerous small overgrowth crystallites. Since each crystallite posses the same parent crystal, each of them will possess near identical lattice continuity. This crystallographic similarity, enables each of them to laterally coalesce with its neighbour as growth proceeds. Intercrystalline void space, present at the initial seeding, may be totally removed by coalescence resulting in inclusion free calcite. Alternatively, if lateral coalescence is less than complete, then as the growth front advances beyond them, fluid or organic impurities present at the time may become trapped between the crystallites, resulting in an inclusion rich calcite. The elliptical openings that occur in many of these inclusions, may represent (1) a fluid escape structure, either liquid or gaseous, or (2) an inclusion bifurcation followed by a re-coalescence, and continued growth as a single inclusion. Conclusive evidence for either is not apparent. Although rare inclusions do bifurcate in the direction of growth, the angle of divergence is approximately 30°, and there does not appear to be any sign of re-coalescence.

Asymmetrical Crystals

Examination of speleothemic calcite from Cayman Brac (sample 1252), shows an unusual growth form that is characterized by a mottled or patchy extinction pattern (Plate 10E). Closer scrutiny of the crystals (Plate 10F) shows the presence of sheaths of columnar calcite with distinct curved crystal boundaries. The degree of curvature is approximately

40° to 45° (Fig. 10). The mottled optical extinction, characteristic of this crystal form, may have resulted from crystal growth asymmetry. Initially, the c-axis of each crystal is orientated normal to the substrate (Fig. 10). As time progressed however, the principal axis of growth deviated from a normal orientation becoming farther inclined as growth proceeded

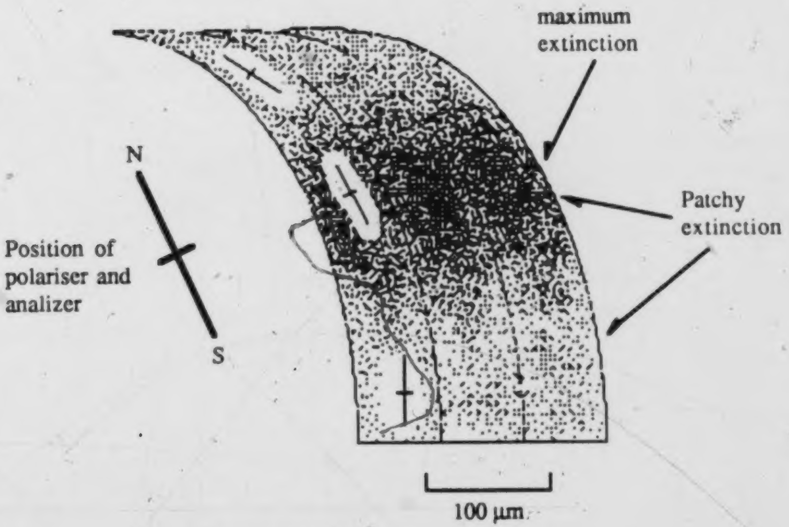

Figure 10. Growth asymmetry and the resulting curvature of the crystals leads to the development of a characteristic 'mottled' optical extinction pattern.

In order to explain the propagation and growth of these asymmetrical crystals, attention must be focussed upon small crystallites (Maleev, 1972; Kendall, 1985). As the crystallites grow up from the substrate, their direction of growth is partly controlled by the forces exerted by neighbouring crystallites. If there is a differential rate of growth across the growing surface, then some crystallites will overtake their slower neighbours. The crystal with the fastest rate of growth, will deflect laterally to partially occupy the free space generated above the slower crystallite (Fig. 11). If the crystallites further subdivide (Fig. 11), then those growing away from the slow rate of growth, will be truncated by their faster growing neighbours. This process naturally selects for those crystallites progressing towards the slow rate of growth, further promoting the overall asymmetry of the crystal as a whole (Kendall, 1985).

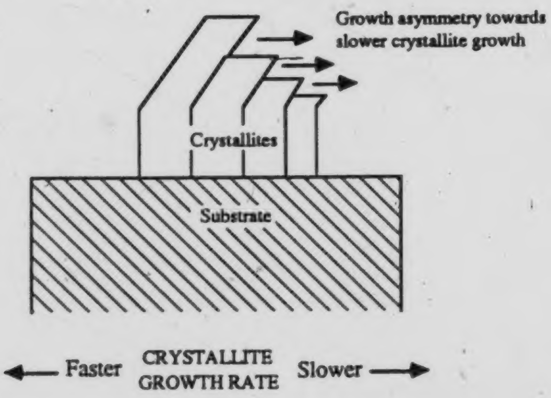

Figure 11. Differential rates of crystal growth can account for the marked asymmetry of the crystal morphology of the speleothemic calcite crystals. After Kendall (1985).

Crystal Junctions

When viewed with crossed nicols, a common feature of the coarse columnar calcite are the interpenetrant margins with digitate processes extending in the direction of growth (Plate 10G, H). This "ragged" intercrystalline boundary, can be explained in terms of variable crystallite c-axis orientations. Overgrowth crystallites will base their c-axis orientations upon either, (1) lattice information attained from the 'parent' or master crystal upon which they are seeded, or (2) their own inherent lattice information. If the surface upon which the crystallites are seeded is flat, then the preferred orientation of the crystallite optic axis will match that of the 'parent' crystal (Fig. 12). However, if the 'parent' crystal has a curved growth surface, then the preferred orientation of the crystallite optic axes will not match that of the 'parent' crystal (Fig. 12). To resolve this problem of incompatible lattice information, the crystallite will compromise its own c-axis orientation, with that of the 'parent' crystal. The result is the further subdivision of the crystallites, and the appearance of ragged, interpenetrant crystal margins (Plate 10G).

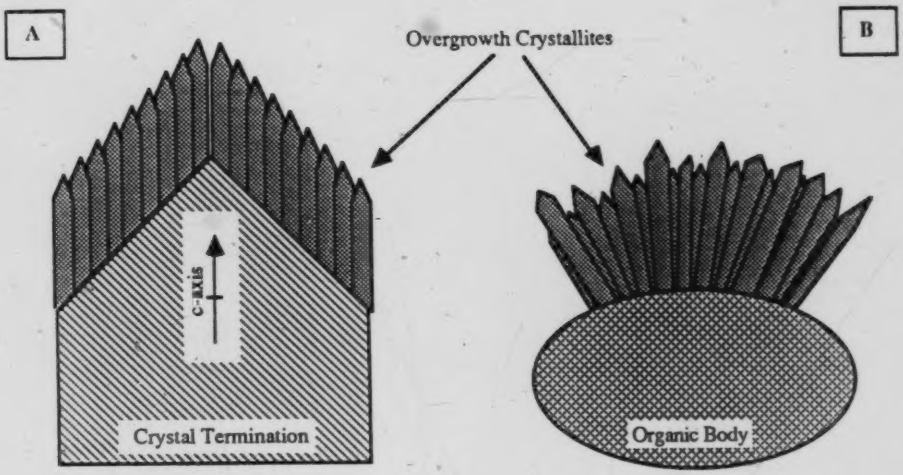

Figure 12. Orientation of the overgrowth crystallites is strongly dependant on the crystallographic lattice information derived from the 'parent' (or substrate). Overgrowth crystallites developed on a crystal termination (A) tend to parallel the parent c-axis, while overgrowth crystallites developed on an organic body (B) tend to grow normal to the substrate.

A detailed SEM examination of the relationship between the parent crystal and the crystallites, shows that if a crystallite is seeded upon a well defined crystallographic face (Plate 11B), the parent crystal lattice information is dominant. The crystallites do not grow normal to the growth surface as suggested by Broughton (1977), but instead show a strong tendency to parallel the growth of the parent c-axis. Any apparent divergence of the crystallites, is probably due to their distal expansion. By comparison, when crystallites are seeded upon an organic host (Plate 11B), or when a thin layer of organic material 'masks' the crystalline substrate, then the controls on growth morphology are quite different. In this situation, it is apparent that it is the inherent lattice information of the crystallite and the irregular surface topography, which control the overall growth morphology. The inorganic substrate can assert no direct crystallographic control by itself, and the crystallites will not be in optical continuity with the substrate. Even when seeded upon an apparently flat parent crystal, some crystallites may not coalesce completely, and an homogeneous extinction pattern will not develop. This failure of the crystallites to fully coalesce is demonstrated in sample EEQ 728 (728.4) (Plate 11B). The lower zone of laterally coalesced 'supercrystals' (Braithwaite, 1979) contrasts sharply with the upper fibrous growth morphology. The upper zone appears to be where the coalescence of the crystallites has been incomplete. This change in morphology is also apparent in plane polarized light, the boundary between the two zones being marked by the change from inclusion rich to inclusion poor calcite (Plate 11F)

A possible interpretation for this change in morphology, is based upon the presence of length slow calcite crystallites at the junction between the two zones. Length slow crystallites growing upon the disconformity surface can be recognized by their contrasting relief and highly inclined extinction angles. Moore and Nicholas (1964) and Folk and Assereto (1976) interpreted similar occurrences of length slow calcite as being due to a pause in crystallization that may have been a period of 'drying out' or even a phase of dissolution. Regardless of the cause, any crystallites subsequently seeded upon this zone of assorted length fast and length slow crystals, will be presented with highly variable lattice information from the substrate. Consequently, the degree of c-axis misalignment, inherent from the substrate, would not allow the crystallites to coalesce completely. The result is a distinctly fibrous habit, defined not by the usual presence of inclusions, but by variation in crystallite extinction patterns. The absence of inclusions in the upper zone suggests a lack of impurities in the medium at the time of precipitation which permits the crystallites to grow in close proximity to each other.

Trigonal Crystals

The trigonal prismatic crystals in the Caymanian flowstone (samples EEQ 726, EEQ 728, and CIQ 1252), which range in size from 50 to 300 μm in maximum dimension, have distinctive growth bands which can be traced laterally between individual crystals (Plate 11

C, D). Smaller trigonal crystals, 50 µm in maximum dimension, are commonly interpenetrant with the larger crystals, apparently truncating the growth bands of the larger crystal. When viewed with crossed nicols, each of the trigonal crystals is defined by an individual optical extinction pattern (Plate 11D). This indicates that each crystallite has its own unique lattice orientation, the smaller crystallites probably being seeded on the surface of the presently expanding larger crystal. A scanning electron micrograph of a similar area of well developed trigonal crystals (Plate 11F), details the manner in which this unusual crystal growth progresses. Once growth of a 'host' trigonal prism is established, then smaller 'parasitic' crystallites may seed onto the side of the first formed crystal (Fig. 13). The boundary between the first crystal and the parasitic crystallite, does not represent a truncation of the growth bands, but a compromise boundary developed as the two crystals grow coevally (Plate 11G). The 'parasitic' crystallite and the 'host' crystal posses differing morphologies. The latter appears to grow from a central location at a constant rate of growth. The former, however, cannot grow at a constant rate on all crystallographic faces, for it abuts against the host crystal. Consequently its morphology reflects an uneven rate of growth away from the point of initial nucleation (Fig. 13). The marked contrast between the two dimensional c-axis view, and a three dimensional view orientated at a high angle to the principal axis, highlights the problem of employing two dimensional morphological terms, to crystals which clearly have a third dimension. At such an oblique angle, the third dimension of the crystallite is now apparent, each forming a trigonal prismatic column (Fig. 13) with a rhombohedral termination. Composite trigonal crystals formed of rising columns of crystallites which taper to a pointed termination occur in the Caymanian samples (Plates 7H and 8A), and appear outwardly very similar to those described by Chafetz and Butler (1983). Examination of a polished and etched slab (1 to 1.5 mins in dilute HCL), shows a number of diagnostic 'etch-figures', or small (< 5 µm) dissolution 'pits' which reflect the internal crystallographic structure (Hohness, 1918; Grigor'ev, 1969). A section cut perpendicular to the c-axis of the crystallites shows a zone of prominent dissolution at the juncture between two crystallites (Plate 12C). A more detailed view of this structure (Plate 12C) shows that dissolution occurs both at the crystal juncture and at 90° to this line, producing a 'carina' structure (Grigor'ev, 1969). The dissolution which produces the carina is expressed as a line of individual solution pits (Plate 12D). Each solution pit is where kinetic and thermodynamic constraints, combine to produce a zone of maximum reactivity. This might be the result of crystal imperfection, the adsorption of impurity ions, or as demonstrated here, the presence of a well defined basal cleavage.

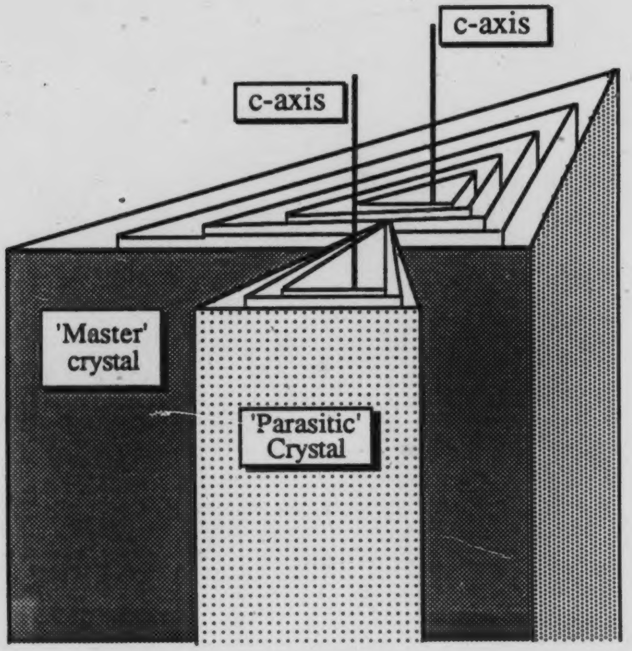

Figure 13. Trigonal crystal development is commonly accompanied by the growth of 'parasitic' crystals, which are seeded on the side of a 'master' or 'host' crystal. Due to the physical confinement of the 'master' crystal, the 'parasitic' crystal tends to grow asymmetricaly away from the 'master' crystal.

The overall trigonal morphology of the crystallites will lead to the creation of distinctly shaped intercrystallite void space, which could be described as an etch figure.

Viewed perpendicular to the c-axis, crystallites which are closely spaced will present intercrystallite void space with a corresponding trigonal morphology (Plate 12E, G). As the 'angle of cut' becomes more oblique to the c-axis, so the pore space will become more elongate (Plate 12H), eventually forming near linear inclusions commonly filled with organic detritus.

One example of a possible screw dislocation was observed in the Cayman samples (Plate 12B). This crystal, approximately 15 μm across is viewed looking down the c-axis, and shows a marked trilete form with a well developed centrally located pit. This figure is similar to those shown in Folk *et al.* (1985, Fig. 10.B, p.365) which propose to show the termination of screw dislocations.

B. INTERNAL SEDIMENT

In addition to the thin (<10 μm) coatings of organic material commonly developed on crystallographic faces, considerable accumulations of similar material form layers of 'internal sediment' up to 1 cm in thickness (Plate 5). Commonly, these layers are 1 mm to 2 mm in thickness, and may be either (1) laminated, with zones of 'chaotic' organic rich calcite (Plate 9E), or (2) homogeneous, opaque zones with no calcite present (Plate 9F).

The relationship of the sediment to the substrate varies between samples. The sediment may occur as (1) layers of uniform thickness, covering a considerable lateral extent (2-3 cm), and showing signs of erosion of the substrate (Plate 9E, F), (2) layers of variable thickness, being 'draped' over crystal terminations (Plate 9G), or (3) isolated pockets of organic material developed between crystal terminations (Plate 9H). SEM examination provides a detailed view of the way in which organic material collects in the intercrystalline spaces (Plate 10C, D).

The internal sediment exerts both a destructive and a constructive influence upon the speleothemic calcite.

Destructive Influences: The substrate below the thick accumulations of sediment commonly exhibit blunt or square terminated crystals that may represent a physically abraded, or scoured surface. The removal of the former crystal terminations, was by the influx of a physically abrasive and/or chemically aggressive fluid, which 'planed off' existing crystal terminations.

There is, however, an alternative explanation for the presence of square terminated crystals. Similar structures have been interpreted by Folk and Assereto (1976), Assereto and Folk (1980) and Mazzullo (1980) as relic structures after aragonite. In describing 'paleo-aragonite crusts', Assereto and Folk (1980, p. 384) stated that, "...they are characterized by crystals of uneven length with square ends...and are now a mosaic of equant 0.01-0.1 mm sparry calcite". On first appearances, a comparison of crystals described in this study (Plate 9E, F, G) with those described by Assereto and Folk (1980, Figs. 13a, 14c) show remarkable similarities. The crystals in the Caymanian samples posses ragged, bluntly terminated growth forms of uneven length. The crystals have a bladed habit, averaging 40 to 50 µm in width, and at maximum 300 µm in length. Despite the outwardly similar morphologies, there is a distinct lack of corroborating evidence to suggest that the Cayman examples possessed an aragonite precursor. There was no evidence from the X-ray diffraction studies, to suggest that aragonite was present in any of the speleothems. Even if former aragonite had been completely replaced by calcite, some aragonite relic structures might be expected. However, there were (1) no linear aragonite relics (Folk and Assereto, 1976, Figs. 8, 9 p.492-493), (2) no 'ghost fibre bundles' indicating the presence of former aragonite crystals (Mazzullo, 1980), and (3) no well developed aragonite needles, as seen in Assereto and Folk (1980, Fig. 14e, p.386). In view of this, the process of physical abrasion is considered most likely.

Constructive influences: Calcite crystals developed above a layer of internal sediment commonly display, (1) a length slow crystallographic habit, (2) a reduced crystal size (Plate 10B), and (3) a xenotopic crystallization fabric (Plate 9H). This is in contrast to the surrounding crystals, and indicates that the organic material exerts a distinct morphological control on calcite crystallization.

D. DISCUSSION OF ABIOGENIC DATA

Early work in the field of crystal morphology dates back to Bravais (1886), Friedel (1907), and Donnay and Harker (1937), who studied crystals from a geometrical viewpoint and provided the foundation on which more recent genetic morphological interpretations are based (Wells, 1948; Grigoriev, 1965; Koster, 1968; Dowty, 1976; Sunagawa, 1977,1981,1982; Rodriguez-Clemente, 1982). These studies proceeded on the premise that (1) varying crystal habits are the result of different combinations of crystal faces, (2) the external form (habit) or morphology, is controlled by the relative rate of growth of each of the crystallographic faces (Rodriguez-Clemente, 1982), and (3) faces with higher normal growth rates will eventually disappear, while those with lower growth rates expand at the expense of others (Sunagawa, 1982, Fig. 6, p.131).

The main controls which act upon crystal growth are (1) structure of the calcite crystal, and (2) the medium in which the crystals are precipitated.

Structure: This involves all aspects of the atomic lattice, and any defects that might be present. These are of great importance to the crystal growth rates and morphology, because the precipitation and dissolution of calcite is controlled by the attachment and detachment of ions at kinks in monomolecular steps (Fig. 14) on the crystalline surface (Berner and Morse, 1974). The existence of kinks depends upon the presence of a step. Possible sites for the formation of a new step, in order of importance are:

(1) at a pre-existing step, as for example in the form of a screw dislocation surface termination (Fig. 14) edges and corners are also sites where the probability of step propagation is very high.

(2) at crystal edge dislocations or point defects, although these are energetically less favourable.

(3) on perfectly flat, two dimensional crystal surface, although energetically this is the least favourable site for step propagation.

The prominent dissolution features seen in the etched speleothemic calcite (Plate 12B ,C, D) occur along crystal junctures, where edge dislocations or point defects are commonly found. These structural defects can result in preferred dissolution and the formation of the etch figures.

The screw dislocation (Fig. 14) commonly provides a preferred growth site, and will exert a strong morphological control upon the calcite crystal. Sunagawa (1982) stated that the morphology of the screw dislocation (growth spiral), would ultimately control the crystal habit, by determining the direction of preferred growth. However, despite their importance, screw dislocations in the Caymanian samples were rare, only one possible example being found (Plate 8B).

Medium: This involves all the physical and chemical characteristics of the solution from which the calcite is precipitated, including pH, ionic concentration, temperature and fluid dynamics. The importance of the 'medium', is highlighted by the work of Given and Wilkinson (1985), who on the basis of earlier research (Dormeus, 1958; Sippel and Glover, 1967; and Lahann 1978), challenged the long held belief that calcite morphology was controlled solely by the Ca:Mg ratio of the medium (Katz, 1973; Folk, 1974; Mucci and Morse, 1983). Given and Wilkinson (1985), suggested that calcite morphology was a kinetic or rate controlled phenomena. If Given and Wilkinson (1985) are correct in their assumptions, then both the saturation state of the medium and the fluid dynamics become important controlling factors in calcite morphology. Consequently, variations in crystal morphology (recorded as a succession of growth bands) can be related to changes in the 'medium'. Transitions from acute to rounded growth bands present in some of the Cayman samples (Plate 8C) record a change in the growth or dissolution rate of specific crystals. In extreme cases of undersaturation, the removal of material can create crystals which become flattened at right angles to their principal growth axis (Plate 9C). The transition from euhedral crystal terminations, to rounded terminations, and finally crystals terminated at 90° to the c-axis, can be explained in terms of a decrease in the saturation state, which leads to loss of material from areas of highest free energy *i.e.* junctions between crystal faces and apical terminations. This is in agreement with more theoretical studies (Burton and Cabrera, 1949; Cabrera and Burton, 1949; Frank, 1949), all of which suggest a similar process, whereby growth (or dissolution) rates at specific sites are dependant largely upon local 'free energy' considerations.

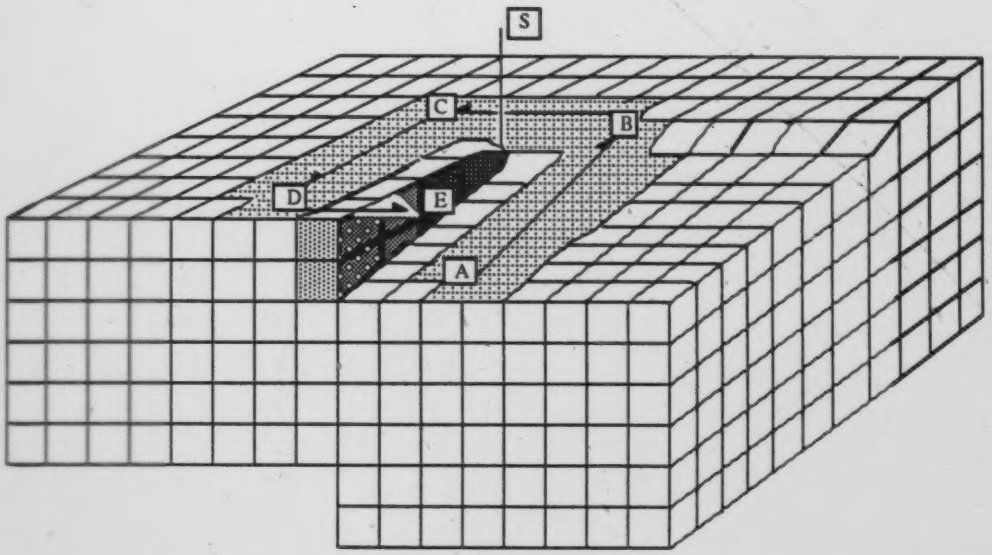

Figure 14. Schematic illustration of a screw dislocation (s). Growth upon the crystal face is achieved in a 'step like' manner, such that upward growth can be achieved by lateral growth around the screw dislocation. The path A through E defines the growth spiral, the distance between A and E, is the 'step'.

Besides controlling the overall crystal morphology the nature of the medium may also determine the presence of inclusions in the calcite. Sunagawa (1982) suggested that in natural fluid environments, fluctuations in the saturation state of calcite are common, and that this can lead to the phenomena of regrowth and dissolution cycles (Sunagawa, 1982;

Fig.4c, p.131). He stated that these cycles lead to, "...perturbed growth, during which interface morphology will be modified and inclusions will be captured." These cycles in the calcite saturation state could feasibly account for the repetition of growth bands, which clearly define the ontogenetic stages of the crystal.

Jannsen-Van Rasmalen (1977) suggested that under certain hydrodynamic conditions, inclusions are formed on the 'near' side of the crystal due to the turbulence of the medium. Interestingly, many of the rhombohedral terminations in the Caymanian examples have an asymmetrical pattern of inclusions (Plate 8 C). When one side of the crystal termination shows a more disseminated pattern of inclusion development, this has been interpreted (Jannsen-Van Rasmalen, 1977) as the result of uneven flow conditions around the crystal termination .

Where ponding of a saturated fluid occurred, free growth of crystals results in well formed rhombohedral and scalenohedral apices. If this saturated, quiescent environment is maintained, calcite crystals will grow to form large 'petal' or 'shrub' like aggregates. Ponding appears to have led to the features in sample EEQ 1219,where large (1 cm) shrubs (Plate 9D) display well defined scalenohedral terminations parallel to the c-axis (made apparent by abundant growth bands), and trigonal prisms perpendicular to the c-axis.

E. BIOGENIC ASSOCIATIONS

Throughout the study of the Caymanian speleothems, numerous enigmatic structures were found which are not immediately attributable to inorganic processes. The composition and morphology of these structures was such that two distinct groups were discernible, (1) subrounded agglomerates of organic material, and (2) rafted calcite bodies. Although it was rare to find both in close proximity, neither type of structure was exclusive to any one sample. The elongate bodies in particular were restricted to zones of dense occurrence,while the organic agglomerates were more widely distributed, it was rare to find both in close proximity.

Petrographic analysis of samples CIQ 1250, CIQ 1252, EEQ 728, EEQ 726, CIQ 1249, EEQ 1220 and CIQ 1253 show the presence of numerous brown, opaque to semi-opaque bodies. These agglomerates, 100 µm (Plate 13C) to 400 µm (Plate 13G) in diameter, are (1) solid, rounded to elliptical (Plate 13C, A), (2) solid, subrounded, with an irregular outline, (3) circular 'ring' structures (Plate 13B), (4) elliptical 'ring' structures (Plate 13E, F), and (5) incomplete, irregular structures (Plate 13 D, H). Their light brown colour in thin section is probably the result of finely disseminated organic material (Lighty, 1985), although Jones and Motyka (1987) have suggested that similar bodies appear opaque in thin section as a result of their Fe and Mn content. The assumptions of Jones and Motyka (1987), would only be correct if the Fe and Mn were in an oxidized form, a fact which has not been conclusively demonstrated. In the course of this study, selected samples of speleothemic calcite were prepared for Atomic Absorption Spectrophotometry (AAS). An insoluble residue which formed as part of this process indicates that these samples were carbon rich. It is therefore suggested that it is the carbon content which gives rise to the light brown colour.

The spatial distribution of all the organic agglomerates is such that they rarely occur in isolation, and are commonly associated with one or more of the differing morphological types. In particular, the small (100 µm) spherical bodies are commonly clustered together as an intercrystallite fill (Plate 13C), or as a dense accumulation (Plate 13B). The opaque, rounded bodies are commonly occur as "free floating" forms, encased in radial-columnar calcite, immediately succeeding crystal growth diconformity surfaces. Amorphous organic material, which commonly forms a distinct band at growth disconformities, may be related to the growth of the large ovate bodies (Plate 13A). Similarly, a large (400 µm) opaque body with an irregular outline, is developed in close association with a very dense zone of amorphous organic material (Plate 13G). The larger 200 µm to 400 µm ovate ring structures, are commonly developed above a dense accumulation of smaller organic bodies (Plate 13G).

The effect that these organic agglomerates have on calcite crystal morphology is profound. In general, the effect of the organic material was to disrupt any former crystal morphology. More specifically, as the surface morphology of the organic bodies is commonly rounded, columnar crystals developing on the substrate assume a divergent radiating pattern (Plate 13F, G)

In addition to the discrete organic bodies, amorphous organic material commonly coats crystal terminations (Plates 13A, 10A, B, C). This coating may be (1) of uniform thickness (approximately 50 µm) covering both the crystal apex and intercrystalline space alike (Plate 13A), or (2) preferentially developed at the apex of the crystal termination (Plate 14A, B). In some cases, the latter can be so pronounced as to produce a crystal termination with all the organic material accumulated at the apex (Plate 14 C). This is most unusual considering the effect that normal gravitational processes should have on the organic material i.e. filling the intercrystalline spaces first.

Calcite 'Rafts'

Petrographic analysis of samples EEQ 726, CIQ 1249 and EEQ 728 showed the presence of large accumulations of elongate bodies, which collectively form dense 'rafted' zones up to 3 cm in thickness (Plate 17D).

Individually, each elongate body is up to 200 µm wide, and up to 1 cm long. The length of each body is a highly variable parameter, dependant upon the 'cut' of the thin section and the orientation of the body itself. Closer observation shows three distinct morphological zones in each elongate body, (1) a central semi-opaque line, which is defined here as the 'core', (2) a zone of xenotopic microspar, commonly organic rich (Plate 14F), and (3) a zone of euhedral rhombic calcite, which may posses well defined organic rich growth bands (Plate 15A).

The core, although well defined at lower magnification, becomes increasingly obscure at higher magnifications. In many cases, there is nothing to suggest the nature of its origin besides a zone of xenotopic microspar. Scanning electron microscopy did, however, show the presence of a small microbial filament at the termination of an elongate body (Plate 14G). This filament, which was not calcified, was less than 4 µm wide, approximately 40 µm in length and showed no evidence of branching (Plate 14H). The surface morphology was irregular, with many randomly spaced surface protrusions approximately 1 µm in size. Surrounding the core is a zone of ill defined microspar which grades into larger (> 10 µm) spar calcite (Plate 14G). In this example the spar calcite does not posses any growth banding.

The spatial distribution of the elongate bodies is such that they rarely occur in with any of the previously described organic bodies. Only one example of organic agglomerates in close association with a filament was observed (Plate 14D).

Uncalcified and Calcified filaments

Two very distinct types of filament occur in samples CIQ 1249 and EEQ 726, (1) uncalcified, convolute branching forms (Plate 15 C, D), and (2) calcified, linear non-branching forms (Plate 16A, B).

The branching forms, attached to the surface of etched trigonal calcite crystals, appear to be colonial. The individual filaments, less than 10 µm in diameter, show an irregular branching pattern, complicated by the convolute nature of each filament (Plate 15D). The surface morphology of the filament consists of fairly regularly spaced (10 µm) collapsed 'ring structures' (Plate 15D).

The linear calcified forms (Plate 16A) are of a highly variable length, but rarely exceed 10 µm in diameter. These filaments commonly employ endolithic, epilithic and chasmolithic modes of life, hence measurement of filament length is highly subjective. Overall, the filament is isodiametric, although local protrusion of the calcite sheath (Plate 16 A) may obscure this fact.

Calcification of these filaments involves irregularly shaped crystals, ranging in size from submicron to 3 µm in length and width. Although not well developed, some of the crystals appear to be orientated with their long axes perpendicular to the filament (Plate 16

B). The degree of calcification appears to remain the same along the entire length of each filament and between each filament.

Microborings

Microborings less than 10 μm in diameter occur in some of the large speleothemic calcite crystals. The borings are straight or slightly sinuous, attaining lengths in excess of 200 μm (Plate 16C). In cross section, they vary from circular, through 'heart' shaped, to irregular (Plate 16D), all in close proximity to each other. A common association was the presence of microborings and small calcified spherules (Plate 16C).

Calcified Spherical Bodies

Spherical bodies, ranging in size from 5 μm to 20 μm were attached to the speleothemic calcite in clusters of between 5 and 10 individual spherules (Plate 15E, F). Each spherule is an agglomerate of near equidimensional, micron sized subhedral calcite crystals. Sections through these spherules (Plate 15E) shows a number of significant differences to those described in the literature, namely that there are, (1) no distinct nuclei of bacterial remains (Chafetz, 1986, Fig. 2F, p.814), and (2) no marked change in crystal size towards the core of the spherule (MacIntyre, 1985, Fig. 1B, p.109). These spherules are outwardly very similar to 'Type I bodies' described by Jones and Motyka (1987), who strongly suggested, "...that the opaque bodies (spherules) and rods in the Caymanian stalactites were of bacterial origin."

F. DISCUSSION OF BIOGENIC DATA

The precipitation and dissolution of calcite is not always the result of exclusively inorganic processes. There is a growing field of knowledge concerning the role that algae, fungi and bacteria play in carbonate diagenesis (Schroeder, 1972; Golubic, 1973; Schneider, 1977; Krumbein, 1979; Golubic *et al.*, 1981; Chafetz and Meredith, 1983; Danielle and Edington, 1983; Folk and Chafetz, 1983; Chafetz and Folk, 1984; Folk *et al.*, 1985; Chafetz, 1986). Of particular relevance to this study being the research concerning the microflora and fauna of the troglobitic (cave) environment (Claus, 1955; Caumartin, 1963; Lefeure and Laporte, 1969) and the controls they exert on carbonate diagenesis.

Microorganisms and their criteria for recognition

Many unusual structures in the Caymanian speleothems may be of algal, fungal or bacterial origin. However, before any such assertion is made, the inherent problems of algal, fungal and bacterial recognition are discussed.

Klappa (1979, Table 1) suggested that certain features, or a combination of morphological features, could be used to determine the affinity of filaments and borings. Although a viable approach, Klappa (1979) noted that there were numerous exceptions to the rule. Size is commonly used as a criterion for distinguishing between algae and fungi. Filaments and borings < 4 µm being assigned a fungal origin while those > 4 µm are regarded as being algal in origin. Again exceptions to this rule have been noted, with fungal filaments reported up to 10 µm in diameter (Klappa, 1979). In trying to separate algae from fungi, Edwards and Perkins (1974) suggested that 1-4 µm borings (filaments), should only be assigned a fungal affinity if sporangia and conidia are found with the filaments.

The supposed dependency of algae upon photosynthetic processes led Klappa (1979) to suggest that light conditions in the environment of deposition could be employed to distinguish algae and fungi. This assumption is incorrect, for many autotrophic algae are capable of sustaining life in low light conditions via the metabolism of organic substances (Nagy, 1965; Lefeure and Laporte, 1969; and James, 1972; Jones and Motyka, 1987). Evidence presented in this study is in agreement with these authors, showing the presence of bacterial and algal associated structures in the low light spelean environment.

The morphological characteristics of bacteria have received less attention than algae or fungi, although they are commonly accountable for many enigmatic 'organic structures' in carbonate rocks (Chafetz and Meredith, 1983; Chafetz and Folk, 1984; Folk *et al.*, 1985). Bacteria commonly occur as rods or chains of spherical bodies, usually less than 1 µm in diameter. Beyond these basic parameters, little is known of the morphology of bacteria in the geological environment.

Micro-organisms In Caymanian Speleothems

The confident identification of microorganisms in carbonate rocks is extremely difficult. This is particularly true in ..."the near surface environment and surface vadose environments which typically contain an abundant, and diverse array of micro-organisms.' (Jones, in press). Despite the limitations, the affinities of certain enigmatic structures in the Caymanian speleothems to specific microorganisms are suggested.

Organic agglomerates: The organic agglomerates found in the Caymanian speleothems are very similar to the 'bacterial' clumps' described by Folk and Chafetz (1980) and Chafetz and Folk (1984) from meteoric travertines. Chafetz and Folk (1984) and Chafetz (1986), liken these 'clumps' to the controversial 'marine peloid' (Macintyre, 1986). Chafetz (1986) cited the presence of a cloudy nucleus, similarity in size (20- 60 µm), a rim of clear euhedral crystals, the colour of the nucleus, and the presence of 'bacterial remains' in both the marine peloids and the travertine examples, as evidence for a similar genesis. The similarity in morphology and composition of the clumps (Chafetz, 1986) and the small organic agglomerates from the Caymanian speleothems (Plate 13C), leads to the conclusion that both have a similar genesis *i.e.* that the small organic agglomerates are of bacterial origin.

It is tempting to relate the larger ovate agglomerates and 'ring' structures to the calcified filaments of Schroeder (1972, Figs. 2, 3, 12). These structures bear many resemblances to the Caymanian examples, except in size. Schroeder (1972) quoted a variable diameter range of 15 µm to 300 µm, where the central core of each filament did not exceed 20 µm. Unlike the examples of Schroeder (1972), the Caymanian examples attain diameters up to 300 µm in the central core alone (Plate 13E, F). Based upon the size of the core, these structures are not of either algal or fungal affinity. Moss tufa, described by Irion and Müller (1968), provides a possible explanation for these large agglomerates. A transverse section of a moss stalk (Irion and Müller, 1968 Fig. 10, p.165 and Fig. 12, p.167) bears striking resemblance to the Caymanian examples (Plate 13 A, G) and (Plate 13 F), suggesting that these larger Caymanian organic bodies are of similar origin . The density of biogenic structures in the moss tufa is, however, far greater than that found in the speleothemic calcite. It is therefore unlikely that the Caymanian example represent a 'moss tufa. If indeed the large agglomerates are moss stalks, then they may represent isolated examples derived from a nearby source.

Calcite rafts: The calcite rafts represent a 'middle ground' between abiogenic and biogenic structures. The encrusting calcite crystals of these rafts represent the abiogenic aspects, their presence being controlled by physiochemical parameter in a manner similar to that described by Klappa (1979, Fig. 4, p.965). The initial site of nucleation, the central core (Plate 14F), is probably composed of organics or organic rich calcite, and in certain examples hosts algae (Plate 14 G, H). The core, therefore, represents the biogenic aspects of these rafts.

Based on the diameter and lack of branching, the uncalcified filament found in close association with an elongate bodies (Plate 14G, H), is probably of blue-green algal affinity. This algal filament may act as a centre for calcite nucleation, where nucleation is both a physical response to the stable substrate, and a chemical response to the suppressed calcite saturation index of the microenvironment surrounding the filament (Berner, 1971; Chafetz, 1986 p.814). The resulting calcified algal filament, when viewed as a longitudinal section (Schroeder, 1972, Fig. 12, p.22; Klappa, 1979, Fig. 4, p.965) is similar to the elongate bodies in the speleothems (Plates 14E, F and 11A). There is, however, a lack of filaments seen in cross section to support this suggestion. It is most unlikely that an accumulation of algal filaments should always produce longitudinal sections (Plate 14E). Therefore, it is suggested that these features represent sections through plate-like bodies, as opposed to rods.

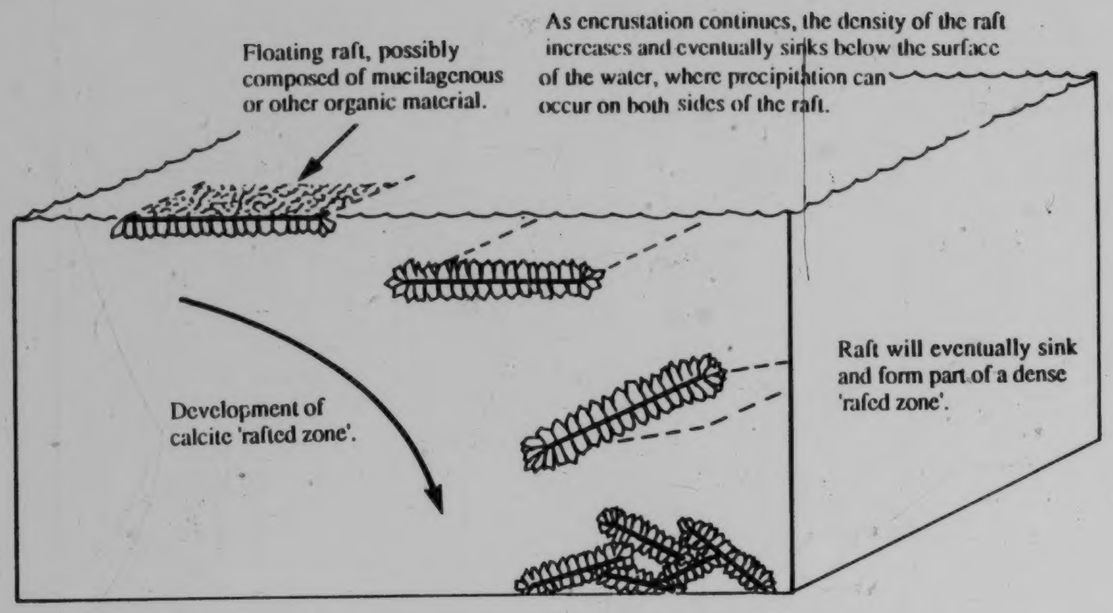
Floating raft, possibly composed of mucilagenous or other organic material.
As encrustation continues, the density of the raft increases and eventually sinks below the surface of the water, where precipitation can occur on both sides of the raft.
Development of calcite 'rafted zone'.
Raft will eventually sink and form part of a dense 'rafed zone'.

Figure 15. Suggested origin for the calcite rafts, involving a mucilagenous organic mat on which calcite crystals are precipitated. As precipitation continues the raft will loose its bouyancy and sink below the surface, where calcite encustation can occur on both sides of the raft. Eventually, the raft will sink to the bottom of the reservoir where it forms part of a dense rafted zone.

Gines *et al.* (1981) described the formation of such a 'plate-like' body, or calcite raft, as thin flakes probably nucleated on "... mucilagenous organic material", with a flat upper surface due to the fact that precipitation occurs below the air-water interface.

This mucilagenous mat, the biogenic component of the raft, may additionally host other microorganisms. Although more plausible, this explanation does not suggest why the elongate bodies are encrusted on both sides. Perhaps encrustation began on the lower surface (Fig. 15), eventually decreasing the buoyancy of the raft until precipitation could occur on both upper and lower surfaces of the raft. Finally, the weight of calcite encrustation caused the raft to settle to the bottom of the reservoir, where it forms a complex rafted zone (Plate 17D). There is no reason to assume that calcite precipitation should be exclusive to the surface of the fluid 'reservoir'. The formation of a crystal compromise boundary, which occurs at the advancing crystal growth front between two juxtaposed 'rafts' (Plate 15B), indicates that crystal growth continued on the rafts after they had accumulated on the floor of the reservoir.

VII. COLOUR BANDING

Calcite in its pure form is colourless. The presence of colour in any of the calcite speleothems, must therefore indicate the presence of impurities. Varying degrees of colour banding occur in flowstone from Grand Cayman Island. This is not a unique feature, since similar colour banded flowstone has been documented elsewhere (Folk and Assereto, 1976; White, 1981). The colours in the Grand Cayman flowstone, vary from white, through tan, to umber, and finally to a pitch black. In addition, bands of a similar colour may exist in varying degrees of opacity. Band thickness is of the order of 5.0 mm to 25.0 mm (Plate17A, B, C, D), and individual bands may be laterally consistent over many metres (Plate from Pirates cave). The cavity into which they are precipitated limits the final lateral extent of the flowstone.

Although the exact cause of pigmentation has yet to be ascertained, it may be due to (1) physical controls, (2) chemical controls, or (3) a combination of both.

Physical controls: Král (1971), suggested that crystal characteristics control the colour of the speleothem. Degrees of irregularity in the crystal structure would scatter light by differing amounts, the degree of scattering controls the spectra of emitted light. This opinion is substantiated by Beck (1978), who concluded that the variation in colour of his "fried egg" stalagmites, was the result of crystallographic (physical), not chemical factors.

Chemical controls: Advocates of the chemical control of pigmentation, suggest that the colour arises from either trace element substitution in the crystal lattice, or from impurities between the crystals (Sergeev *et al.*, 1974; Hill, 1976). White and Van Gundy (1974), demonstrated that Ni^{2+} substitution for Ca^{2+} imparts a yellow coloration. However, for most tan to umber coloured speleothems, Gascoyne (1977) concludes that, "...there is no obvious relation between colour and trace element content.", and that the colour is due to organic pigments, possibly humic or fulvic acid. This opinion is shared by White (1981), who after completing a reflectance spectrometric study of similarly coloured material, noted a lack of correlation between colour, and concentration of known pigments. He concluded that the common colours observed in calcite speleothems are not due to the oxides and oxyhydroxides of iron, but to a single pigmenting substance which is dispersed through the calcite grains as well as over grain surfaces. His reflectance data, leads indirectly to the conclusion that organic pigments are most likely responsible.

It is noteworthy that colour banding in caymanite (Rigby and Roberts, 1976; Jones *et al.*, 1983), a lithology closely associated with the flowstone, has been attributed to bacterial concentration of manganese and iron oxides (Lockhart, 1986). In order to ascertain if the colour banding in the flowstone was the result of similar manganese and iron concentrations, or one of the mechanisms outlined above, three samples of varied colour were analysed using atomic absorption spectrophotometry (AAS). The absorption wavelengths of Fe, Mn, Pb, Ni, Cu, Cr and Zn were scanned, as they have been proven to be pigmenting agents in other speleothems (Sergeev *et al.*, 1974; White and Van Gundy, 1974; Hill, 1976). The results from this analysis (Table 3), suggests that there is a fundamental difference exists between the colouring of caymanite and that of flowstone. Unlike the caymanite, the pigment for these particular flowstones, does not appear to be an oxide of either Mn or Fe. The Mn content for *all* the samples ranged from 8.5 μg/g to 22.0 μg/g (for comparative purposes, dark caymanite has upwards of 3% Mn). The sample with the highest Fe content (100.0 μg/g), sample EEQ 1219, was remarkably a *white* calcite; clearly the Fe was not acting as a pigment in this instance. The answer may lie in the form of an insoluble residue, which forms in HCl as part of the AAS process. This residue, following filtration and ignition in a furnace, looses its characteristic coloration and becomes completely soluble in the acid solution. A comparison of the trace element content of the solution before and after removal of the residue, shows little variation (≈8.0 μg/g). This appears to suggest, in agreement with the work of Gascoyne (1977) and White (1981), that the pigmentation was probably the result of an organic carbon component, which can be selectively removed in the ignition process.

		SAMPLE					
		1219	726	1257	1220	1257 ign	1220 ign
ELEMENT	Fe	100.0	111.9	71.5	62.5	57.5	65.0
	Mn	18.5	22.0	5.5	10.0	8.5	9.5
	Pb	35.0	33.5	33.5	35.0	33.5	33.5
	Mg	0.71%	▨	▨	▨	▨	▨
	Ni	50.0	50.0	50.0	50.0	50.0	50.0
	Cu	6.5	6.5	5.43	6.5	6.5	6.52
	Cr	28.6	28.6	28.6	28.6	28.6	28.6
	Zn	6.5	6.5	5.9	5.9	5.9	7.1
	Co	33.3	30.6	27.8	30.6	30.6	27.8

Table 3. Results of the atomic absorption spectrophotometry on three flowstone samples of varied colour. Sample 1219 (white), 726 (blonde), 1220 (dark brown), and 1257 (black). Samples 1220 ign and 1257 ign, refer to those samples in which the insoluble organic residue was ignited prior to AAS. All results are reported as parts per million for the element, except for Mg which is reported as percent elemental composition.

VIII. CATHODOLUMINESCENCE

A. INTRODUCTION

The realization that the distribution of luminescent zones in calcite crystals can be related to the development of ambient pore water chemistry has led to the increasing use of cathodoluminescence in the study of ancient strata, in what has been termed "cement stratigraphy" (Evamy, 1969; Meyers, 1974). Cement stratigraphic studies rely on the premise that in a particular pore space or around a particular grain, there will be a fluid system, the pore water. In the phreatic diagenetic environment its presence is total, while in the vadose environment air may take its place.

Pore water chemistry is a dynamic feature and will change in a body of rock according to a number of variables (Longman, 1980), the most influential of which is probably sea level fluctuation. As sea level changes, its passage will result in a series of chemically and physically distinct hydrological zones, which are herein referred to as "diagenetic environments". The passage of a particular diagenetic environment will be recorded as a series of chemically and luminescently distinct cements. If the luminosity remains constant it is assumed that the pore water chemistry remained constant throughout the precipitation of that cement zone. A variation in the luminescence, resulting from a variation in the concentration of impurity ions, is an indication of a change in the chemistry of the pore fluids (which may or may not be caused by a change in the diagenetic environment). A persistent combination of zones with distinctive morphology and luminescence, is termed a "luminescent signature" (Meyers, 1974; Carpenter and Oglesby, 1976).

There is a fundamental difference between the cement stratigraphic studies of Meyers (1974) and Evamy (1969) who dealt with ancient strata, and the present study on the Caymanian speleothems. These speleothems are geologically very young and it is possible (based on growth rates from recent caves) that they formed within recent history.

Consequently, they probably have not passed through many differing diagenetic environments. Despite these considerations, some of the speleothemic calcites display complex luminescent zonation.

B. THEORETICAL CONSIDERATIONS

Luminescence is the phenomenon of electromagnetic radiation in excess of thermal radiation (Marfunin, 1979). Luminescence may be regarded as a way of converting many different kinds of energy input, optical, nuclear, mechanical, chemical, into a light emission output. Excitation by one or more of these sources is a prerequisite for luminescent emission. Ionizing irradiation by electrons is a common method of excitation, the resulting emmision being known as *cathodoluminescence*.

Cathodoluminescence is the end product of a very complex series of energy storage and transitions in the irradiated substance, involving complex semi-conductor theory (Marfunin, 1979; Levrenz,1948). Nickel (1978), suggested that the entire process of cathodoluminescence could be simplified into three distinct stages, (1) absorption of energy or excitation, (2) temporary storage of energy, and (3) emission.

All three stages will be dependant upon both impurity ions incorporated into the growing crystal lattice and atomic lattice distortions. The elemental nature and valency state of the impurity ion involved will determine the role that the ion plays in the production of a luminescent spectra. Such an impurity ion may perform one of three functions,

(1) As an **activator** it is capable of absorbing the energy provided and later releasing it as a photon emission, or luminescence.

(2) As a **sensitizer** the ion is capable of absorbing a specific wavelength of energy that is unavailable to a second ion by virtue of the position of its absorption band. The energy is then transferred to a second activator or 'acceptor' ion, which can then release the energy in the form of luminescence. The method of energy transfer will

vary, depending upon the nature of the impurity ion, and the mode of excitation (Marfunin, 1979).

(3) As a **quencher** the ion is capable of reducing the emission from an activator or sensitizer/activator pair.

The concepts of sensitizing and quenching are of great importance to this study, for they provide an explanation for the patterns of cathodoluminescence observed in the speleothemic calcite.

C. RESULTS

Most of the speleothemic calcite, and in particular the inclusion free variety, is non-luminescent. Under electron excitation these calcites appear as black or blue-black, with no apparent variation beyond this (Plate 18 D). Where luminescence does occur, it is commonly of one of two forms.

(1) Bright orange, sharply defined "hairline" luminescence (Plate 20), forming a succession of zones or narrow bands. The emission intensity throughout each zone is usually homogeneous, which reflects the constant chemical composition of that zone. The morphology of these zones often corresponds to different stages of crystal growth (Plates 19A and 20B), reflecting the spatial distribution of the activator and quencher ions throughout the ontogeny of the calcite. This luminescent pattern is typical in inclusion (organic) rich calcite (Plate 19D, F) or porosity occluding cements (Plate 18B).

(2) Dull to moderate orange, broad transitional zones, the intensity and colour of which are commonly inhomogeneous, varying between dull orange to moderate orange/red luminescence. These zones typically occur in dolostone clasts of the Bluff Formation (Plate 19B), or organic agglomerates (Plate 18B).

The luminescence in the secondary porosity occluding calcite is very distinctive (Plate 18B, D), with well defined transitions from bright to dull orange luminescence. No conclusive match could be made with luminescent zones from similar cements in any one sample, or from comparison with other samples. The failure to recognize a luminescent signature can be related to the highly individual physical and chemical characteristics which develop within the pore spaces, and the speleothemic environment in general. It appears that luminescent calcite will evolve very different luminescent characteristics in two closely spaced pores (Plate 18B).

Some luminescent zones mimic the inclusion defined growth banding common in the Caymanian speleothems (samples EEQ 726 and PCQ 1241). Although retaining the same morphology as the growth bands, the luminescence is commonly displaced to either side (Plate 19D). Although a causal relationship appears to exist between the growth banding and the luminescence, it is not always the organics contained in the inclusions which actually emit the luminescence.

In order to interpret these luminescent patterns, it is necessary to rationalize the morphology of the luminescent zones in relation to the physical and chemical controls which are acting upon the luminescent zonation. Some of the more distinctive luminescent zones comprise numerous very bright orange, 'hairline' luminescence (Plates 19A and 20B). Individually, these imply (1) rapid incorporation of trace elements responsible for either sensitizing or activation, and (2) a limited supply of those ions. A repetition of the hairline zones (Plate 19D), further suggests a diagenetically "open" system which allows for the periodic replenishment of the appropriate trace elements. The repetition of these zones, which commonly mimic the growth bands, infers that organics are intrinsically linked to the luminescence.

D. DISCUSSION OF DATA

Dolostone Luminescence

The dull to moderate orange/red luminescence of the Bluff Formation clasts (Plate 19 B) is a common phenomenon that occurs in many luminescent dolostones (Sommer, 1972a; Pierson, 1981), the apparent luminescent colours being the result of the moderate Fe quenching of Mn activated luminescence. The common occurrence of these colours being attributable to the higher Fe^{2+} contents of many dolostones (Machel, 1985).

Organics - Their Influence On Luminescent Properties

The common occurrence of bright orange luminescence in association with organic accumulations may be an indication of the origin of the impurity ions responsible for activation and sensitization. It is common to find both in close proximity to one another (sample 728b, 1291) (Plate 18C and Plate 19D, F), suggesting that the luminescence may be the result of the uptake of activators and /or sensitizers from the organics. Both clay minerals and organic matter are known to preferentially host trace metals (Parekh *et al.*, 1979), however, since X-ray studies of the speleothemic calcite did not reveal the presence of any clay minerals, only the trace metals commonly hosted in organic matter are considered. Machel (1985) suggested that these were Ag, C[illegible], Cu, Ga, La, Mn, Mo, Ni, Pb, with minor Eu and Co; some of which are important activators and sensitizers (Table 4). Throughout diagenesis these trace elements are released into the ambient fluids and incorporated into the growing calcite lattice according to the partitioning coefficient of each element (Hem, 1972; Pingitore, 1978; Brandt and Veizer, 1980). Thus, calcite precipitated in association with organics may possess distinctive luminescent properties as a direct result of the differential release of trace elements into the ambient fluids. In view of this, a number of equally viable scenarios are possible for the production of the common luminescent pattern, whereby organics are followed by a hairline zone of bright luminescence, which then gradually decays into a dull luminescence.

ACTIVATORS	SENSITIZERS	QUENCHERS
Mn^{2+}	Pb^{2+} Ce^{2+}	Fe^{2+}
Pb^{2+}	Ce^{2+} Ce^{4+}	Ni^{2+}
REE's (Eu^{3+} Tb^{3+})	Several REE's	Co^{2+}
Cu^{2+}		
Zn^{2+}		
Ag^{+}		
Bi^{+}		

Table 4. Some of the more common impurity ions which are involved as activators, sensitizers and quenchers in luminescence in calcite. Modified after Machel (1985).

(1) If the release of activators from the organics, (eg. Mn^{2+} and Pb^{2+}), was initially very rapid and then began to decline, this could account for the distinctive luminescent pattern

(2) If the observed luminescence is Mn^{2+} activated, then the increased release of Ni^{2+} over time, will result in a similar subdued luminescence in later calcite.

(3) If the cathodoluminescence was Pb^{2+} activated, then Medlin (1959) has suggested that Ni^{2+} may sensitize the luminescence. Consequently a depletion in the Ni^{2+} content over time could also produce this cathodoluminescence pattern.

The nature of the trace element host and the effect that partitioning coefficients may play can be speculated on, the practicalities of testing such theories are, however, prohibitive. Firstly, there are the *minimum effective concentrations* to consider, which have been the source of much debate in the past (Schulman *et al.*, 1947; Pierson, 1983: Fairchild, 1983; Machel, 1985). Mn^{2+} activated luminescence has been reported with Mn^{2+} concentrations between 20-40 ppm (Richter and Zinkernagel, 1981), but when sensitized, Mn^{2+} concentrations need only be 10-20 ppm. Machel (1985) quoted a Mn^{2+} concentration figure required for luminescence as low as 5ppm. Quenchers, such as Fe^{2+}

become active at concentrations of approximately 35 ppm, while Co^{2+} and Ni^{2+} are effective at still lower concentrations (Machel, 1985).

When variation in the wavelength and intensity of cathodoluminescence is controlled by concentration changes in the order of 10 ppm, it becomes important to realize the experimental limits of the sampling techniques employed. Although both organic rich and organic poor calcites were studied using an x-ray dispersive analysis unit employed in conjunction with the scanning electron microscope, the detection limits of this technique are of the the order of 1 wt %. Thus, the presence of important activators, quenchers and sensitizers below 1 wt % can not be recorded with any degree of accuracy.

In an attempt to try to resolve this problem, four samples of calcite of varying organic content and colour were prepared for atomic absorption spectrophotometry (AAS), which has detection limits within 10 ppm. Despite analyzing samples of varying organic content, concentrations of Fe, Mn, Pb, Mg, Ni, Cu, Cr, Zn and Co, were remarkably low and consistent (Table 3). Only Mn and Fe displayed a significant variation between samples, with the trace element content decreasing with increased organic content. This was not the expected result if indeed the organics were preferentially hosting certain trace elements. This apparent discrepancy is likely attributed to the precision of sampling that can be achieved with this method. To sample only the calcite which possess the hairline luminescence is beyond the sampling resolution of this technique. By the time this small area is incorporated in a 1 gramme sample necessary for the AAS process, a 'dilution effect' could have drastically reduced the apparent trace element concentration of these very narrow zones.

Changes In The Redox Potential

The precipitation of luminescent calcite, in a fluid which contains above minimum concentrations of activator and sensitizer ions is not *ipso facto*. The valency state of an impurity ion must also be assessed, as this will control its effectiveness as a sensitizer, an activator, or a quencher. For example, the valency state of Mn will affect its role as an activator. In order for it to be effective it must be able to substitute for Ca^{2+} in the calcite lattice, this is only possible in the reduced Mn^{2+} state. If the waters are oxidizing, then the Mn present will be in the oxidized Mn^{3+} and Mn^{4+} states, which are inhibited from entering the calcite lattice by virtue of their ionic radii. In addition, both Fe^{2+} and Fe^{3+} are common quenchers, with the latter having the potential for considerably more effect upon luminescent intensities (Marfunin, 1979). The size and intensity of the charge transfer band for Fe^{3+}, causes it to have an absorption band which overlaps the emission bands of the activators. The result is a total, non-selective quenching of luminescence for low concentrations of Fe^{3+}, while a similar concentration of Fe^{2+} will allow for luminescence. However, the radius and charge of the Fe^{3+} ion, makes substitution into the calcite lattice an improbable event; consequently, Fe^{2+} is considered the more important quencher in luminescent calcite.

For the sake of simplicity, the assumption is made that the Caymanian speleothemic calcites owe their luminescent properties to the presence of a Mn activator and an Fe quencher. This is not unrealistic, considering the emphasis placed upon these trace elements as important luminescent contributors in the literature (Schulman *et al.*, 1942; Long and Agrell, 1964; Sommer, 1972; Meyers, 1974, 1978; Carpenter and Oglesby, 1976; Nickel, 1978; Pierson, 1981; Frank *et al.*, 1982; Fairchild, 1983; Grover and Read, 1983; Machel, 1985). Furthermore, high concentrations of Mn have been noted in association with the Bluff Formation. Jones and Kahle (1985) documented biogenically controlled Mn rich surficial coatings on karst breccia clasts in the Bluff Formation, and Lockhart (1986) recorded the presence of large Mn dendrites in association with Caymanite. The source of this Mn might be from the overlying 'terra rosa' soil, which contains approximately 0.25 % Mn (Lockhart, 1986), or from a highly concentrated source of Mn which is biologically 'fixed' beneath the mangrove swamps (Woodroffe, 1983).

A knowledge of the redox potential of the groundwater is of great importance, for it is the redox potential which determines the valency state of the important impurity ions.

In any groundwater system, Drever (1982) suggested that the redox level is determined by the relative rate of introduction of O_2. The concentration of O_2 in the groundwater is determined by, (1) the circulation of the groundwater, and (2) the consumption of O_2 by the bacterially mediated decomposition of organic matter. According to Drever (1982) the most important variables associated with these controls are:

(1) The O_2 content of the recharge water, which is determined by its passage through overlying rock or soil.

(2) The distribution and reactivity of organic material present at the site of precipitation.

(3) The concentration of specific ions, and the likelihood of potential redox buffer reactions eg. MnO_2/Mn^{2+}, $Fe(OH)_3/Fe^{2+}$, Fe_2O_3/Fe^{2+}.

(4) The circulation rate, or 'residence time' of the groundwater in any one particular pore.

With these variables in mind, the major cathodoluminescent zoning of the Cayman speleothems can be related to the redox potentials of the precipitating fluid.

Activators and the redox potential: The poorly developed soil zone covering much of Grand Cayman Island results in a meteoric water entering the speleologic environment with a strong redox potential. If the precipitating fluid has a strong redox potential, then Mn^{3+} and Mn^{4+} (which are not capable of activating luminescence) will predominate (Fig. 16), and the calcite will be non-luminescent. This would correspond to a "'dead' type 1 precipitation environment" of Frank *et al*. (1982). Furthermore, the mechanism of flowstone precipitation via a thin film of fluid (Dreybrodt, 1979), allows for constant O_2 replenishment (redox buffering) via the cave atmosphere. Theoretical constraints correspond well with the lack of cathodoluminescence in the speleothemic calcites. If the precipitating fluids at any time become more reducing, then Mn^{2+} would be the expected manganese state (Fig. 16), resulting in bright luminescence. This would correspond to a "type 2 precipitation environment" of Frank *et al*. (1982).

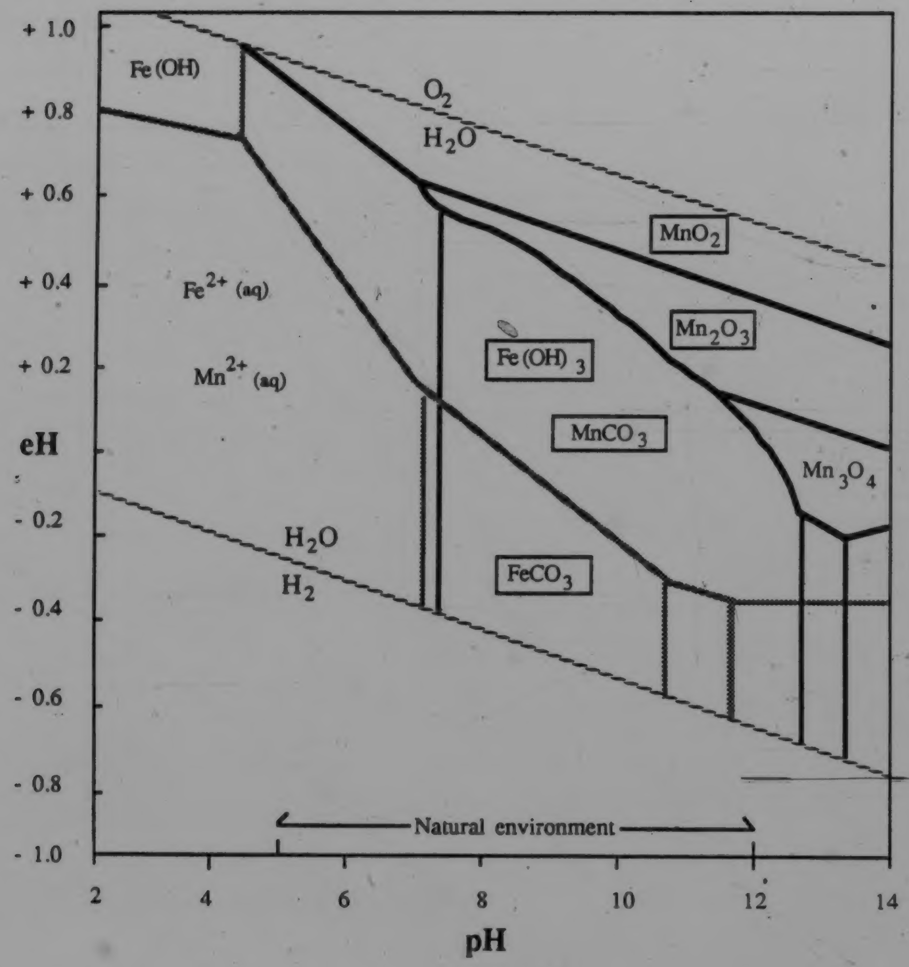

Figure 16. Eh-pH diagram of the stability fields of iron and manganese compounds at 25 °C and 1 atmosphere. Reasonable limits of pH in the natural environment are shown (Garrels and Christ, 1965). Modified after Machel (1985).

The transition from an oxidizing to a reducing environment in a fairly large aquifer, can be achieved via certain thermodynamically favoured redox reactions (Champ *et al.*, 1979, Table 2, p. 14). These reactions in the absence of a catalyst are, however, very slow and require a catalyst to be of any significance. The presence of microbial enzymes and the subsequent metabolic degradation of organic matter has been shown by Champ *et al.* (1979) and Grover and Read (1983) to be a suitable catalyst. This provides a possible answer, to the very interesting relationship which places bright orange luminescence in common association with 'bacterial clumps' and detrital organic matter. Firstly, the detrital organic matter will act as a source for important activator and sensitizer impurity ion. Secondly, bacterial reactions, which are associated with the metabolic decomposition of the organic matter, will catalyze important reducing reactions which lower the redox potential of the immediate environment. Consequently, the reduction of Mn^{4+} to Mn^{2+} in a mildly reducing environment will lead to the precipitation of luminescent calcite (Fig. 16).

Quenchers and the redox potential: If the redox potential of the precipitating fluid decreases further, then the reduction of iron to the Fe^{2+} state increases the probability of quenching (Fig. 16). Thus, if a pore fluid becomes too reducing, calcite precipitated in this environment is not expected to luminesce.

At this point the concept of 'residence time' can be expanded upon. In normal flowstone precipitation, fluids pass rapidly over the calcite surface, the residence time is thus very short, and the cave waters remain in an oxidized state. The high redox potential prevents the occurrence of manganese in the Mn^{2+} state, and the result is the precipitation of non-luminescent calcite (Fig. 16). If the residence time is significantly increased, as for example in a small pore space, then the bacterially mediated reducing reactions of Champ *et al.* (1979) will have more time in which to lower the redox potential of the fluid. If a sufficient residence time is maintained, then the redox potential of the water may approach that which permits manganese activated calcite to be precipitated. A further increase in the residence time may cause the water to stagnate, which could lower the redox potential of the water to a point where the precipitation of Fe^{2+} quenched calcite is possible (Fig. 16).

The ability of the residence time to control the redox potential of the cave waters, can provide the answer to a number of questions. Firstly, a close examination of the relationships between organics, luminescence and crystal growth morphology, shows that luminescent calcite can occur **before** the presence of organics (Plate 10 B), inferring that organics may not be a prerequisite for luminescence. If a sufficiently long residence time can be maintained (i.e. stagnation of the water), this may allow non-biologically catalyzed reactions to lower the redox potential of the water sufficiently for the precipitation of luminescent calcite. Secondly, residence times could account for the dissimilar luminescence patterns in juxtaposed porosity occluding cements (Plate 18 A, B). Inhomogeneous permiabilities will produce differing rates of fluid exchange through a pore system. Consequently, different pores will have different residence times, which will result in a variation of the redox potential throughout localized areas of the speleothem.

The Significance of REE's

Rare Earth Elements (REE's) are known to be activators and sensitizers of cathodoluminescence in calcite (Machel, 1985), particularly Eu^{3+} ,Tb^{3+} and Ce^{3+}, Ce^{4+} respectively (Table 4). This presents yet another possibility to account for the luminescent zonation of the speleothems.

Based upon an early concept by Balashov *et al.* (1964), who stated that the increase in the Ce:Y ratio was, "...a result of preferential capture of the heavy lanthanides by organic matter.", Scherer and Seitz (1980) suggested that REE's may actually be fractionated by a bacterial influence. Thus a bacterial presence within the speleothemic calcite, could increase the concentration of Ce, which would increase the sensitization of Mn activated calcite (Table 4). Due to the difficulty of separating and calculating the concentration of REE's (Krauskopf, 1967, p.577) this would be very difficult to verify experimentally. This method of sensitized luminescence in calcite is, however, a very real possibility and one which cannot be totally discounted.

D. SYNOPSIS

Cayman speleothemic calcite is in general non-luminescing due to the fact that it was precipitated from a fluid with a high redox potential i.e. in an oxidizing environment. The common coexistence of bright orange luminescence and organic material strongly suggests that a causal relationship exists between them. The organic material acts as both a host for common activator and sensitizer impurity ions, and for bacteria which can effectively lower the redox potential of the pore fluid. The combination of activator and sensitizer ions in a sufficiently reducing environment, will result in the precipitation of luminescent calcite.

The variation in luminescent zonation is the result of the complex interplay of many factors, including, (1) the trace element content of the organic material, (2) partitioning coefficients of each element present in the organics, (3) occurrence of bacterially mediated reducing reactions in the pore fluid and the effect upon the redox potential of the environment, and (5) the residence time of the fluid in any one particular pore.

The rare occurrence of bright orange 'hairline' luminescence in the absence of any organics, indicates that the pore fluids alone are capable of precipitating luminescent calcite. The development of a sufficiently reducing environment in the absence of bacteria would require a long residence time, or "stagnation" of the fluid responsible for the precipitate. A situation such as this may occur during periods of reduced meteoric influx.

IX. STABLE ISOTOPE GEOCHEMISTRY

A. INTRODUCTION

Physical and chemical characteristics of the fluids responsible for the precipitation of speleothems and calcite in general can be deduced from their stable carbon and oxygen isotope geochemistry (Clayton and Degens, 1959; Hendy, 1971; Meyers, 1974; Allan, 1976; Thompson *et. al.* 1976; Meyers and James, 1978; Allan and Mathews, 1977, 1982). To study the isotope geochemistry of the Caymanian speleothems, samples which possessed well defined morphological and compositional variations, were collected from localities on Grand Cayman Island and Cayman Brac (EEQ 1219, CIQ 1250, CIQ 1252, EEQ 726, EEQ 727, EEQ 728, BH 730). As successive layers of calcite were deposited to form these speleothems, so a record of the isotope geochemistry of the pore waters was retained. When sampled sequentially, selected layers on each slab can provide information on the evolution of the pore waters through time.

In order to provide an accurate record of the $\delta^{18}O$ and $\delta^{13}C$ ratios, a unique number was assigned to each calcite layer sampled. Each 'sample number' eg. EEQ 728.4, therefore consists of, (1) a location number code and number (**EEQ 728**.4) which places the sample at a specific site on Grand Cayman Island (Fig. 1), and (2) a decimal number (EEQ 728.**4**) which is assigned to an individual calcite layer in that sample.

B. SPELEOTHEMIC ISOTOPE DATA

Carbon and oxygen isotopic data was determined for forty four samples from speleothems collected at seven different localities on Grand Cayman Island and Cayman Brac (Table 5). Data for the isotope geochemistry of selected Caymanian waters has also been obtained (Table 6), samples being collected from the marine, meteoric and mixing zone environments.

SAMPLE NO.	δ^{18}O SMOW	δ^{13}C PDB	δ^{18}O PDB
EEQ 1219.1	25.5	-10.3	-5.2
EEQ 1219.2	24.8	-9.8	-5.9
EEQ 1219.3	25.4	-10.2	-5.3
EEQ 1219.4	24.9	-8.3	-5.8
EEQ 1219.5	25.5	-9.7	-5.2
CIQ 1250.1	26.6	-9.9	-4.1
CIQ 1250.2	24.6	-11.6	-6.0
CIQ 1250.3	25.3	-10.9	-5.4
CIQ 1250.4	24.3	-11.6	-6.3
CIQ 1250.5	24.7	-10.5	-6.0
CIQ 1250.6	24.7	-9.5	-6.0
CIQ 1250.9	25.5	-9.9	-5.2
CIQ 1250.10	26.9	-9.6	-3.9
CIQ 1252.2	29.0	-7.2	-1.8
CIQ 1252.3	29.0	-4.8	-1.9
CIQ 1252.4	25.6	-10.8	-5.1
CIQ 1252.5	24.1	-10.7	-6.5
CIQ 1252.6	24.1	-10.5	-6.5
CIQ 1252.7	29.5	-6.9	-1.3
EEQ 726.1	32.6	1.6	1.7
EEQ 726.2	25.9	-10.2	-4.8
EEQ 726.3	25.2	-10.6	-5.5
EEQ 726.4	24.3	-11.9	-6.4
EEQ 726.5	25.2	-10.6	-5.5
EEQ 726.6	25.2	-10.5	-5.5
EEQ 726.7	26.1	-11.1	-4.6
EEQ 727.1(Dol)	28.2	0.6	1.6
EEQ 727.1(Calc)	28.5	-6.3	-2.6
EEQ 727.2	28.5	-7.1	-2.3
EEQ 727.4	25.7	-9.6	-5.0
EEQ 727.5	26.0	-9.8	-4.7
EEQ 728.1	25.3	-8.4	-5.4
EEQ 728.2	26.1	-8.5	-4.6
EEQ 728.3	25.3	-11.0	-5.4
EEQ 728.4	27.6	-5.4	-3.2
EEQ 728.5	25.3	-9.9	-5.4
EEQ 728.6	25.0	-9.9	-5.7
EEQ 728.7	25.3	-10.0	-5.4
EEQ 728.8	25.0	-10.0	-5.7
EEQ 728.9	25.0	-9.6	-5.2
BH 730.4	24.9	-7.1	-5.8
BH 730.3	24.0	-8.7	-6.6
BH 730.2	24.3	-7.9	-6.4
BH 730.5	25.3	-7.9	-5.4

Table 5. δ^{18}O and δ^{13}C values for all the speleothems sampled, all values are reported in parts per thousand (permill).

CAYMANIAN WATER ISOTOPE DATA	
WATER TYPE	**$\delta^{18}O$**
Sea Water	+ 1.48
	+ 1.44
Brackish Water	- 4.09
Fresh Water	- 4.27

Table 6. $\delta^{18}O$ ratios for selected water samples taken from diverse hydrological environments on Grand Cayman Island. Sample courtesy of Sam Ng.

When the $\delta^{13}C$ data is plotted versus $\delta^{18}O$ (Fig. 17), it is apparent that:

(1) The general field defined by all the speleothemic data lies in the range $\delta^{18}O$ = -6.6‰ to +1.3 and $\delta^{13}C$ = -11.9 to -4.7‰. The $\delta^{18}O$ data lies within the well established range of meteoric waters (Hudson, 1977). This is in agreement with both the isotopic values measured for Caymanian fresh water ($\delta^{18}O$ = -4.27‰), and petrographic and field observations, all of which suggest that the sampled calcite is of a speleothemic origin from the meteoric realm.

(2) Selected layers from samples CIQ 1252, EEQ 728, and EEQ 727 form a distinct and separate zone from most of the data (Fig. 17). Consequently, the data can be divided into two zones, zone A ($\delta^{13}C$ = -11.9 to -7.1‰ and $\delta^{18}O$ = -6.6 to -3.9‰) and zone B ($\delta^{13}C$ = -4.7 to -7.2 and $\delta^{18}O$ = -1.3 to -3.2‰).

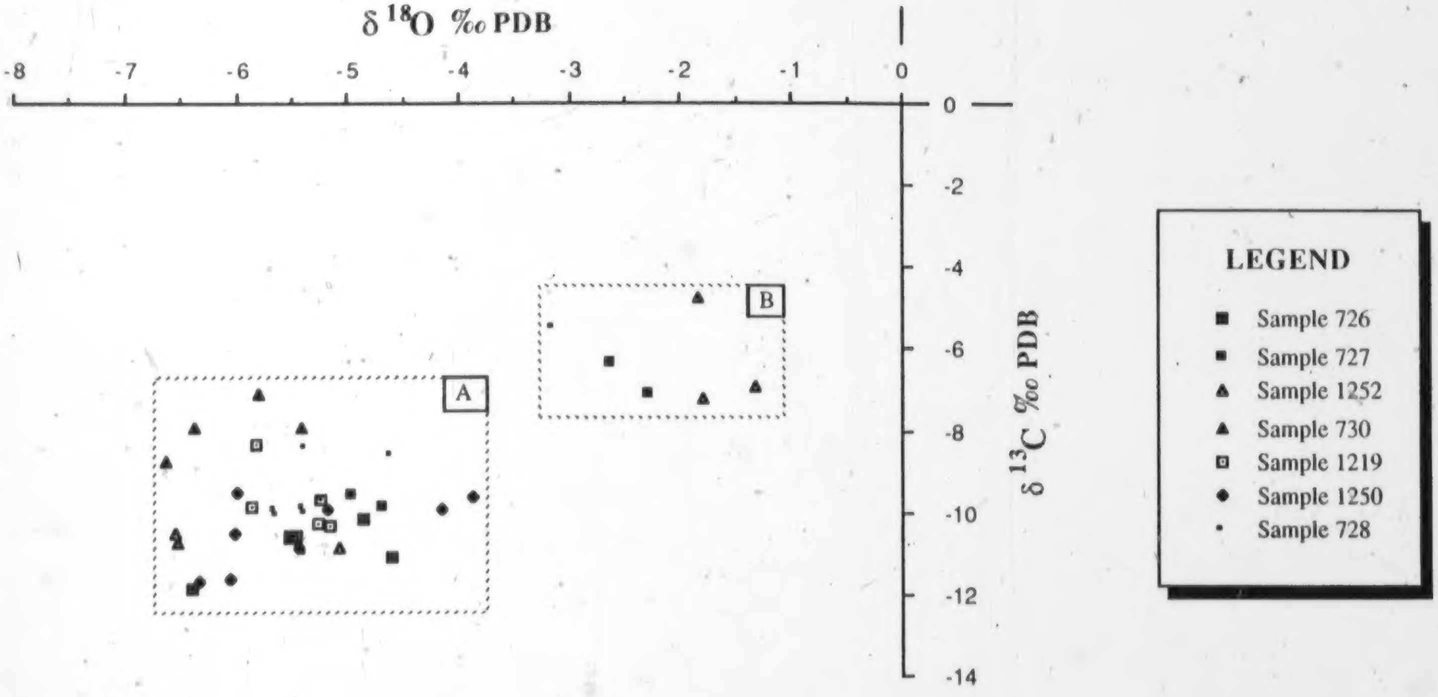

Figure 17: Stable isotope geochemistry of all the speleothems that were selected for analysis. The genaeral field of data is clearly divided into two zones, 'Zone A' - with more negative $\delta^{18}O$ and $\delta^{13}C$ ratios and 'Zone B' - with more positive $\delta^{18}O$ and $\delta^{13}C$ ratios.

In an attempt to rationalize this zonal distinction, isotopic data from each of the sampled speleothems are treated sequentially in order to illustrate the evolution of the pore waters responsible for calcite precipitation.

Sample 728: The initial precipitates, EEQ 728.9 through EEQ 728.5, which lie in a narrowly defined isotopic range, contrasts with the large variation between the later calcites, EEQ 728.4 through EEQ 728.1 (Fig. 18). Sample EEQ 728.5 (-8.5 $\delta^{13}C$, -4.6 $\delta^{18}O$) was followed by EEQ 728.4 (-11.0 $\delta^{13}C$, -5.4 $\delta^{18}O$), showing a considerable increase in both the $\delta^{13}C$ and the $\delta^{18}O$ values. The isotopic variations which define the transition between these two layers, may be related to (1) a decrease in the water:rock ratio (Sverjensky, 1981), (2) an increase in the temperature, or (3) an influx of marine waters.

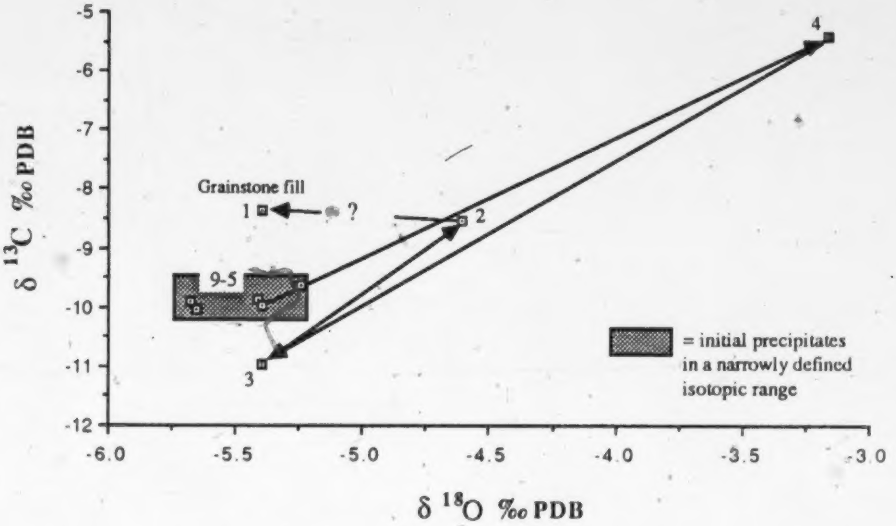

Figure 18. Evolution of the isotopic geochemistry of the pore waters responsible for the precipitation of sample EEQ 728.

The water:rock ratio in this instance can be treated as a simple measure of the amount of dissolution of the host Bluff Formation. In a closed system, where dissolved CO_2 is totally removed from any atmospheric CO_2, there are two distinct sources of carbon, that derived from the dolostone of the Bluff Formation, and a finite source derived from the initial absorption of soil CO_2. Dissolution of the Bluff Formation is important, since isotopic values from the dolostone are considerably enriched in $\delta^{13}C$ and $\delta^{18}O$ (Pleydell, 1987). Consequently, during dissolution, the Bluff Formation will act as a reservoir for ^{13}C and ^{18}O. In a similar situation on Barbados, Allan and Mathews (1977) indicated that the groundwater bicarbonate is isolated from isotopic exchange with the soil gas CO_2 soon after passing through the soil profile. Thus as dissolution proceeds, the water:rock ratio will decrease as proportionally more carbon and oxygen are derived from the host carbonate, and less from the soil zone. If this is the situation occurring between samples EEQ 728.5 and EEQ 728.4, then both the $\delta^{13}C$ and $\delta^{18}O$ ratios of the precipitated calcites would be expected to increase.

The increase in $\delta^{13}C$ and $\delta^{18}O$ could also be accounted for via a temperature effect. In the closed system, Hendy (1971) suggested that variability in the $\delta^{13}C$ will be dominated by the PCO_2 *i.e.* $CO_{2(aq)}$, the effects of temperature being negligible. The only way in which significant changes in the $\delta^{13}C$ value could occur, would be if the change in temperature caused a change in the vegetation pattern, leading to an indirect control of PCO_2 in the soil . If, however, the system were open to atmospheric CO_2, then carbon derived from the absorption of soil CO_2 is no longer a finite source. The presence of an excess PCO_2 allows isotopic equilibrium to be maintained between $CO_{2(g)}$(soil derived) and $CO_{2(aq)}$. In this open system, the $\delta^{13}C$ of the fluid is no longer controlled by PCO_2 but by temperature. The relationship between temperature and $\delta^{13}C$ has been quantified by Craig (1954) and labeled the 'Enrichment Factor' (E). Expansion of Craig's work by Vogel *et al.* (1970), and Hendy (1971) showed that the temperature dependence of $\delta^{13}C$ in the open system will be approximately 0.6‰ $°C^{-1}$. Applying this theory to the data from sample 728, an increase in $\delta^{13}C$ of +4.5‰, can be attained from the enrichment factor via a rise in temperature of approximately 7.5 °C.

If the above scenario is continued, then a rise in temperature must also effect the $\delta^{18}O$ values. If isotopic equilibrium is maintained, then the precipitated calcite will be in isotopic equilibrium with the water. The relationship between the $\delta^{18}O$ of the fluid and the $\delta^{18}O$ of the speleothem, will be determined by the isotopic equilibrium fractionation factor. Following the experimental work of O'Neil *et al.* (1969), the calcite-water fractionation can be described by equation (1.0)

$$10^3 \ln \alpha\, CaCO_3 - H_2O = (2.78 \times 10^6 . T^{-2}) - 2.89 \qquad (1.0)$$

Where T = Temperature (°K)

In order to calculate the effect a 7.5 °C increase would have on the calcite being precipitated, equation (1.0) was rearranged.

$$\text{Ln } 1000 + \delta^{18}O_{CaCO_3} = \frac{((2.78 \times 10^6) - 2.89) + \text{Ln } 1000 + \delta^{18}O_{H_2O}}{10^3} \qquad (1.1)$$

If T = 25°C and $\delta^{18}O_{H_2O}$ = -4.27‰ SMOW, then $\delta^{18}O_{CaCO_3}$ = 24.4‰ SMOW. Following an increase in temperature of 7.5 °C, and assuming a constant value for $\delta^{18}O_{H_2O}$, then $\delta^{18}O_{CaCO_3}$ becomes 25.8‰ SMOW. The temperature increase therefore gives rise to a theoretical 1.4‰ $\delta^{18}O$ enrichment. In reality, a 2.3‰ $\delta^{18}O$ enrichment was measured between samples 728.5 and 728.4 (Table 5); either the temperature increase was greater, or the assumption that the $\delta^{18}O_{H_2O}$ ratio remained constant was incorrect.

(3) The third possibility involves the influx of marine fluids into the cave system. From the data in Table 6, it can be shown that mixing of marine and meteoric waters, could produce a water with a suitable isotopic composition (Fig. 19).

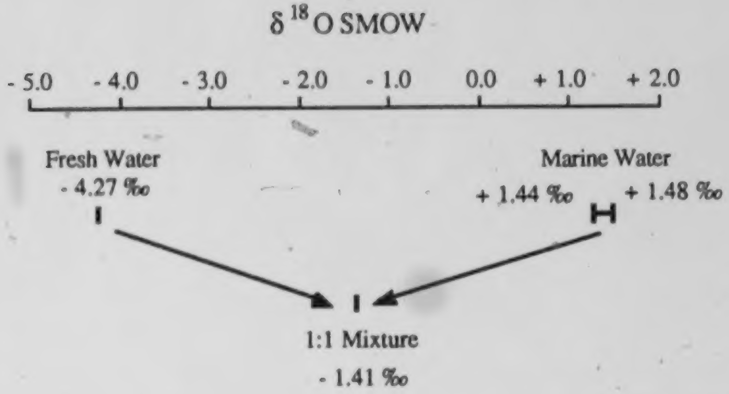

Figure 19. The mixing of Caribbean sea water and fresh water from Grand Cayman Island, will produce a water with a $\delta^{18}O$ ratio of approximately - 1.41 ‰ SMOW.

From equation (1.1) it is possible to construct a set of hypothetical curves, based upon the maximum and minimum $\delta^{18}OCaCO_3$ ratios from sample 728, which describe the range of possible $\delta^{18}OH_2O$ and temperature values capable of precipitating the sampled calcite (Fig. 20). Measured temperatures for the shallow fresh water phreatic zone range from 27 ° to 31°C (Ng, 1987, pers. comm.), and are considered adequate an approximation for the near surface vadose fluids.

Despite the large range of temperatures capable of precipitating the calcite at a $\delta^{18}OH_2O$ ratio of -1.4‰, the fact remains that the mixing of marine and meteoric fluids could have produced the observed $\delta^{18}OCaCO_3$ ratios at an acceptable temperature for the depositional environment.

Sample 728 was collected from a small exposed cave system, approximately 200 m from the present day shoreline, at an elevation of about 20 m above sea level. In view of this one of two mechanisms for deriving the marine fluids can be suggested. Within recent history, catastrophic events have been recorded which have driven sea water right across the entire island. Clearly, sufficient marine waters can be driven onto coastal sites which then rapidly drains through solution conduits in the karst (Plate 17F).

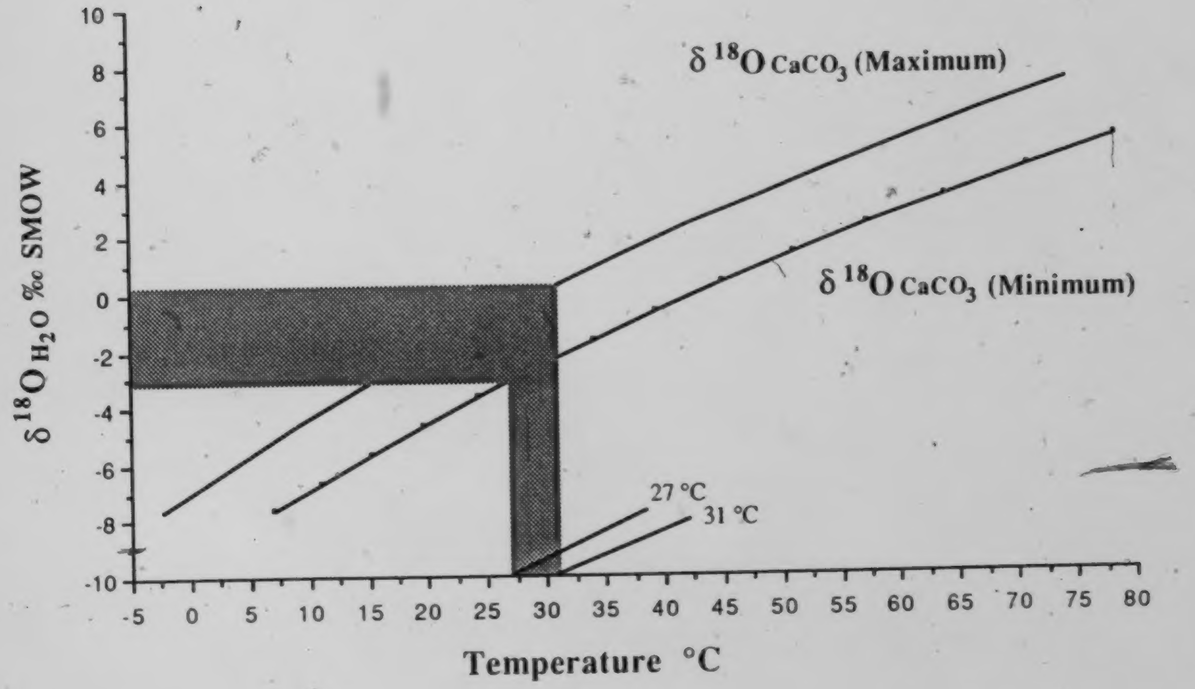

Figure 20: From the standard calcite-water fractionation equation of O'Neil *et. al.* (1969), a set of hypothetical curves can be created. These curves indicate the range of possible temperatures and water compositions which are capable of precipitating the measured calcite ratios in sample EEQ 728. The stippled area indicates the $\delta^{18}O_{H2O}$ ratios capable of precipitating the calcite at temperatures between 27°C and 31°C.

Alternatively, the marine infiltration may have been a subsurface phenomenon. Hydrologically the Bluff Formation possesses a high infiltration rate, which allows marine water to influx into the islands fresh water lenses along joints and fissures on a diurnal basis (Ng, 1985). However, sample EEQ 728 was collected from the east end of the island where infiltration rates are known to be considerably lower. Consequently, the former hypothesis of surface infiltration is thought the most likely.

Sample EEQ 728.3 which follows EEQ 728.4, is considerably depleted in both ^{13}C and ^{18}O (Fig. 17). The substantial decrease in $\delta^{13}C$ (-5.6‰) resulted from either (1) a meteoric influx bringing ^{12}C enriched water from the soil zone above, (2) the fractionation of a ponded fluid reservoir, or (3)*in situ* organic decay.

(1) During more pluvial periods, perhaps even seasonally, the amount of meteoric water entering the cave system from the surface will increase. This meteoric water, generally assumed to be isotopically enriched in ^{12}C due to its passage through the soil zone, will then impart a depleted $\delta^{13}C$ signature upon near surface speleothems. Although it is commonly assumed that meteoric water must first have passed through a soil zone, at which point the isotopic signature of the water becomes enriched in ^{12}C (Wickman, 1952; Brinkman *et al*., 1959; Bender, 1968), on Grand Cayman Island this is not always the case. While there are areas of well developed clays and clay loams (Baker, 1974), the depth of soil cover in general is very thin, varying from pockets of 1m to large areas with no soil at all (Plate 17F). It is therefore possible for meteoric water to enter the cave system without being substantially enriched in ^{12}C, the result of this which would be speleothemic calcite with a more enriched $\delta^{13}C$ ratio.

(2) Equilibrium fractionation of a ponded fluid reservoir could also account for the decrease in both the $\delta^{13}C$ and $\delta^{18}O$ values of sample 728.3. If the rate of loss of CO_2 is sufficiently slow, such that chemical equilibrium can be maintained between bicarbonate ions and aqueous CO_2, then the calcite deposited will be in oxygen isotopic equilibrium with the water. In a closed system, two separate processes are occurring which can greatly

effect the the isotopic values of the flowstone. Thermodynamic considerations reason that the $^{12}CO_2$ molecule will be preferentially removed over the $^{13}CO_2$ molecule. The fractionation factor which describes this process (α $CO_{2(g)}$- HCO_3^-), equals -9.0‰ $\delta^{13}C$ (Friedman and O'Niel, 1977). Consequently, the remaining fluid reservoir should become enriched in ^{13}C. However, $CaCO_3$ precipitated should be enriched in the $^{13}CO_3^{2-}$ molecule via the process of Rayleigh distillation, thereby maintaining the *status quo* in the reservoir. The $\delta^{13}C$ fractionation factor between HCO_3^- and $CaCO_3$, however, results in a $\delta^{13}C$ of only +1.7‰, hence when combined with the fractionation factor between $CO_{2(g)}$- HCO_3^- a net fractionation of -7.3‰ $\delta^{13}C$ results.

(3) The process of *in situ* organic decay, which refers to the localized degradation of surface derived soil in the karst system (James and Choquette, 1985), may be responsible ~~for the~~ isotopic trend between EEQ 728.4 and EEQ 728.3 (Fig 18). Evidence of the insurgence of surface organic material is apparent at both Pedro Castle quarry and at the Old Man Bay village caves (Fig. 1). At Pedro Castle quarry, fractures developed in the dolostone of the Bluff Formation have been filled with surface terra rossa (Plate 17G, H). At Old Man Bay village, the caves are floored with a thick layer of soil, and many of the now inactive speleothems are 'dusted' with a liberal (3 to 5 mm) coating of organic debris. The origin of this coating appears to be suspended material, washed into the karst system from the soil zone above, which has then been physically deposited on the surface of the speleothems.

Sample 1252: The complex sequence of precipitation present in sample CIQ 1252 (Plate 19B) precludes any attempts to sample the calcite sequentially. Consequently, the sequence of pore water evolution is not known for this sample. It is apparent from Figure 17, however, that sample CIQ 1252 has precipitates of markedly dissimilar isotopic geochemistry.

Sample CIQ 1252.1 was extracted from conspicuous white aphanitic elongate bodies (Plate 17B). Through the use of alizarin red staining it was apparent that these bodies are laminated cavity linings, composed of alternating dolomite and calcite. X-ray diffraction studies of this sample further conclude the presence of dolomite. Sample CIQ 1252.2 was extracted from an enigmatic pink clastic cavity fill, X-ray analysis of which again shows the presence of dolomite. It is likely that the ^{13}C and ^{18}O enriched dolomite probably accounts for the presence of this sample in zone B (Fig. 17). Sample CIQ 1252.7 was extracted from a geopetal fill (Plate 17 B), which contains numerous skeletal (Foraminiferal) fragments. Additionally, X-ray analysis of this sample shows greater then 20% dolomite.

Both the petrographic and X-ray diffraction analysis of sample CIQ 1252, indicate that the cause of the separation of these isotopic data from the main filed of speleothemic calcites (Fig. 17), may be due to the presence in each sample of, (1) some component of the Bluff Formation, or (2) biogenic (skeletal) calcite of recent origin.

The relationships between the contaminant phases and these samples which comprise the zone B speleothems (Fig. 17), becomes more apparent when the recent skeletal sediments, Bluff Formation, and the speleothemic data are plotted on the same graph (Fig. 21). The spar calcite cements associated with the Bluff dolostone defines a distinct linear trend, which passes through the zone B speleothemic calcite field. The implications of this are that the isotopically distinct samples (CIQ 1252.1, CIQ 1252.2, and CIQ 1252.7) are the result of precipitation from a geochemically distinct cave water, one which is related to that which precipitated the spar calcite cements. This relation may take one of two forms, either (1) both the speleothemic calcite and the spar calcite cements were precipitated coevally from the same fluid, or (2) dissolution and re-precipitation of the spar calcite cements provides the saturated fluids which precipitates the later speleothemic calcites.

The effects of dolostone dissolution should not be discounted either, as with the spar calcites, the isotopic geochemistry of the dolomite also lies the same covariant trend (Fig. 21).

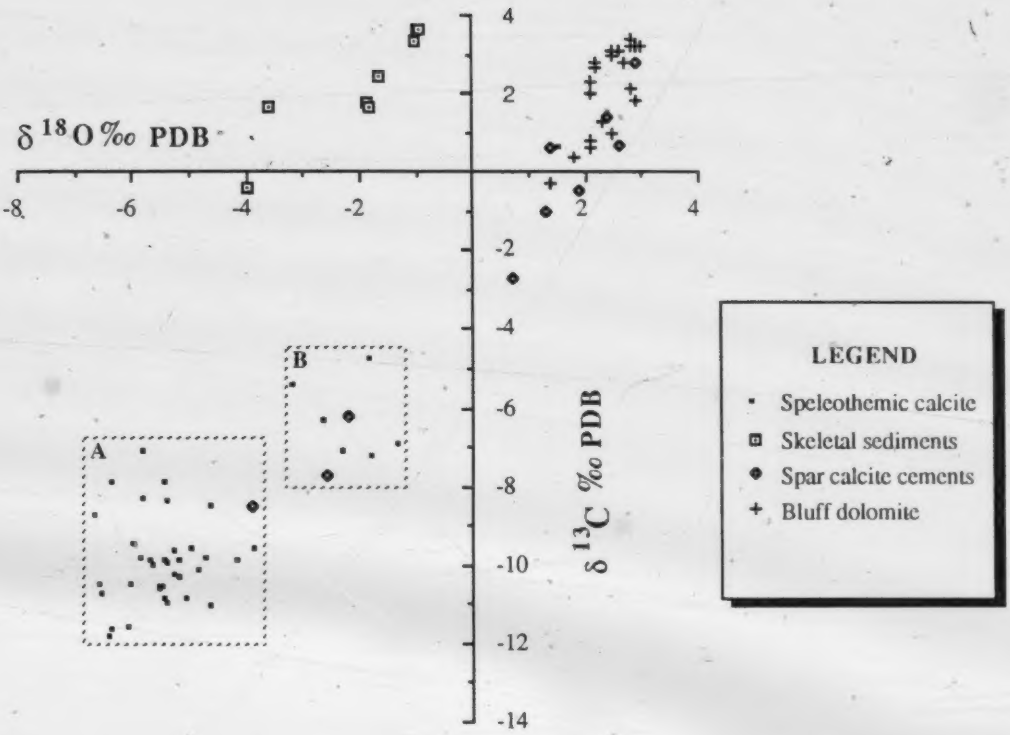

Figure 21: The covarient trend between the isotopic geochemistry of the Bluff Formation and the closely related spar calcite cements, transects the Zone B speleothemic calcite. Biogenic calcites (skeletal sediments) do not appear to be related to the geochemistry of the Zone B calcites. Additional isotopic data courtesy Suzanne Pleydell.

It is possible that the dissolution of the host dolostone and/or physical contamination by dolostone clasts could have produced the measured increase in the $\delta^{18}O$ and $\delta^{13}C$ ratios in these samples. The presence speleothemic calcite in the zone B range may, therefore, be the result of a decreasing water:rock ratio *i.e.* greater dissolution of the host dolostone.

Sample 727: The isotopic data from this sample further corroborates the view that the isotopic ratios of the zone B calcites are related to those of the host dolostone and associated spar calcite cements. Isotopic geochemistry of the spar calcite present in sample EEQ 727.1 had $\delta^{18}O$ and $\delta^{13}C$ ratios of - 2.6‰ and - 6.3‰ respectively. These are very similar to the $\delta^{18}O$ and $\delta^{13}C$ ratios of the flow banded calcite (EEQ 727.2) which coats the dolostone clast (Fig. 22).

Sample EEQ 727.2 is (1) enriched in ^{13}C and ^{18}O in comparison to most of the speleothemic calcites, and (2) of a similar isotopic composition to the spar calcite cements. One possible explanation for this, is the fact that they were precipitated from a similar fluid, one which is distinct from the zone A calcites. Alternatively, the higher $\delta^{18}O$ and $\delta^{13}C$ ratios may be representative of a mechanical (artifact) or chemical (natural) contamination of the calcite layer juxtaposed with the dolostone clast. Mechanical contamination is ruled out on the grounds that X-ray analysis of this sample did not show the presence of any dolomite. The increased $\delta^{18}O$ and $\delta^{13}C$ ratios may, therefore, be the result of dissolution of the dolostone clast, which has released $\delta^{18}O$ and ^{13}C into the ambient fluid to be later incorporated in the calcite of sample EEQ 727.2. Once the dolostone clast is coated in calcite, it is effectively removed from the system, hence subsequent calcite layers, EEQ 727.4 and EEQ 727.5 (Fig. 22) plot in the zone A range.

Sample 726: Sample EEQ 726 (Plates 6 and 17D) displays a great variety of calcite morphologies, varying from white palisade calcite (EEQ 726.3), 'rafted' calcite bodies (EEQ 726.5), to well developed 'calcite shrubs' (EEQ 726.6). If fluid composition is a

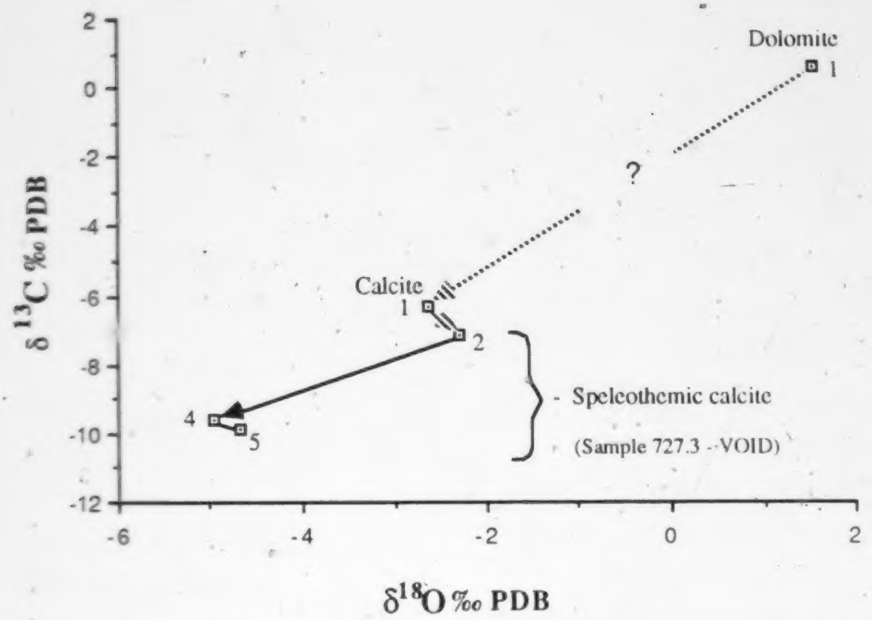

Figure 22. Evolution of the isotope geochemistry of pore waters responsible for the precipitation of sample EEQ 727.

controlling influence upon crystal morphology, then these changes in morphology may be reflected in the isotopic geochemistry of the layers. A comparison of the geochemical evolution of the fluids responsible (Fig. 23) and the morphology changes (Plate 17D), however, fails to reveal any significant correlation. For example, the isotopic values of EEQ 726.5 (the algal filament zone) are -10.6 $\delta^{13}C$ and -5.5 $\delta^{18}O$. The following zone, a very distinct botryoidal and 'shrub' calcite has $\delta^{13}C$ and $\delta^{18}O$ values of -10.5‰ and -5.5‰ respectively. Clearly a considerable morphological change has occurred without a corresponding change in the carbon and oxygen geochemistry.

There does appear to be a more positive morphological and geochemical correlation between samples 726.6 and 726.7 (Fig. 23). A small decrease in the $\delta^{13}C$ ratio of -0.6‰, is accompanied by a larger increase in the $\delta^{18}O$ ratio of +0.9‰, as the morphology changes from euhedral crystalline shrubs to an orange pelloidal fill. This zone consists of many subrounded spherical clasts of Bluff dolostone, surrounded by a spar calcite cement. The presence of these inverse graded peloids represents the influx of sediment laden fluids into a previously ponded reservoir. The clasts of the dolostone can account for the enrichment in $\delta^{18}O$, while the orange coloration (possibly derived from terra rossa) may be the cause of $\delta^{13}C$ depletion, via *in situ* organic decay.

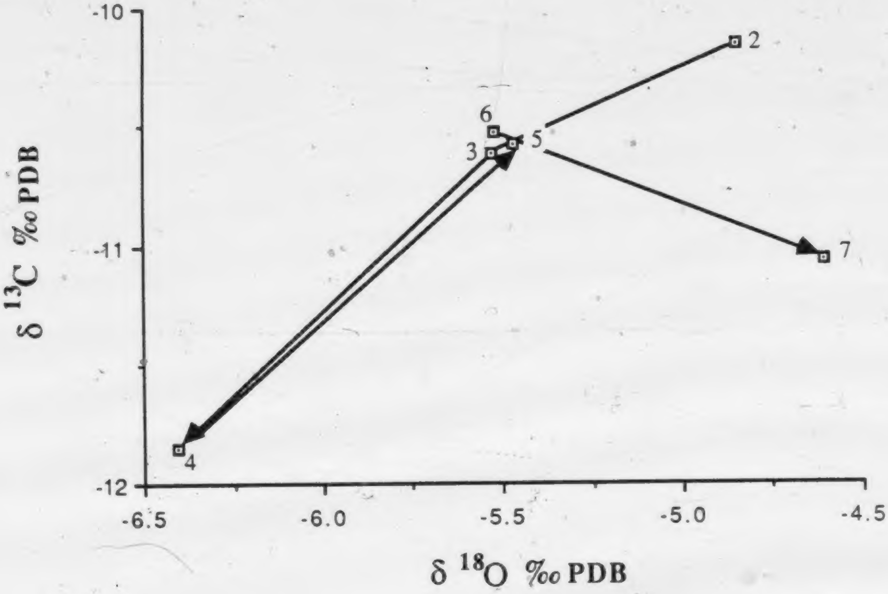

Figure 23. Evolution of the isotope geochemistry of pore waters responsible for the precipitation of sample EEQ 726.

Sample 1250: The isotopic trend displayed between samples CIQ 1250.1, CIQ 1250.2, CIQ 1250.3 and CIQ 1250.4 (Fig. 24) may be the result of variations in the water:rock ratio. For example, as the rate of meteoric influx increases, so the trend towards depleted $\delta^{13}C$ and $\delta^{18}O$ values will occur since the carbon and oxygen from the meteoric water will gradually become predominant. During periods of lowered meteoric influx, or where the fluids responsible for precipitation have been ~~in~~ contact with the host dolostone for longer periods of time, then a trend towards enriched $\delta^{13}C$ and $\delta^{18}O$ values is expected.

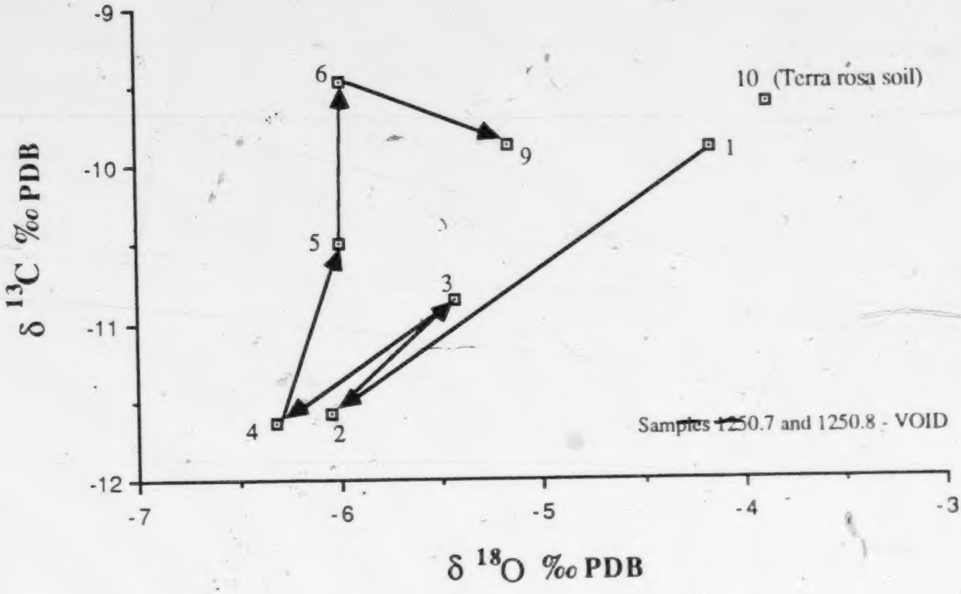

Figure 24. Evolution of the isotope geochemistry of pore waters responsible for the precipitation of sample CIQ 1250.

Samples CIQ 1250.5 and CIQ 1250.6 show a trend of increasing $\delta^{13}C$, while the $\delta^{18}O$ value remains fairly constant. If an increased rate of CO_2 degassing occurred, then because the fluid $\delta^{13}C$ ratio will be enriched by +9.0‰ (Assuming equilibrium conditions at 15°C), subsequently precipitated calcite will be similarly enriched.

Samples 730 and 1219: The isotopic values from samples BH 730 and EEQ 1219, all lie in a very narrow isotopic range (Figs. 25 and 26). As neither the morphology nor the isotopic geochemistry show any marked variation, these samples are considered no further.

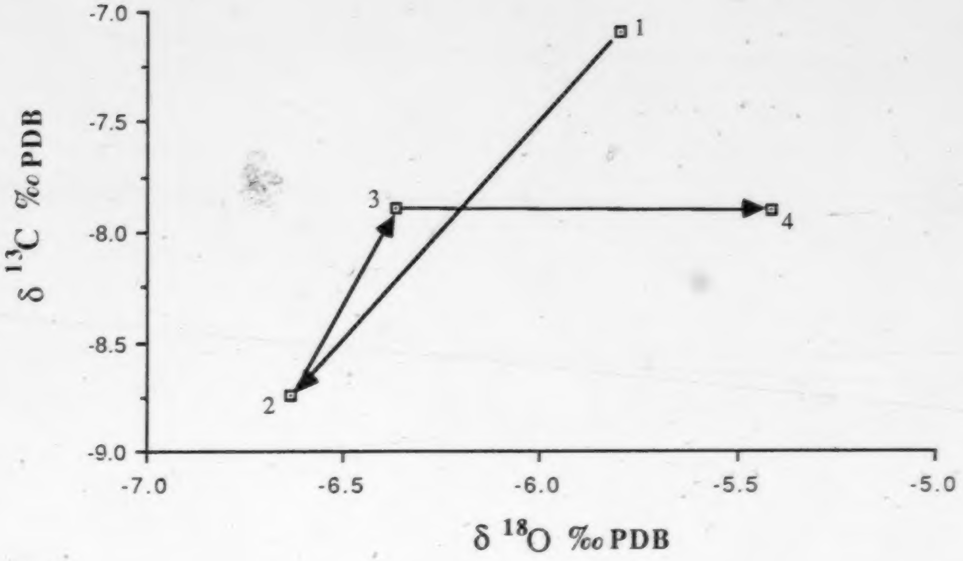

Figure 25. Evolution of the isotope geochemistry of pore waters responsible for the precipitation of sample BH 730.

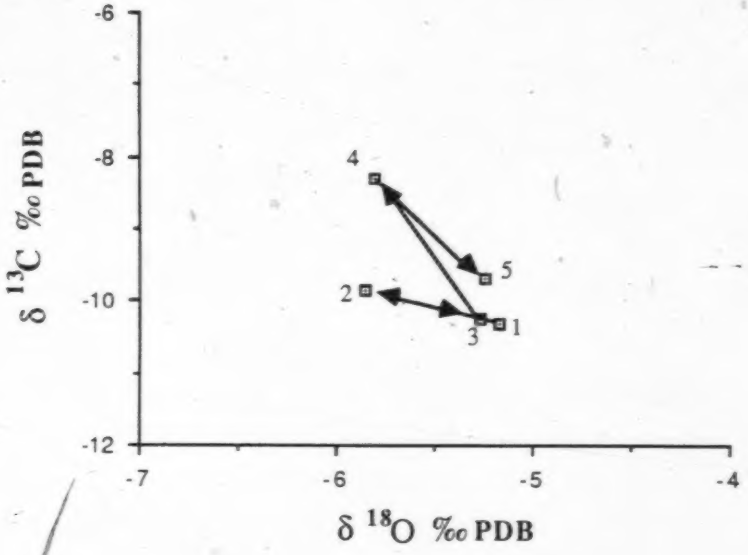

Figure 26. Evolution of the isotope geochemistry of pore waters responsible for the precipitation of sample EEQ 1219.

D. DISCUSSION OF DATA

A distinctive change in the isotopic ratios, recognized in more than one sample, may indicate a regional isotopic signature. Layer 728.4 with $\delta^{13}C$ and $\delta^{18}O$ ratios of -5.4‰ and -3.2‰ respectively, is isotopically very distinct and it was hoped that this may be used as an 'isotopic signature'. However, analysis of all the other samples from both Grand Cayman Island and Cayman Brac failed to reproduce this particular signature. The evidence therefore suggests that this was a localized event. This is not surprising in view of the fact that speleothems will form in a micro-environment of a highly individual geochemical and physical nature. It is apparent that many variables can be considered influential in determining the carbon and oxygen isotopic geochemistry in these environments (Fig. 27), the most important of which are;

Meteoric Water: The $\delta^{18}O$ ratio of rainwater in the Caribbean in general, is known to vary between -2.0 and -4.0‰ SMOW (SEPM course #10). At this stage, variation in the $\delta^{18}O$ ratio of the rainwater is a direct result of fractionation in all condensation and evaporation processes (Dansgaard, 1964). Extremes in latitude and altitude can therefore have marked effects upon the $\delta^{18}O$ ratio. The low latitude of Grand Cayman Island (19°20'N) and the lack of substantial relief, however, ensures that the $\delta^{18}O$ ratio of the precipitation is close to that of the initial fractionation of the Caribbean sea reservoir (0.0 to +1.0‰ SMOW). Despite the high mean daily temperatures, 29.5°C and 26.0°C for August and January respectively (Proctor, 1984), the effect of evaporational fractionation is minimized by high humidity and rapid surface drainage. Thus, it appears valid to assume that meteoric waters entering the groundwater cycle, have similar regional and annual $\delta^{18}O$ ratios.

Groundwater: The isotopic geochemistry of the groundwater is primarily a function of four major elements;

(1) The initial $\delta^{18}O$ value of Caymanian rainwater (above).

(2) The $\delta^{13}C$ ratio of atmospheric CO_2, which is approximately -7.0‰ (Hudson,1977).

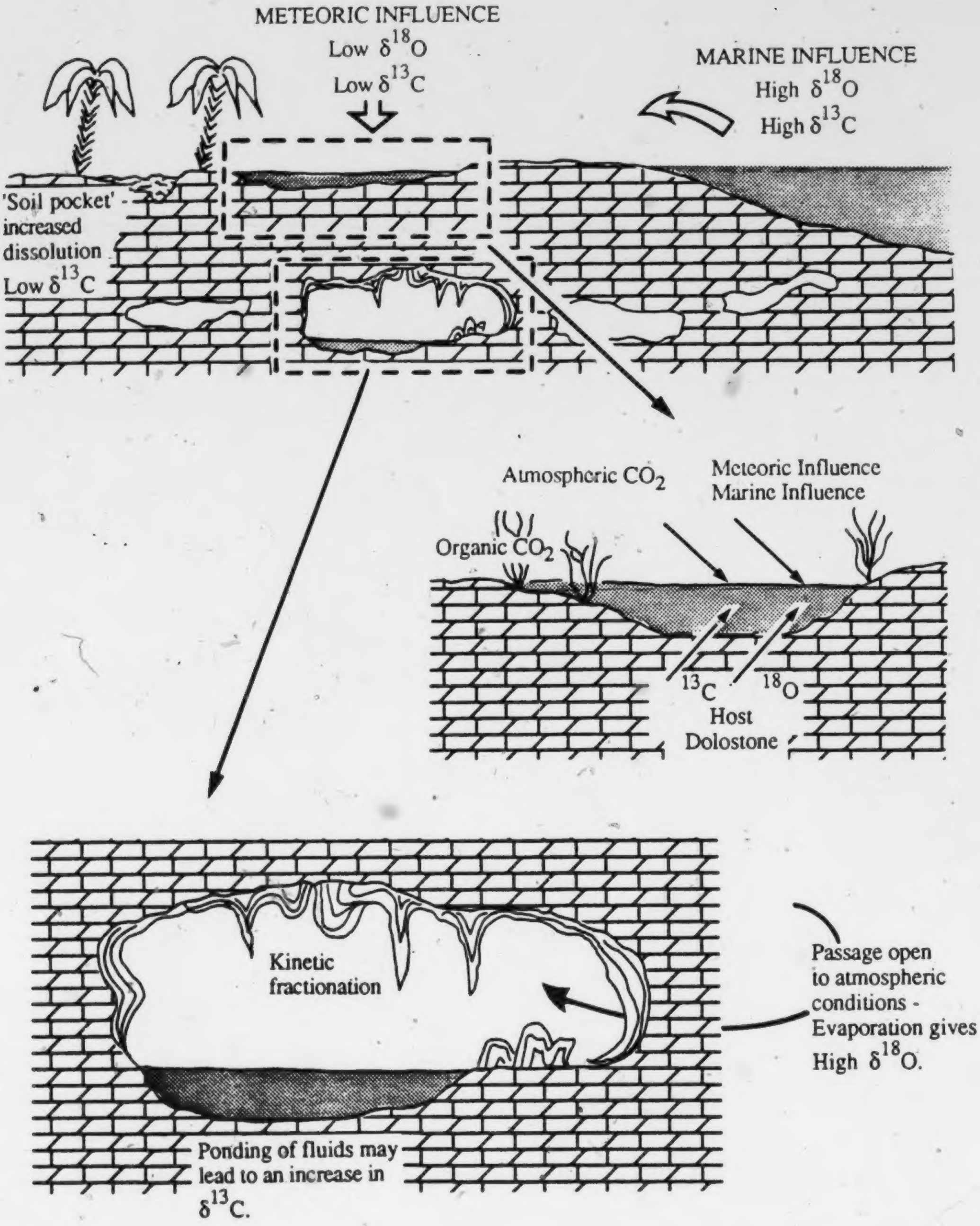
METEORIC INFLUENCE
Low $\delta^{18}O$
Low $\delta^{13}C$
MARINE INFLUENCE
High $\delta^{18}O$
High $\delta^{13}C$
'Soil pocket' - increased dissolution
Low $\delta^{13}C$
Atmospheric CO_2
Meteoric Influence
Marine Influence
Organic CO_2
^{13}C
^{18}O
Host Dolostone
Kinetic fractionation
Passage open to atmospheric conditions - Evaporation gives High $\delta^{18}O$.
Ponding of fluids may lead to an increase in $\delta^{13}C$.

Figure 27. The isotopic geochemistry of the Caymanian speleothems is controlled by many factors of both local and regional significance. This summary diagram illustrates those factors which are most influential, and the ares in which they are effective.

(3) The $\delta^{13}C$ of organic derived CO_2, an approximate range for which is -12.0 to -20.0‰. This is based upon, (a) the vegetation types (Brinkman *et al.*, 1959), (b) the fact that no isotopic fractionation occurs between living and decaying organic material (or that produced via respiration), and (c) no isotopic fractionation occurs between the organic material and gaseous CO_2 (Bender, 1968).

(4) The $\delta^{13}C$ and the $\delta^{18}O$ values of the Bluff Formation, where the $\delta^{13}C$ ratio ranges from -0.3 to +3.4‰ (Pleydell, 1987).

The $\delta^{13}C$ ratio of the groundwater is a combination of the above elements 2, 3 and 4. The interaction between the organic material and the host carbonate, commonly referred to as 'soil weathering' (Hudson, 1977), involves the formation of a bicarbonate molecule, one carbon atom being contributed from the Bluff formation and one from the organic material. Therefore, knowing the $\delta^{13}C$ ratios of the organic CO_2 and the Bluff dolostone, an approximation of the $\delta^{13}C$ ratio of the groundwater can be made (Fig. 28). Discrepancies between the measured value for Caymanian groundwater (Table 6), and that predicted in Figure 28, can be explained in view of the fact that the $\delta^{13}C$ ratio is very much dependant upon time. The greater the period of time that groundwater is in contact with either organic material or host carbonate, the greater the influence of each will be.

Marine influx: The combination of marine fluids ($\delta^{18}O$ = 1.4 to 1.5‰) with groundwater, can produce a fluid enriched in both ^{13}C and ^{18}O.

Equilibrium and Kinetic Fractionation Factors: Precipitation of calcite through the slow loss of CO_2 allows chemical equilibrium to be maintained between bicarbonate ions and gaseous CO_2, hence isotopic equilibrium is maintained. In a ponded fluid reservoir for example, isotopic equilibrium fractionation factors (Friedman and O'Neil, 1977), will eventually lead to a fluid depleted in ^{13}C.

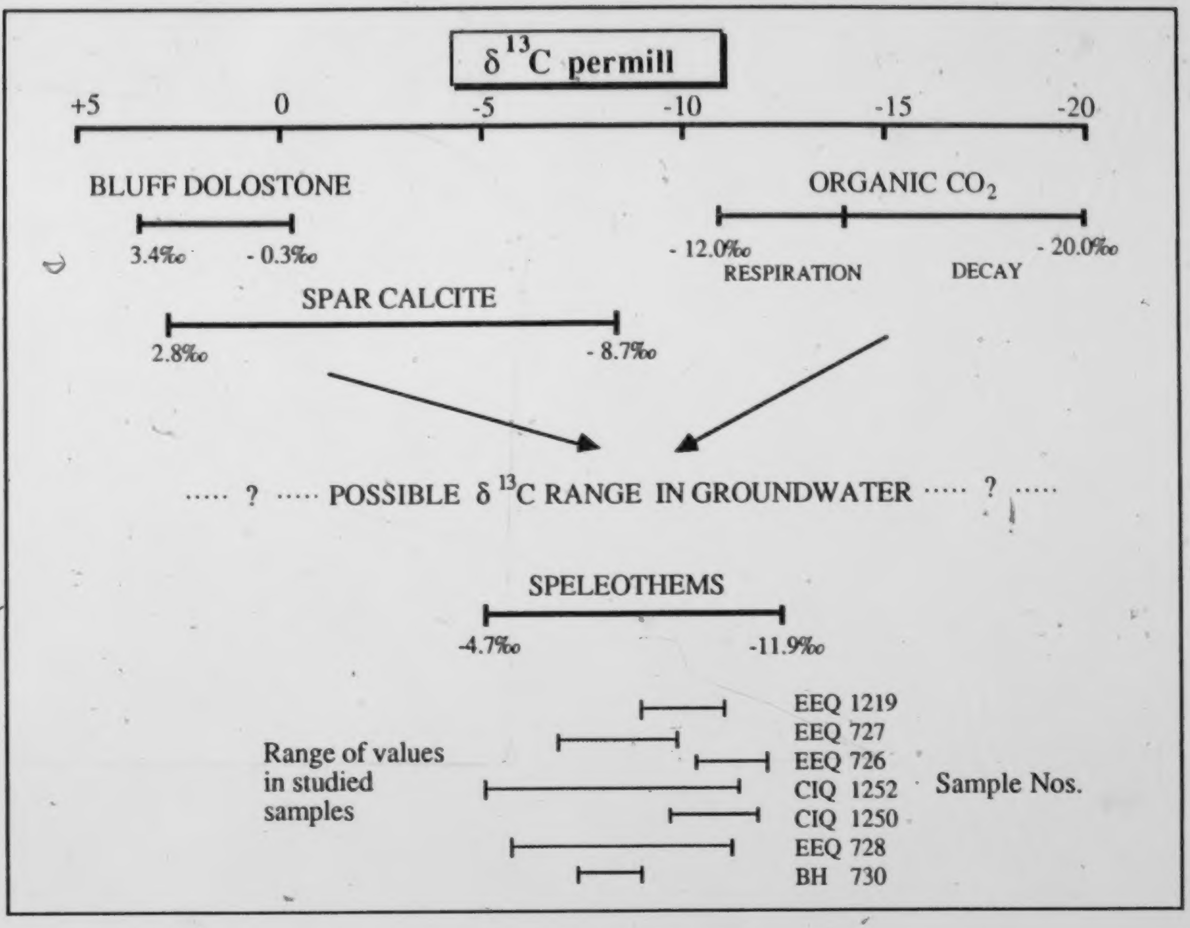
$\delta^{13}C$ permill
+5
0
-5
-10
-15
-20
BLUFF DOLOSTONE
3.4‰
- 0.3‰
ORGANIC CO_2
- 12.0‰
- 20.0‰
RESPIRATION
DECAY
SPAR CALCITE
2.8‰
- 8.7‰
..... ? ..... POSSIBLE $\delta^{13}C$ RANGE IN GROUNDWATER ..... ? .....
SPELEOTHEMS
-4.7‰
-11.9‰
Range of values in studied samples
EEQ 1219
EEQ 727
EEQ 726
CIQ 1252
CIQ 1250
EEQ 728
BH 730
Sample Nos.

Figure 28 . Suggested evolution of the $\delta^{13}C$ ratios of the Caymanian groundwater and its relation to the isotopic geochemistry of the speleothemic calcite.

If the rate of loss of CO_2 is too rapid, then a kinetic isotopic fractionation factor is introduced between HCO_3^-, CO_2 and H_2O. Under such circumstances, the precipitated calcite is no longer in isotopic equilibrium with the water. Hendy (1971) has presented the theory of kinetic isotopic fractionation in great detail, and suggested its effects are so great, as to totally mask all recognizable features of isotopic equilibrium fractionation. In order to recognize the features of kinetic isotopic fractionation however, samples would have to be collected sequentially **along** the calcite layers, in the direction of fluid flow (Fantidis and Ehalt, 1971). As the samples used in this study were not collected *in situ*, information as to the direction of flow was not available. In view of this, kinetic isotopic fractionation is considered no further.

Evaporation: Evaporation can induce precipitation of calcite via the increased ion concentration of the solution. Subsequently precipitated calcite will posses a distinctive $\delta^{18}O$ signature, the result of $H_2{}^{16}O$ being preferentially removed from the reservoir. As the reservoir is enriched in the $H_2{}^{18}O$ molecule, so the calcite will become enriched in the $C^{18}O_3^{2-}$ radical. Clearly the degree of $\delta^{18}O$ enrichment is dependant upon the rate of evaporation. In the cave environment however, humidity is usually high and the degree of evaporation low (Holland *et al.*,1964), hence unusual conditions are required for this process. A cave entrance, or any subterranean cavity which is open to surface atmospheric conditions, may be subject to evaporative fractionation processes. Unusual petrographic features may also be associated with this type of deposit. As water evaporates, other soluble salts in solution may approach saturation; their presence during the precipitation of calcite may result in a calcite phase which is impure and microcrystalline in texture.

E. SYNOPSIS

Idiosyncrasies abound in the carbon and oxygen stable isotopic geochemistry of the Caymanian speleothems. Each individual sample possesses a different trend of isotopic variation, although all the studied samples do lie within a restricted $\delta^{18}O$ and $\delta^{13}C$ range

(Fig. 17). The range of isotopic values, and the isotopic variation observed between the samples can be related to, (1) the source of the carbon and the oxygen, (2) the temperature of the precipitational environment, and (3) the hydrodynamics of the precipitational environment. The source of carbon and oxygen apparently exerts a strong control on the final isotopic enrichment of the speleothemic calcites. The fact that many of the sampled speleothems have isotopic ratios which lie along a covariant trend with both the host dolostone and related spar calcite cements, suggests that their dissolution may control the isotopic geochemistry of the speleothemic calcites to large extent.

X. CONCLUSIONS

1. Speleothems are common in the solution cavities, joints and skeletal molds of the Oligocene-Miocene dolostones of the Bluff Formation.
2. Speleogenesis was a result of cyclic fluctuations of the shallow vadose and phreatic hydrologic regimes. (i) Ceiling solution pockets indicate that the large solution cavities were initially formed by mixing corrosion in the phreatic zone. (ii) These phreatic cavities were later modified in the vadose zone to produce gravitationally controlled speleogens. (iii) These cavities were further overprinted by phreatic dissolution features.
3. The dense accumulation of speleothems at some localities, and the paucity at others, is the result of a partial lithological control.
4. A wide range of crystal morphologies in the speleothemic calcite was a response to (i) fluctuating chemical and physical conditions, and (ii) biogenic controls in the vadose zone. Those crystals that are precipitated on organic bodies are strongly substrate controlled, whereas those precipitated on a crystalline substrate receive additional crystallographic control.
5. The presence of (i) calcified filaments, (ii) uncalcified filaments, (iii) microborings, (iv) organic bodies, and (v) calcified spherules indicates that speleothem formation is not solely an abiogenic process.
6. The formation of colour banded flowstone emphasizes the significant role of organics in the macroscopic, as well as microscopic features of the speleothems. AAS showed no correlation between the colour bands and the trace element content, whereas the distribution of organics was correlative.
7. δ^{18}O and δ^{13}C ratios of the flowstones from Grand Cayman Island range from -6.6‰ to +1.3‰ and -11.9‰ to -4.7‰ respectively. This range of data is indicative of precipitation in the meteoric diagenetic realm.

8. Systematic $\delta^{18}O$ and $\delta^{13}C$ analysis of the individual flowstones laminae showed that although isotopic variation occurred in any one sample, these trends could not be correlated between samples. This suggests that in any one cavity, the controls acting upon $\delta^{18}O$ and $\delta^{13}C$ ratios fluctuated, but that these fluctuations were unique, localized events *i.e.* each cavity existed as a partially isolated microenvironment.
9. Speleothemic calcite in general exhibited no cathodoluminescence. Exceptions are dull to bright orange luminescence occurring in (i) organic rich zones, (ii) undefined 'hairline' zones, and (iii) cements that occlude coeval porosity in the flowstones.
10. With the emergence of Grand Cayman Island after middle Miocene times, came the development of a meteoric hydrological system. This provided the potential for speleogenesis. Subsequent sea level fluctuations during the Tertiary and Quaternary have had a marked influence on the gross morphology and spatial distribution of speleological features.

XI. PHOTOGRAPHIC PLATES

PLATE 1

Vertical speleothems from the Old Man Bay Village Caves.

(A) Saw tooth stalactite with elaborate cuspate drapes. Photograph courtesy B. Jones. Scale bar = 20 om.

(B) Type I stalactite, with a small drape developing. Note the geometry of the banded calcite where the speleothem has ben damaged. Scale bar = 15 cm.

(C) Spectacular growth of vertical speleothems, with stalactites, stalagmites and stalacto-stalagmites (S). Note the eccentric stalactite in the left background (arrow), the distinct curved nature of which may be due to an uneven flow of water down the stalactite. Scale bar = 25 cm.

(D) Fractured type II stalactite, showing a near concentric arrangement of calcite laminae. Note the preservation of the fine central 'soda straw', and the coalescence of juxtaposed stalactites, a result of their dense growth. Scale bar = 10 cm.

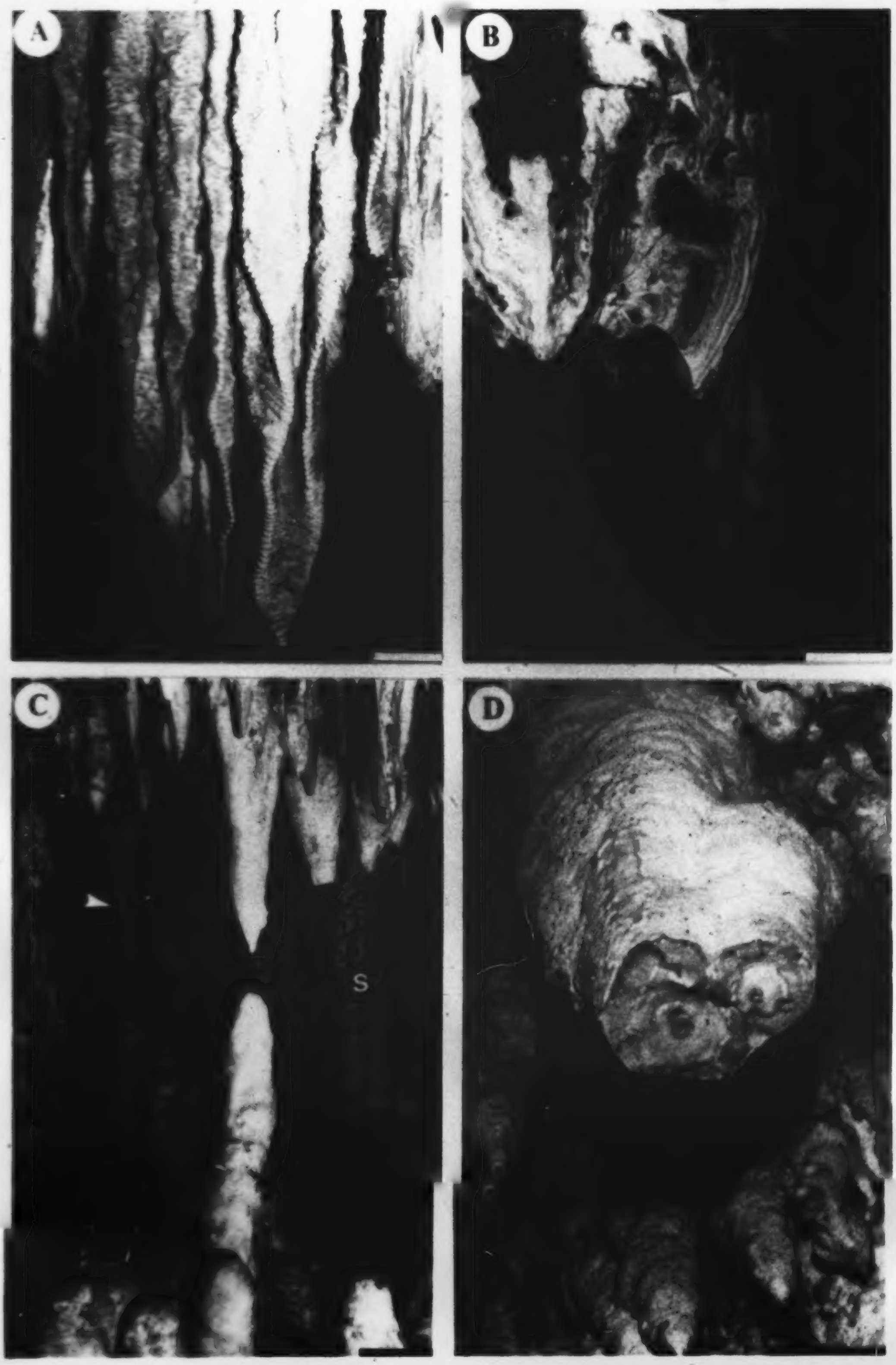
A
B
C
S
D

PLATE 2

(A) Fractured stalagmite showing the geometry of the internal calcite laminae, note that they do not form concentric structures as do the stalactites (Old Man Bay Village Caves). Scale bar = 15 cm.

(B) Dense growth of stalactites, many of which still display the central soda straw. Growth was so dense, that many of the stalactites have laterally coalesced to form a composite structure (Old Man Bay Village Caves). Scale bar = 25 cm.

(C) A loose block of the Bluff Formation showing preserved speleothems. The concentric laminae and the characteristic sinter tube indicate that these speleothems are inverted stalactites (High Rock Quarry). Scale bar = 5 cm.

(D) Horizontal flowstone filling former solution conduits in a loose block of the Bluff Formation (Pedro Castle Quarry). Hand lens for scale.

(E) Large saw tooth sinter 'flag', note the well developed crenulations along the entire length of the speleothem (Old Man Bay Village Caves). Scale bar = 25 cm.

(F) Massive flowstone formation, which shows the beginning of a 'meduse deposit'. Note the cuspate growth which develops as increased CO_2 degassing on protuberances, leads to enhanced calcite precipitation (Old Man Bay Village Caves). Scale bar = 20 cm.

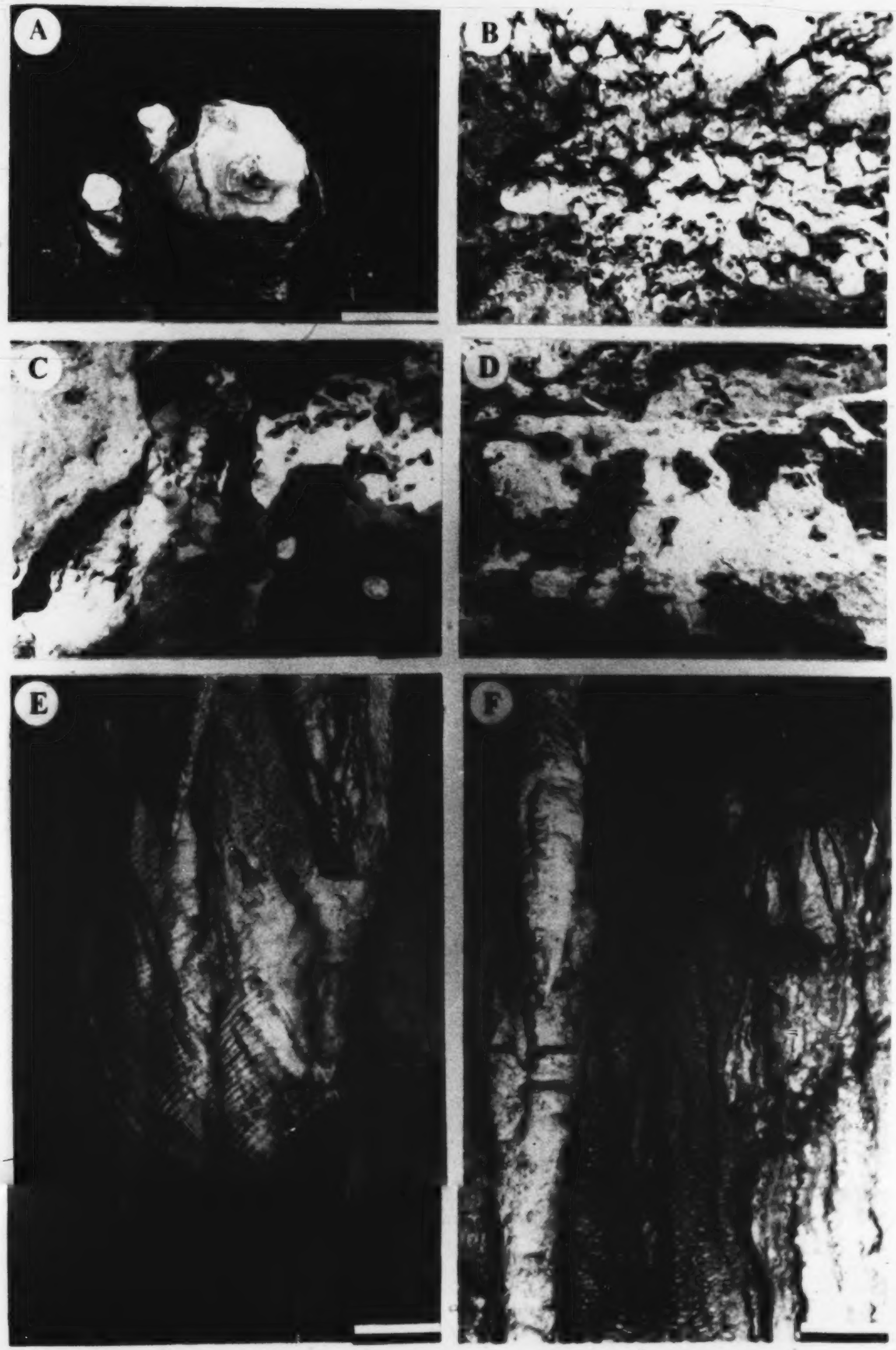
A
B
C
D
E
F

PLATE 3

(A) Unusual cave deposit formed of fragmented stalactites, which have collected as debris on the cave floor, and later become lithified. Note the coarse cave sediment which fills the interstices between the fragmented stalactites (Old Man Bay Village Caves). Scale bar = 10 cm.

(B) A two cycle cave; the upper elliptical phreatic tube (PT) shows many well developed phreatic speleogens i.e. solution pockets and ceiling scallops. The lower portion of this passage shows vadose canyon incision (V), down cutting approximately 2 m (Pirate Caves). Scale bar = 1 m.

(C) Inverse solution pocket, in which pre-existing flowstone is shown corroded. This is indicative of a phreatic phase of dissolution following a vadose stage of development (Pirate Caves). Scale bar = 5 cm.

(D) Large inverse solution pocket, the lack of vertical groves inside of which, indicates that this is not a "vadose solution pocket". Note the presence of algae (arrow) growing in this low light environment (Pirate Caves). Scale bar = 25 cm.

(E) Entrance to the Pirate Caves system shows the presence of a former phreatic tube (PT) very close to the surface (possibly the result of ephemeral phreatic conditions). Note the large collapsed block (In), evidence of incasion in this particular cave system (Pirate Caves). Scale bar = 1.5 m.

(F) Large elliptical phreatic tube, showing a well formed inverse solution pocket (SP). The elliptical cross section of this passage, may be the result of some poorly defined bedding control. Evidence of later vadose downcutting (white arrow) is clearly marked (Pirate Caves). Scale bar = 15 cm.

(G) Multiple generations of flowstone filling a former solution conduit; note how the flowstone has conformed to the former topography. One of the later generations of flowstone has developed small vertical speleothems (arrow) (Pirate Caves). Scale bar = 15 cm.

(H) Former solution conduit which has been filled with laminar flowstone, is now exposed in the wall of a phreatic tube. This indicates that a late stage of phreatic dissolution has followed a period of development in the vadose zone
phreatic dissolution has followed a period of development in the vadose zone
(Pirate Caves). Scale bar = 15 cm.

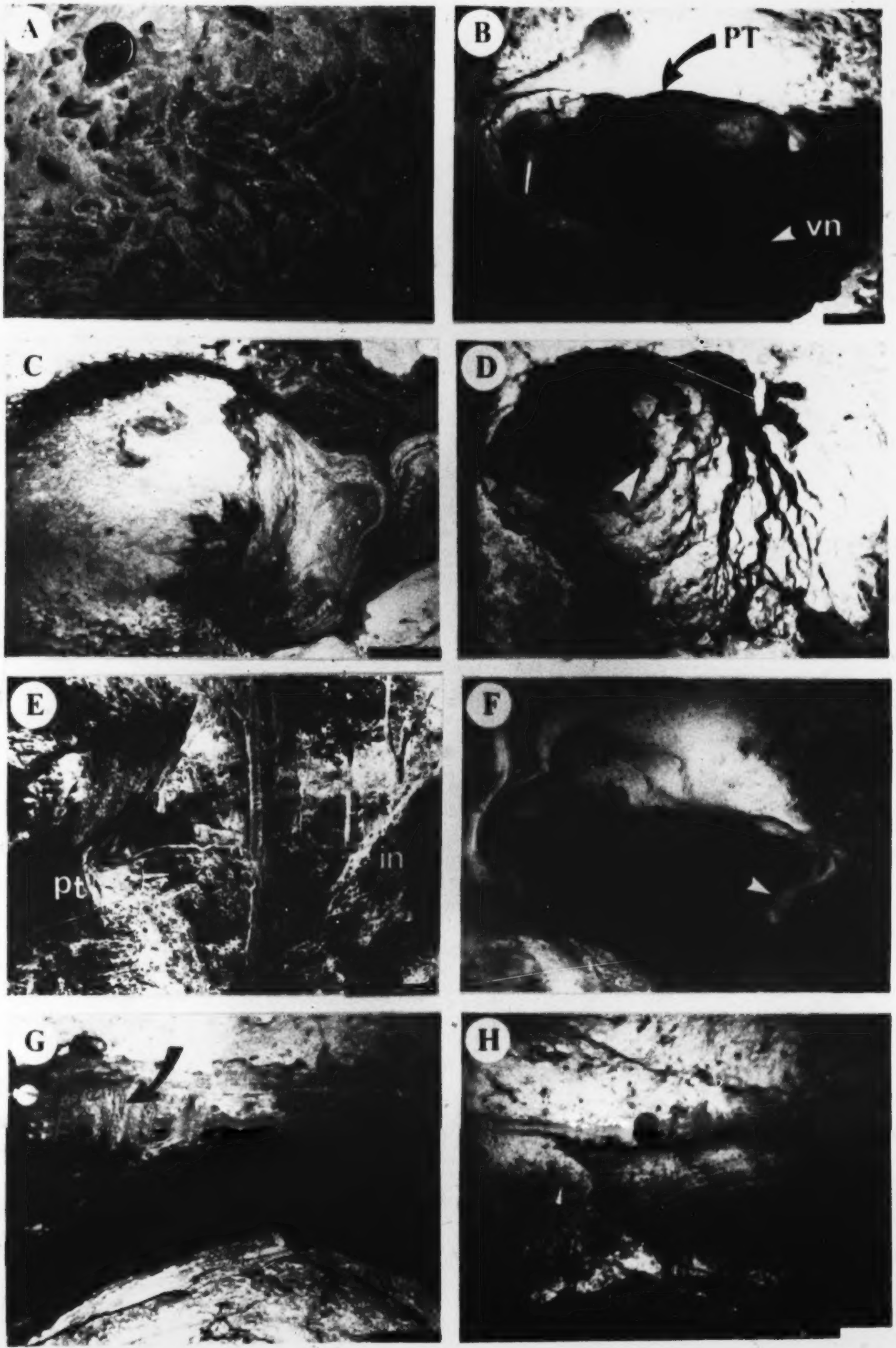
A
B
PT
vn
C
D
E
pt
in
F
G
H

PLATE 4

(A) Massive 'meduse' flowstone, with well developed rimstone deposits (RD) in the foreground. Where the gradient has become excessive, rimstone and flowstone speleothems have developed into large stalactite curtains (SC) (Old Man Bay Village Caves). Scale bar = 50 cm.

(B) Circular solution conduit cut into the host Bluff Formation, and then later filled with horizontal layers of flowstone. Note the vertical flowstone (arrow), which encrusts part of the wall of the former conduit (Pirate Caves). Scale bar = 25 cm.

(C) Large, inactive vertical solution shaft, a vadose flow feature which has been exposed in the side of the main phreatic tube. Surface water entered from above (arrow), and fell approximately 2.5 m to the lower cave level. The prominent bowl at the base of the shaft is the result of increased dissolution, probably the result of mixing corrosion (Pirate Caves). Scale bar = 50 cm.

(D) A large sinter band (arrow) has formed as a result of saturated waters flowing down the passage wall. Note the prominent banding which occurs as a result of differing impurity concentrations in the water responsible for precipitation (Old Man Bay Village Caves). Scale bar = 50 cm.

(E) Solution shaft (arrow) links two inactive cave passages. The exact origin of the shaft is unknown, but probably represents the situation where a lowered water table has caused downcutting into a lower cave level (Pirate Caves). Scale bar = 1m.

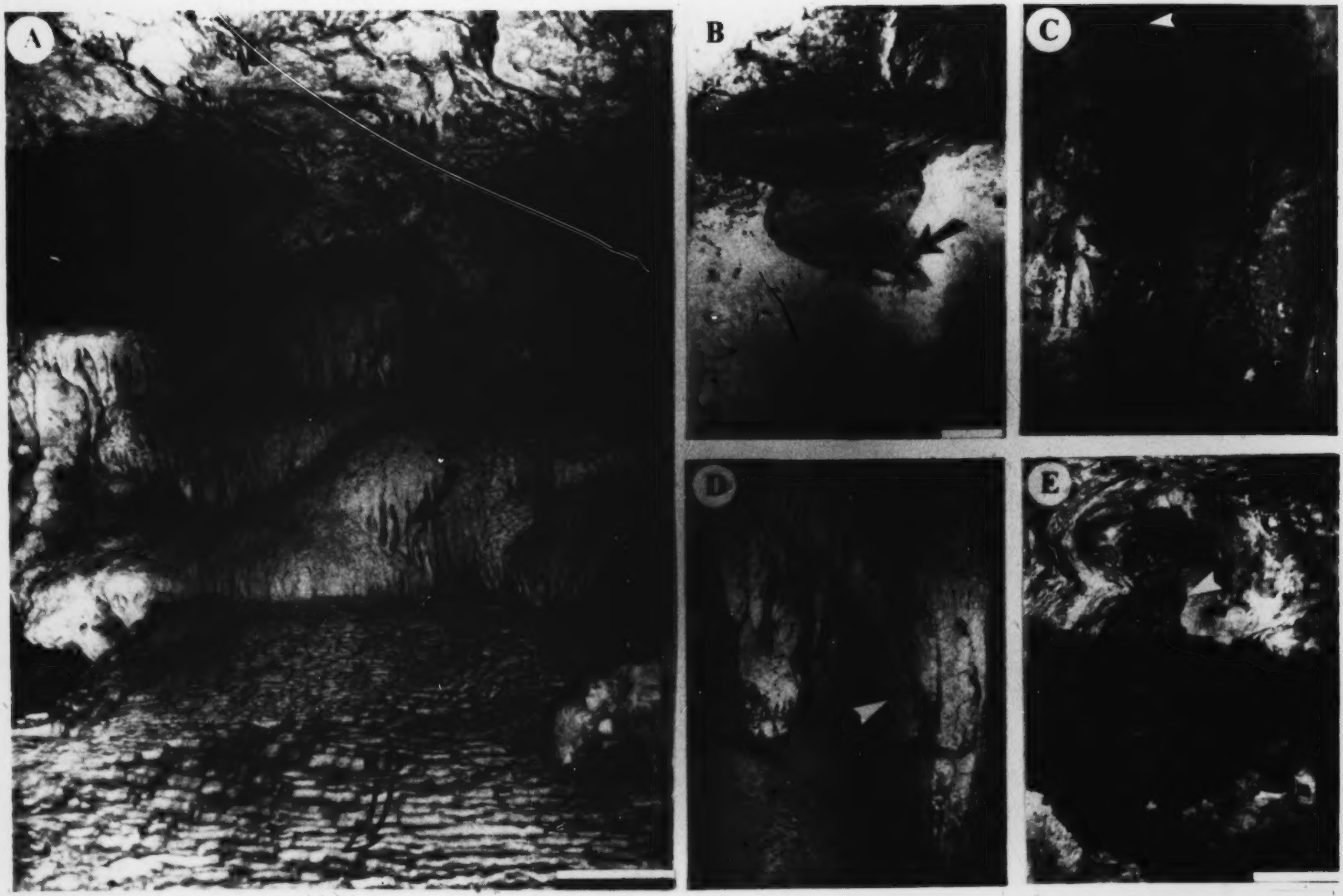
A
B
C
D
E

PLATE 5

Thin section EEQ 728a, showing a thick accumulation of laminated internal sediment (LS) between vertical speleothems (VS). To the left, the sediment has truncated the crystals (TC), while to the right, the sediment is draped over the crystal terminations (DS). The lower portion represents a well developed flowstone, with inclusion rich (IR) and inclusion free (IF) calcite. Growth banding (GB) and palisade calcite (PC) are shown. Scale bar = 4 mm.

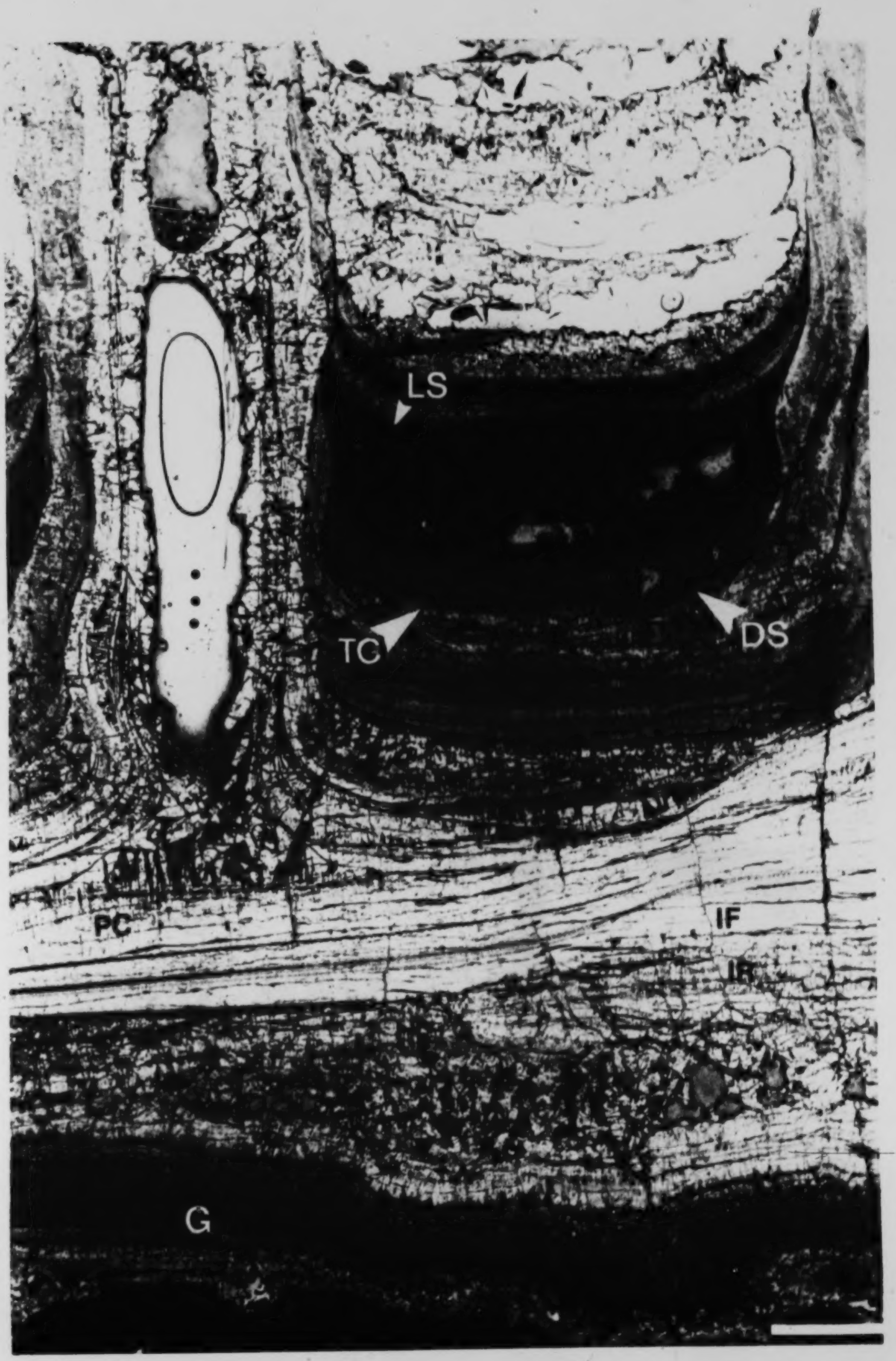
LS
TC
DS
PC
IF
IR
G

PLATE 6

Thin section EEQ 726a showing palisade calcite (PC), with growth banding (GB) defined by internal sediment. Above the palisade calcite, algal filaments (AF) form a prominent 'rafted zone'. Following this zone, there is a succession of radiating calcite bundles (RB) and finally trigonal crystals (TC) in the uppermost part of the thin section. Scale bar = 5 mm.

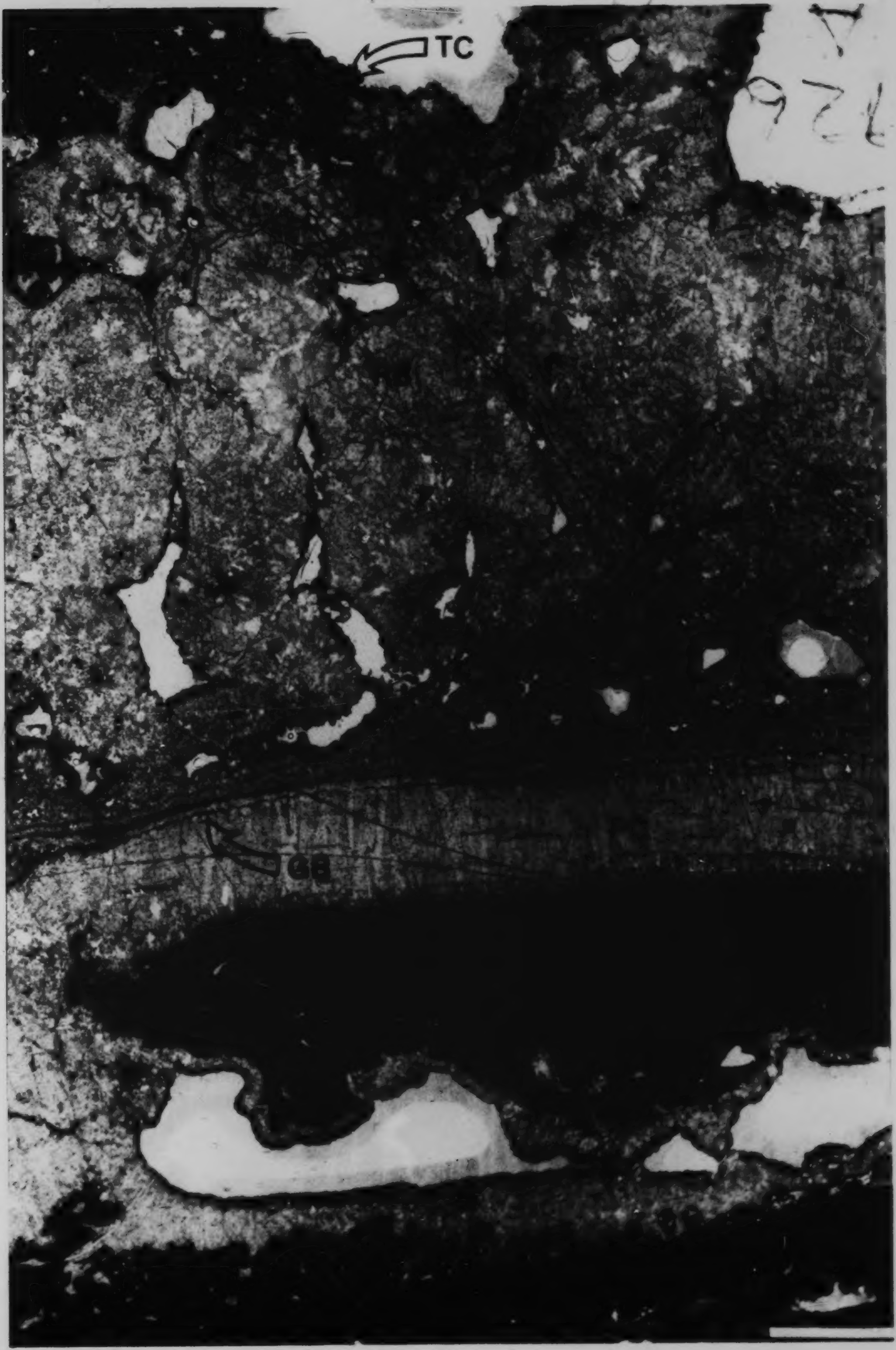
TC
GB
126
A

PLATE 7

(A) A marked change in calcite morphology occurs at the truncation of the lower growth surface. Crystal growth following the period of erosion is clearly inclusion rich. Scanning electron micrograph (Sample CIQ 1291). Scale bar = 20 µm.

(B) Boundary between inclusion poor to inclusion rich calcite. The change in morphology is not marked by a truncation, but is possibly a growth hiatus incorporating an influx of organic material. Scanning electron micrograph (Sample CIQ 1291). Scale bar = 10 µm.

(C) Former crystallographic faces are defined by an abundance of inclusion rich growth bands, of varying density and type. Photomicrograph, crossed nicols (Sample EEQ 726). Scale bar = 150 µm.

(D) Master crystal with well developed crystallites (C) . Note the growth phases defined by type III inclusions (I) (Kendall and Broughton, 1978). Photomicrograph, crossed nicols (Sample EEQ 726). Scale bar = 300 µm.

(E) Detailed view of very fine, sharply defined type III inclusions. Photomicrograph, plane polarized light (Sample EEQ 726). Scale bar = 100 µm.

(F) Change from type V inclusion rich calcite to type VI inclusion free calcite. Photomicrograph, plane polarized light (Sample EEQ 728). Scale bar = 240 µm.

(G) Former crystallographic faces defined by organic rich zones, contain abundant elongate inclusions. Note the asymmetric development of organic accumulation and inclusion growth. Photomicrograph, plane polarized light (Sample EEQ 726). Scale bar = 120 µm.

(H) Detailed view of G showing that the principal direction of growth, parallel to the inclusion, is not normal to the crystallographic faces. Photomicrograph, plane polarized light (Sample EEQ 726). Scale bar = 30 µm.

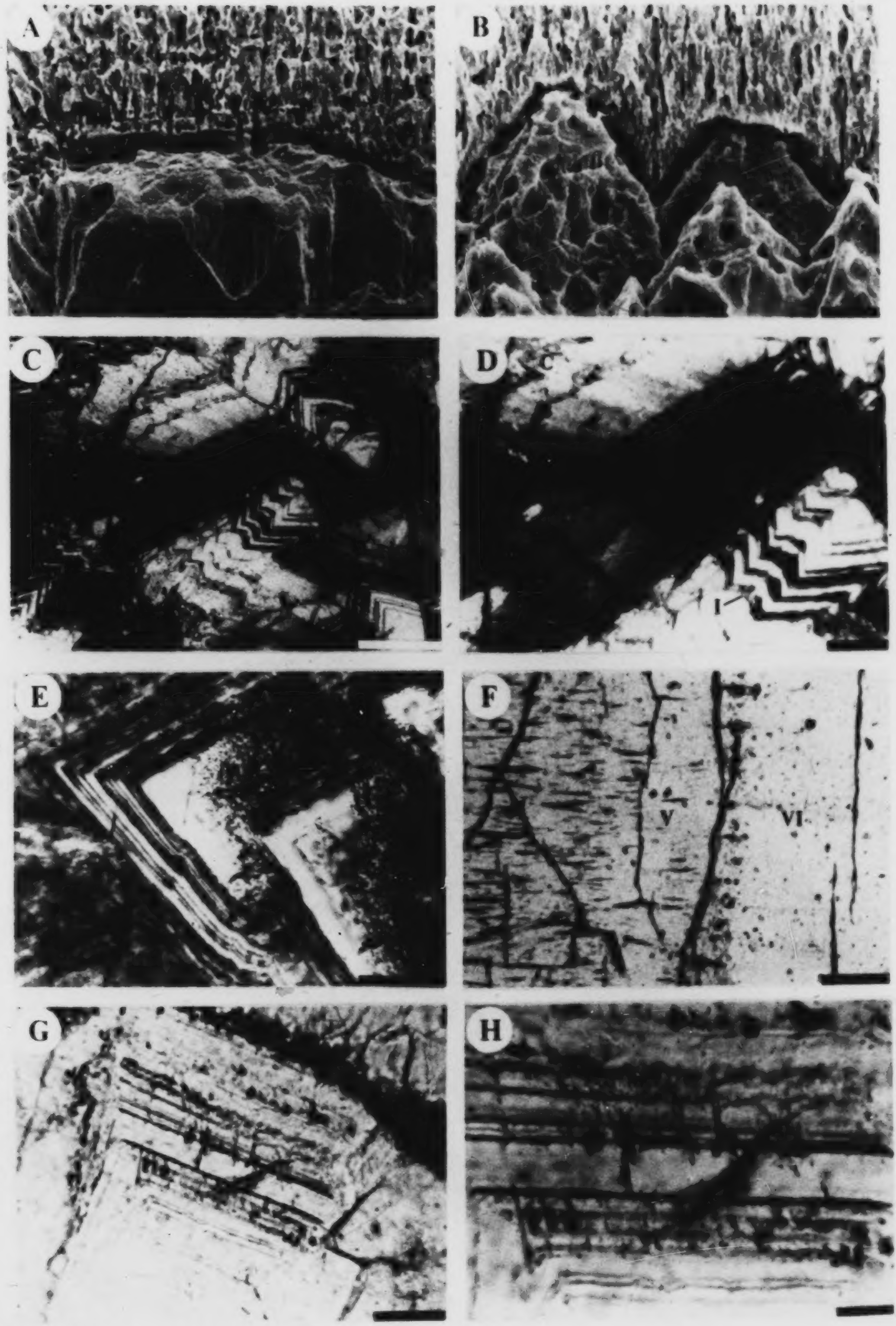
A
B
C
D
c
I
E
F
V
VI
G
H

PLATE 8

(A) Well developed palisade calcite crystal fabric with individual crystals having rhombohedral terminations. Photomicrograph, crossed nicols (Sample EEQ 726). Scale bar = 100 µm.

(B) End on view of a possible screw dislocation; note the well formed centrally located pit, which represents the axis of the dislocation. Scanning electron micrograph (Sample EEQ 728). Scale bar = 4 µm.

(C) Well formed asymmetrical inclusion pattern on both the large crystal terminations. One side of each crystal shows a more abundant and random arrangement of inclusions. Photomicrograph, plane polarized light (Sample EEQ 726). Scale bar = 100 µm.

(D) Spindle or needle like inclusions developed parallel to the principal direction of growth. Note the elliptical holes (H) developed in three of the inclusions. Scanning electron micrograph (Sample EEQ 1219). Scale bar = 40 µm.

(E) Example of a bifurcating inclusion, in this instance, the inclusion bifurcates in the direction of growth.Scanning electron micrograph (Sample EEQ 1219). Scale bar = 40 µm.

(F) Submicron calcite crystals (C) deposited on a truncated growth surface (TS). Organic material present at this interface has been removed during the etching process. Scanning electron micrograph (Sample EEQ 1219). Scale bar = 1 µm.

(G) Crystallographic faces defined by detrital organic material (O). Scanning electron micrograph (Sample EEQ 726) Scale bar = 1 µm.

(H) Former crystallographic faces, once defined by an abundance of organic material, are now represented by void spaces (V). Scanning electron micrograph (Sample EEQ 726). Scale bar = 20 µm.

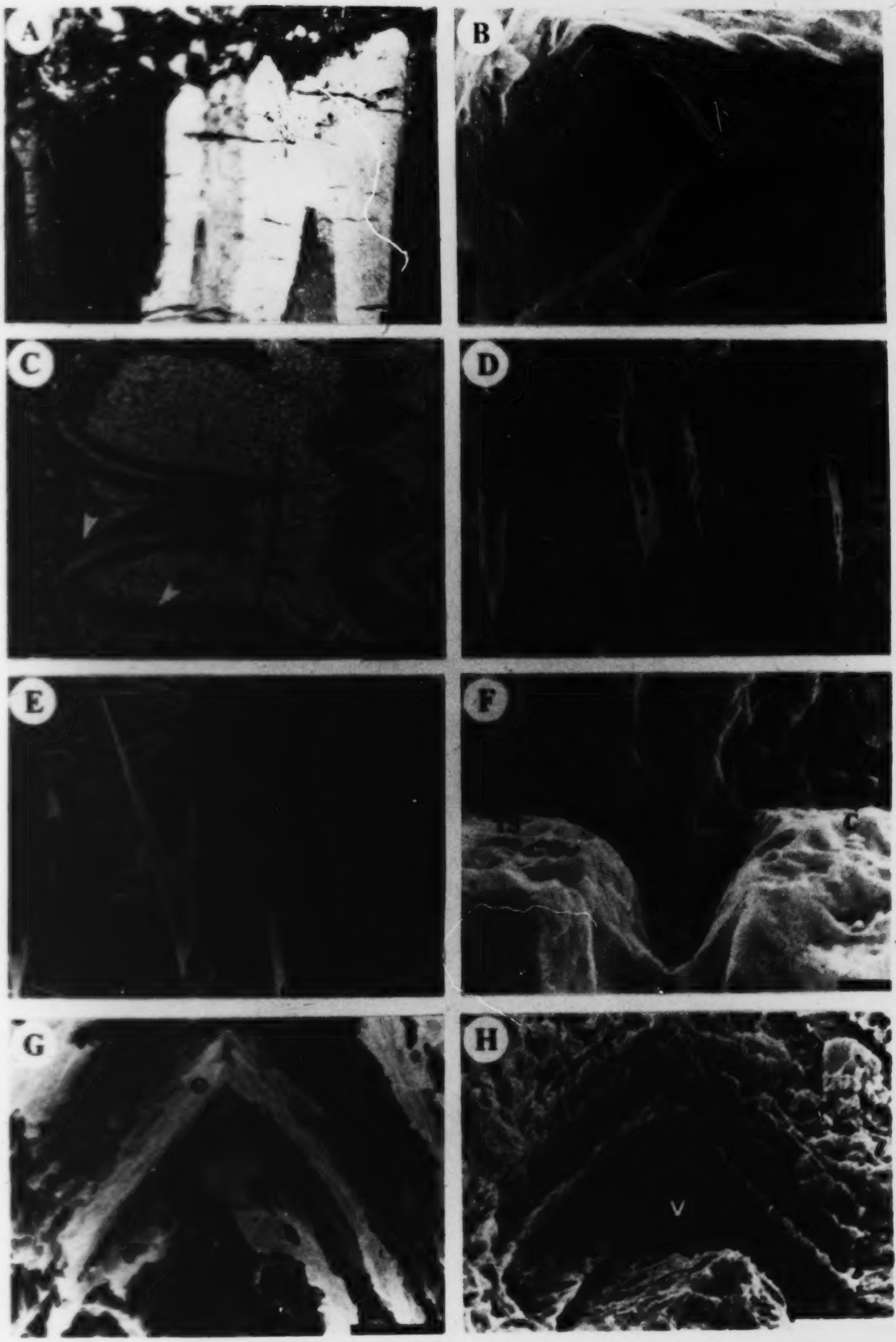
A
B
C
D
E
F
C
G
H
V

PLATE 9

(A) Large, well defined inclined inclusion, propagated from the juncture between two truncated crystals. The inclination of the inclusion marks the principal growth direction. Scanning electron micrograph Scanning electron micrograph (Sample EEQ 726). Scale bar = 10 µm.

(B) Cross cutting, pseudo-pleochroic type II inclusion bands, thought to be the result of differential flow rates over the exterior of the stalactite. Photomicrograph, plane polarized light (Sample EEQ 1220b). Scale bar = 200 µm.

(C) Former crystal growth surfaces have been truncated at right angles to the principal growth direction, by intensive physical and/or chemical erosion. The final stage of crystal growth, before a major change in crystal morphology, is marked by an organic rich zone. Photomicrograph, plane polarized light (Sample EEQ 726b). Scale bar = 60 µm.

(D) Negative print from thin section 1241 showing calcite crystal shrubs (S), which are probably the result of fluid 'ponding' above the disconformity surface (D). Scale bar = 2 mm.

(E) Former crystal growth surface has been truncated by the laminated internal sediment fill. Note how disordered the crystal growth is following each sucessive organic fill. Photomicrograph, plane polarized light (Sample EEQ 728). Scale bar = 300 µm.

(F) Thick deposit of internal sediment, which has planed off the columnar crystals to produce distincdy square tipped crystals. Photomicrograph, plane polarized light (Sample EEQ 728). Scale bar = 300 µm.

(G) Ragged, uneven crystals with square terminations, overlain by a thick deposit of internal sediment. Note the change in crystal morphology as calcite resumes growth above the sediment layer. Photomicrograph, plane polarized light (Sample EEQ 728). Scale bar = 300 µm.

(H) Presence of organic material (O) between scalenohedral crystal terminations, has a marked effect upon the morphology of the proceeding calcite crystal growth. Photomicrograph, plane polarized light (Sample EEQ 1219). Scale bar = 150 µm.

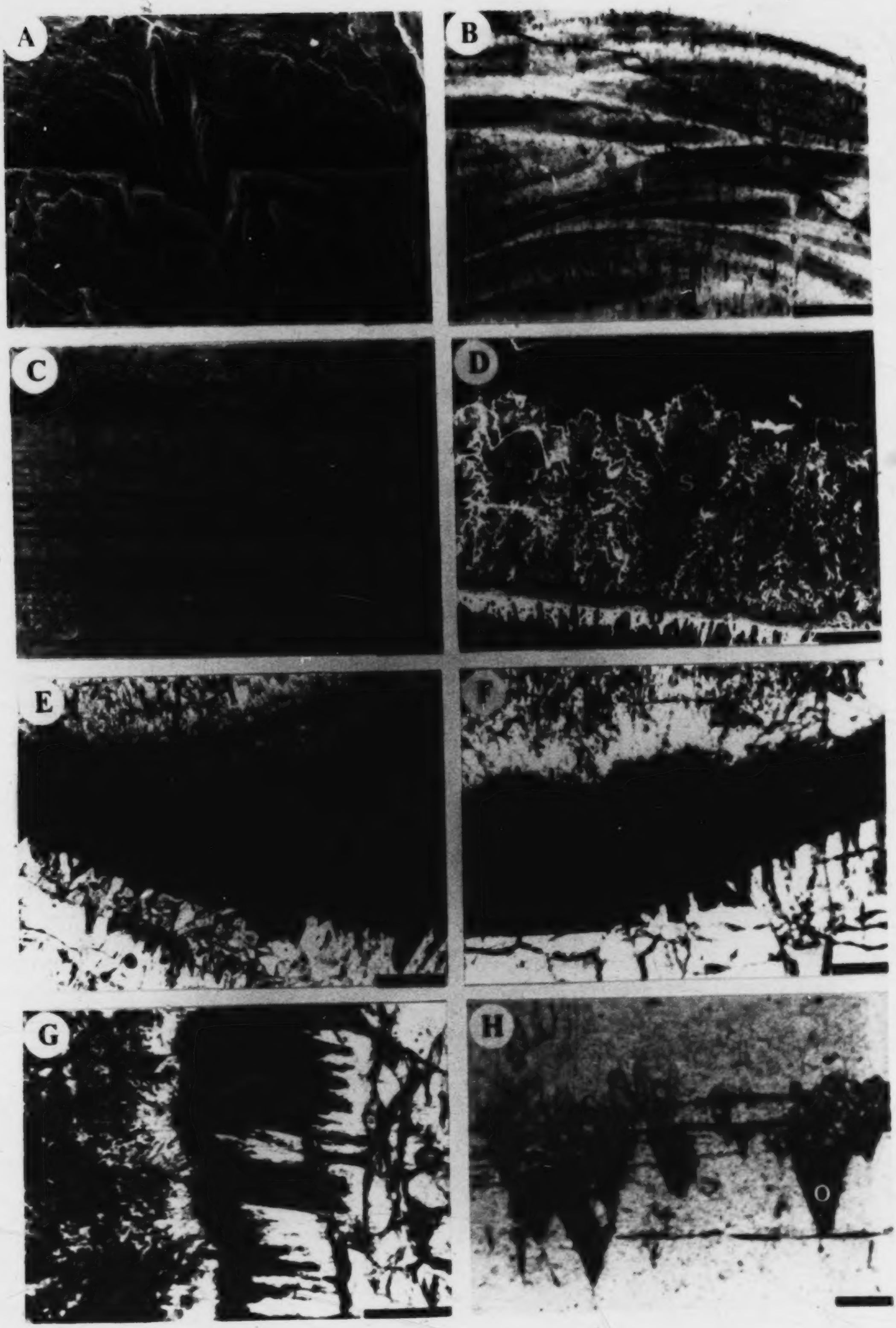
A
B
C
D
S
E
F
G
H
S
O

PLATE 10

(A) Layer of 'perched' internal sediment, which produces a marked change in the crystal morphology. Below the sediment are large well formed palisade crystals, while above the sediment, the crystal morphology consists of small, disorientated 'fibres'. Photomicrograph, plane polarized light (Sample EEQ 1220). Scale bar = 150 µm.

(B) Same field of view as A. The new crystal growth above the internal sediment, which have a different crystallographic orientation, are length slow. Photomicrograph, crossed nicols (Sample EEQ 1220). Scale bar = 150 µm.

(C) Palisade calcite crystal terminations, with accumulation of organic detritus in the intercrystalline voids. Scanning electron micrograph (Sample EEQ 1219). Scale bar = 100 µm.

(D) Enlarged view of plate VI (C), detailing the nature of the organic material which drastically alters crystal growth morphology . Scanning electron micrograph (Sample EEQ 1219). Scale bar = 20 µm.

(E) Mottled or 'patchy' extinction pattern, characteristic of zones where asymmetrical crystals (A) have developed. Photomicrograph, crossed nicols (Sample CIQ 1252a). Scale bar = 150 µm.

(F) Asymmetrical crystals showing markedly curved crystal boundaries (CB). Photomicrograph, plane polarized light (Sample CIQ 1252a). Scale bar = 200 µm.

(G) Calcite crystals with interpenetrant margins and digitate processes extending in the direction of growth. Photomicrograph, crossed nicols (Sample EEQ 726b). Scale bar = 150 µm.

(H) Calcite crystals showing the characteristic radial growth pattern of stalactites. Note hoe the crystallites have coalesced to form 'ragged' compromise boundaries. Photomicrograph, crossed nicols (Sample EEQ 1220b). Scale bar = 200 µm.

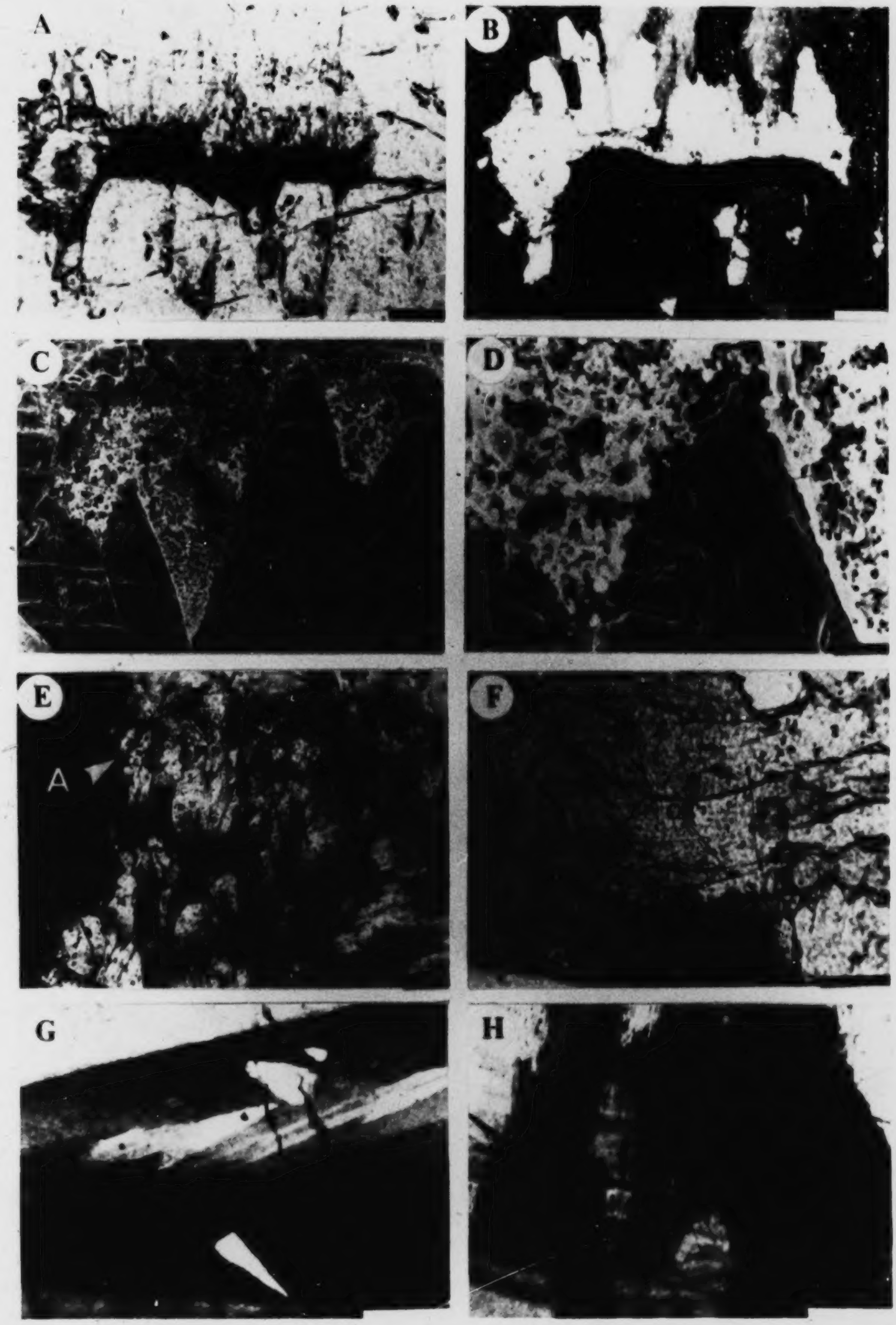
A
B
C
D
E
A
F
G
H

PLATE 11

(A) Detailed view of crystallites which propagated on a well defined crystal termination. Note that the crystallites do not develop perpendicular to the growth surface, but retain a considerable degree of 'lattice information' from the parent crystal (Sample EEQ 726b). Scale bar = 40 µm.

(B) A distinctive change in morphology from the lower zone, in which lateral crystallite coalescence has been relatively complete, to an upper zone in which lateral crystallite coalescence has been relatively incomplete. Photomicrograph, crossed nicols (Sample EEQ 728). Scale bar = 100 µm.

(C) Trigonal crystals defined by organic rich growth bands, showing numerous 'parasitic crystallites' (arrow). Photomicrograph, plane polarized light (Sample EEQ 726). Scale bar = 140 µm.

(D) Extinction pattern highlights the individual crystallographic nature of both the host crystal and the crystallite. Photomicrograph, crossed nicols (Sample EEQ 726). Scale bar = 140 µm.

(E) Trigonal crystal morphology highlighted by the etching of the thin section. Note the multiple crystallite propagation in the lower potion of the photomicrograph. Photomicrograph, plane polarized light (Sample CIQ 1252). Scale bar = 120 µm.

(F) Laterally interfering trigonal crystals, one of which displays a well formed parasitic crystal (arrow). Scanning electron micrograph (Sample EEQ 726). Scale bar = 50 µm.

(G) Enlarged view of plate F, showing the manner in which the parasitic grow on the flanks of the host crystal. Scanning electron micrograph (Sample EEQ 726). Scale bar = 40 µm.

(H) Three dimensional view of a trigonal host crystal, or master crystal (MC), with numerous secondary, or parasitic crystallites (SC) growing on its flanks. Scanning electron micrograph (Sample EEQ 1069). Scale bar = 50 µm.

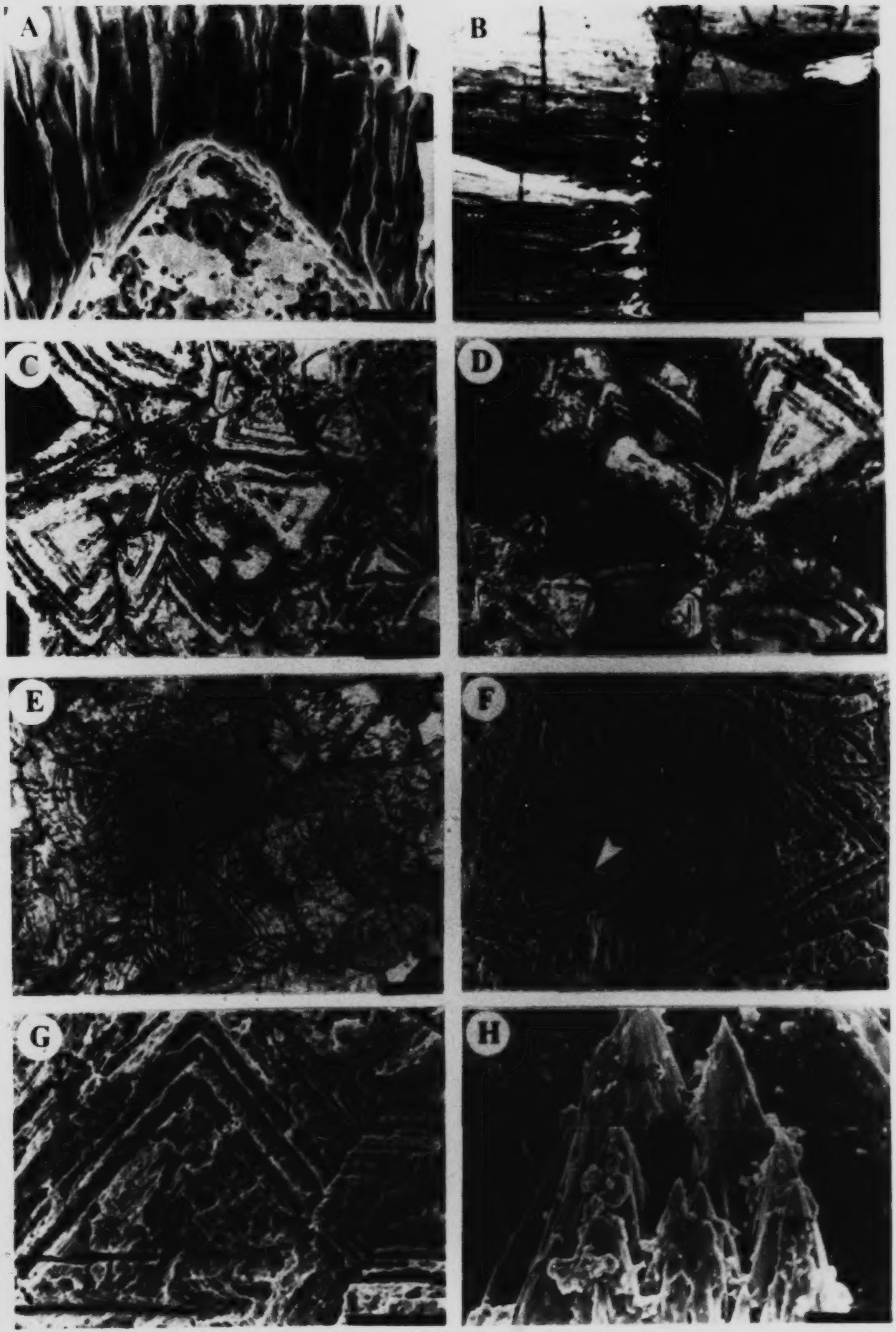
A
B
C
D
E
F
G
H

PLATE 12

(A) Profusion of syntaxial overgrowth crystallites growing on the flanks of the larger host crystal. Scanning electron micrograph (Sample EEQ 728). Scale bar = 20 μm.

(B) Columnar crystals seen parallel to the {001} plane, with prominent dissolution features between individual crystals, highlighted by etching with HCl. Scanning electron micrograph (Sample EEQ 726b). Scale bar = 100 μm.

(C) A prominent 'carina' structure (arrow) developed at the regular intervals along the crystal boundaries. Scanning electron micrograph (Sample EEQ 726b). Scale bar = 25 μm.

(D) Enlarged view of the 'carina' structure which is formed from a succession of individual solution pits (arrow). Scanning electron micrograph (Sample EEQ 726b). Scale bar = 10 μm.

(E) Columnar crystals viewed perpendicular to the {001} plane, highlighting the trigonal nature of these crystals, and the control that this has on the morphology of the intercrystalline pore space. Photomicrograph, plane polarized light (Sample EEQ 728). Scale bar = 200 μm.

(F) An ordered arrangement of trigonal intercrystalline pore space, which produces a very distinctive pattern of voids. Scanning electron micrograph (Sample CIQ 1252). Scale bar = 20 μm.

(G) Enlarged view of trigonal intercrystalline pore space. Scanning electron micrograph (Sample CIQ 1252). Scale bar = 20 μm.

(H) More elongate intercrystalline void space occurs, as the section through the crystals is more oblique to the c-axis. Scanning electron micrograph (Sample CIQ 1252). Scale bar = 10 μm.

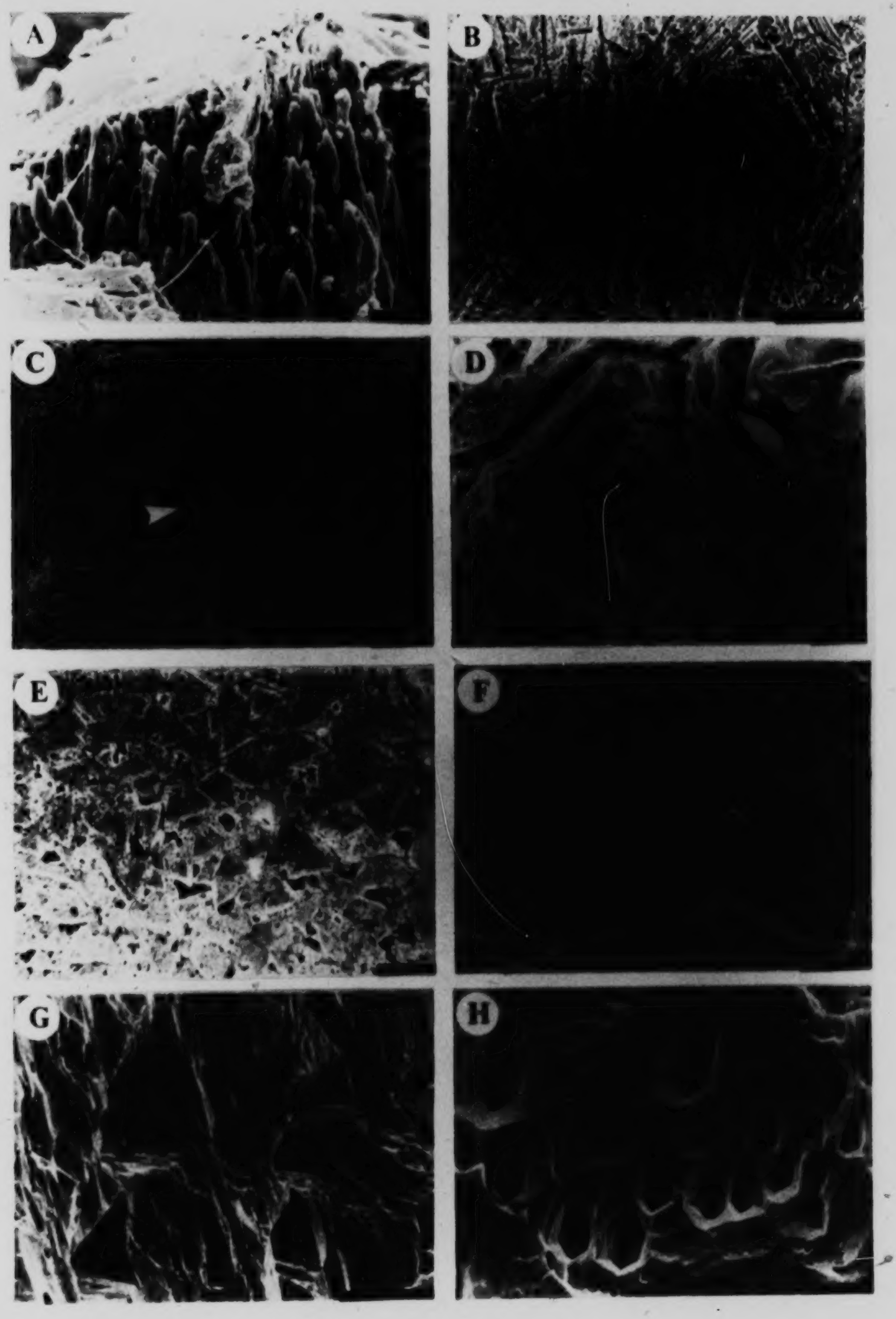
A
B
C
D
E
F
G
H

PLATE 13

(A) A large bacterial 'clump' developed above a disconformity in the crystal growth. The disconformity surface is marked by an abundance of amorphous organic material. Photomicrograph, plane polarized light (Sample EEQ 1219). Scale bar = 150 µm.

(B) 'Ring' accumulations of organic material, possibly a cross section through either an algal filament or stem of a higher taxonomic plant form eg. a 'moss stalk'. Photomicrograph, plane polarized light (Sample EEQ 728). Scale bar = 200 µm.

(C) Bacterial peloids have accumulated between two large composite calcite crystals (C), as coarse internal sediment. Photomicrograph, plane polarized light (Sample CIQ 1250). Scale bar = 200 µm.

(D) Bacterial clumps acting as a nucleus for the growth of calcite spherocrystals. Photomicrograph, crossed nicols (Sample CIQ 1250). Scale bar = 150 µm.

(E) Elliptical ring structure with a central zone of organic rich xenotopic calcite. Photomicrograph, plane polarized light (Sample CIQ 1250). Scale bar = 150 µm.

(F) Crystals seeded upon the bacterial clumps follow the curved morphology of the substrate, resulting in a divergent pattern of crystal growth. Photomicrograph, crossed nicols (Sample CIQ 1250). Scale bar = 150 µm.

(G) Large, very dense bacterial clump, which acts as a nucleus for a large spherocrystal. Photomicrograph, crossed nicols (Sample EEQ 726). Scale bar = 350 µm.

(H) Mutually interfering crystals arising from a large a spherocrystal. These crystals have again used the bacterial clump a centre for nucleation. Photomicrograph, crossed nicols (Sample CIQ 1250). Scale bar = 150 µm.

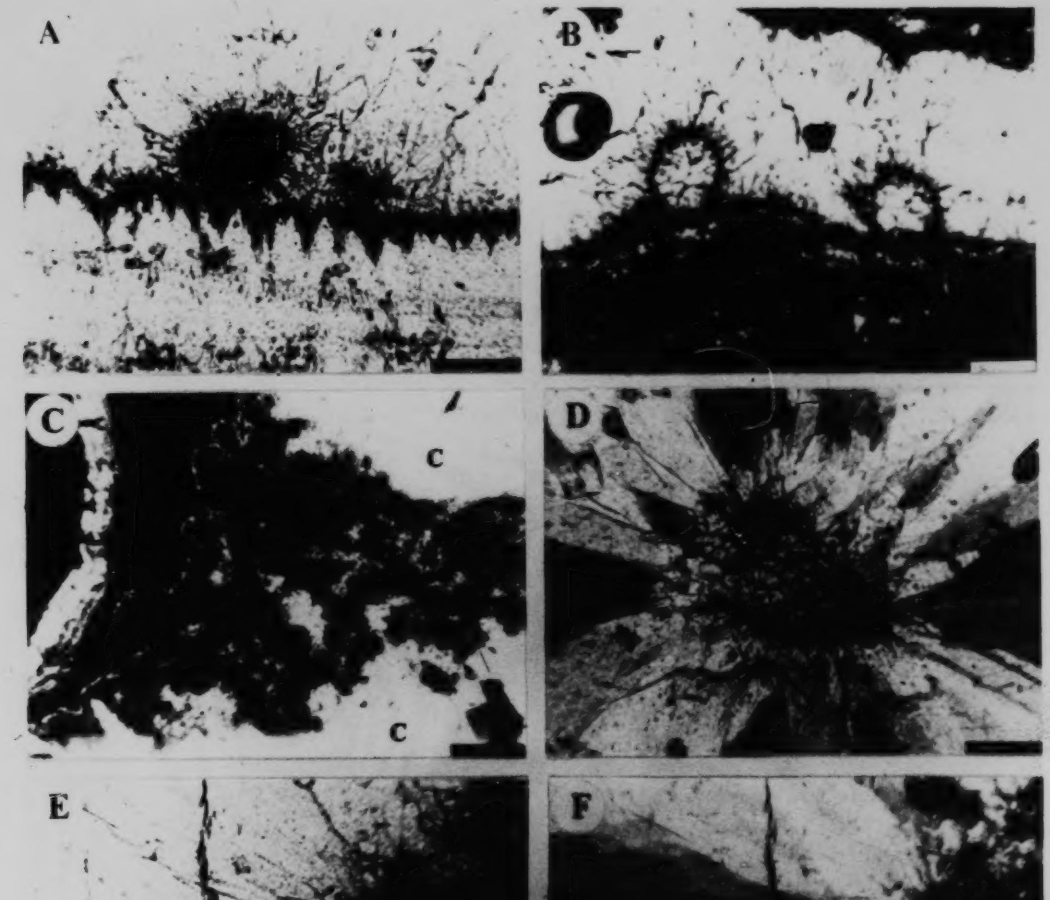
A
B
C
c
c
D
E
F
G
H

PLATE 14

(A) Preferential accumulation of organic material at the apices of the crystal terminations. This may be due to either an inorganic or organic control mechanism. Photomicrograph, plane polarized light (Sample CIQ 1250). Scale bar = 240 µm.

(B) Crystal regrowth after the organic accumulation follows the morphology of the organic substrate, producing distally divergent columnar crystals. Photomicrograph, crossed nicols (Sample CIQ 1250). Scale bar = 240 µm.

(C) Large columnar calcite crystal with organic material accumulated at its apex, the organic material has not filed the intercrystalline spaces (arrow) as would be expected under gravitational forces. Photomicrograph, plane polarized light (Sample CIQ 1250). Scale bar = 220 µm.

(D) Calcite raft with a well defined central core (arrow). Bacterial peloids have accumulated on either side of the raft. Photomicrograph, plane polarized light (Sample CIQ 1250). Scale bar = 200 µm.

(E) Dense zone of elongate bodies with many disordered cross cutting relationships. These may at first appear as branching forms of filaments, but is probably the result of a random arrangement of calcite rafts. Arrow zone is enlarged in plate F. Photomicrograph, plane polarized light (Sample CIQ 1249). Scale bar = 300 µm.

(F) Enlarged view of an elongate body, showing the well defined central core. Note how the crystal morphology changes from xenotopic microspar (MS) which surrounds the core, to coarse spar calcite (SC) between the elongate bodies. Photomicrograph, plane polarized light (Sample CIQ 1249). Scale bar = 75 µm.

(G) Enlarged view of the rounded termination of one of the elongate bodies projecting into pore space (P). Note the xenotopic nature of the microspar, and the termination of an algal filament (arrow). Scanning electron micrograph (Sample CIQ 1249). Scale bar = 40 µm.

(H) Enlarged view of the particularly small algal filament, which may form the central 'core' of the larger elongate bodies (Plate x (E)). Scanning electron micrograph (Sample CIQ 1249). Scale bar = 4 µm.

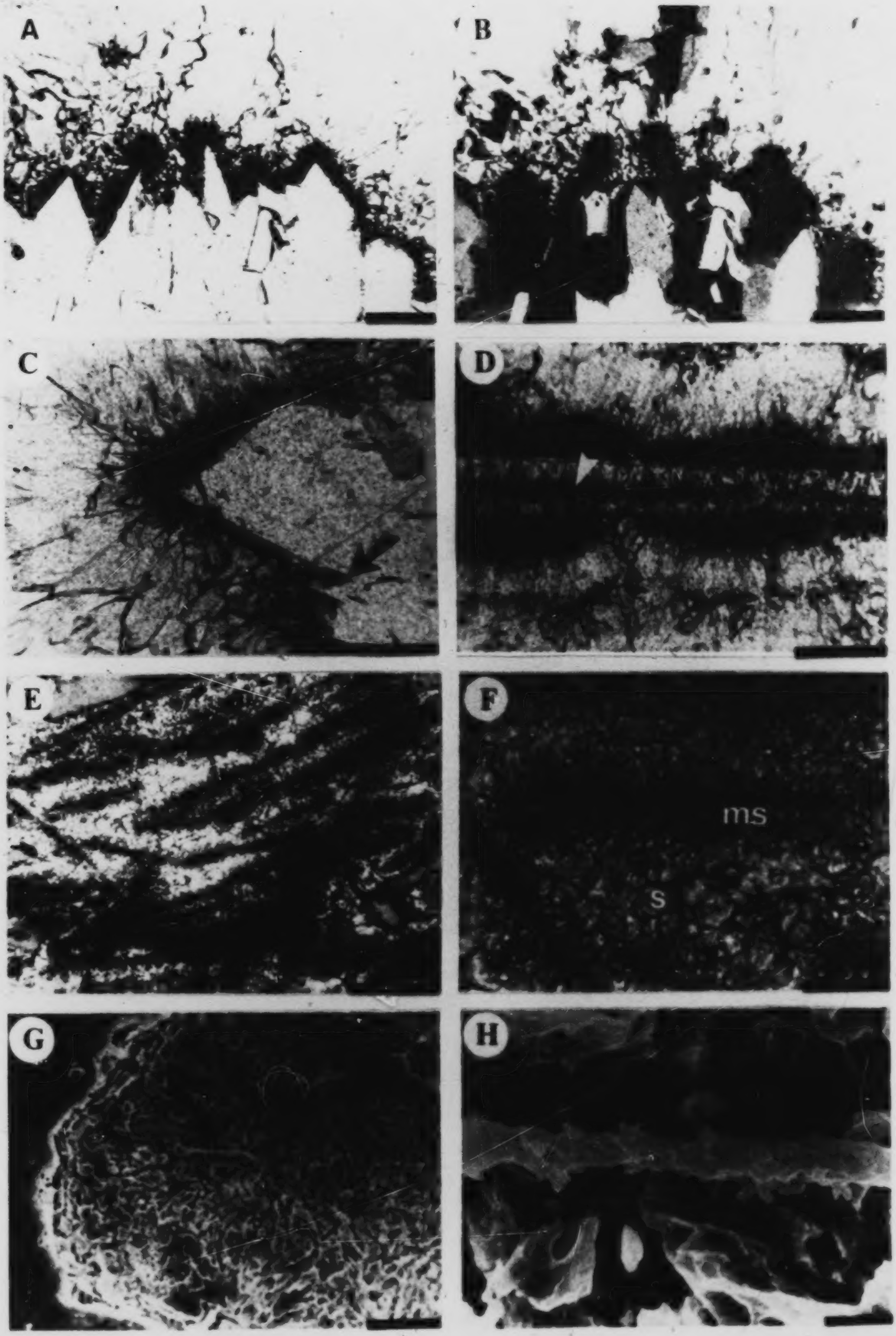
A
B
C
D
E
F
ms
s
G
H

PLATE 15

(A) Large elongate body with a poorly defined central core, which has been encrusted with microspar, and later by larger rhombohedral crystals. The larger encrusting crystals show well developed growth banding, formed during the latter stages of crystal growth. Photomicrograph, plane polarized light (Sample EEQ 726). Scale bar = 80 µm.

(B) Where two elongate bodies are juxtaposed, the advancing growth front of the overgrowth calcite will mutually interfere, forming a compromise boundary (arrow) between the two bodies. Photomicrograph, crossed nicols (Sample EEQ 726). Scale bar = 150 µm.

(C) Colony of fungal filaments attached to the surface of etched trigonal crystals. Note the characteristic dichotomous branching (arrow). Scanning electron micrograph (Sample EEQ 726). Scale bar = 100 µm.

(D) Enlarged view of the branching fungal filament, with an unusual surface morphology which may be the result of collapsed fruiting bodies. Scanning electron micrograph (Sample EEQ 726). Scale bar = 10 µm.

(E) Cluster of calcified spherules, composed of submicron to 3 µm sized calcite crystals. The fractured spherule in the foreground shows that there is no marked compositional change, or bacterial colony at the nucleus of the spherule. Scanning electron micrograph (Sample EEQ 726). Scale bar = 10 µm.

(F) Cluster of calcified spherules, ranging in size from 4 µm to 12 µm. Note the close association of an algal? filament in the upper right. Scanning electron micrograph (Sample EEQ 726). Scale bar = 10 µm.

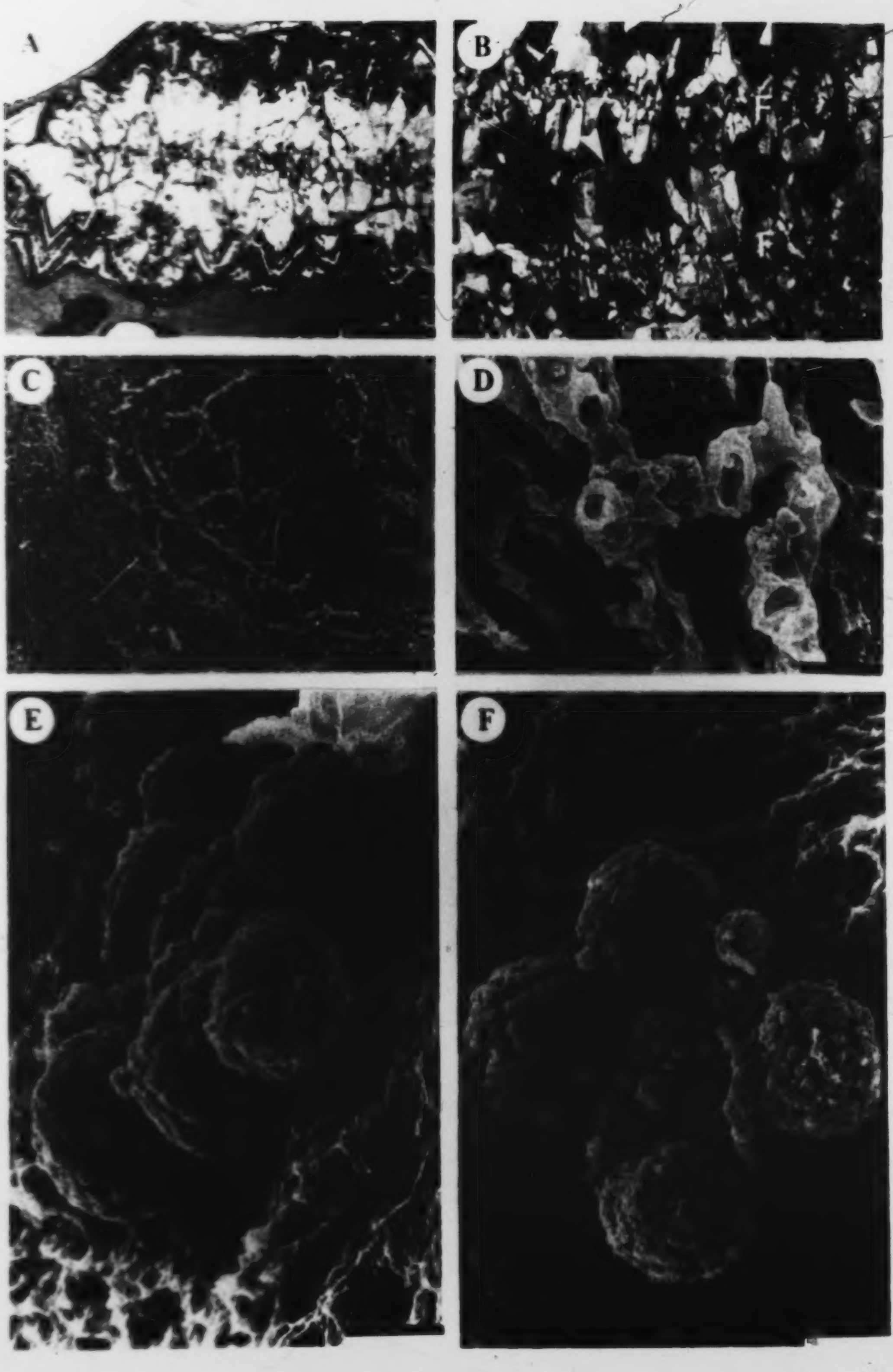
A
B
F
F
C
D
E
F

PLATE 16

(A) Linear chasmolithic alga, which has been encrusted in microspar calcite. Note the distinct lack of branching of algal body, as opposed to the fungal body. Scanning electron micrograph (Sample CIQ 1249). Scale bar = 20 µm.

(B) Enlarged view of the algal filament which showing micrite rhombs encrusting? the filament. Scanning electron micrograph (Sample CIQ 1249). Scale bar = 5 µm.

(C) Bored calcite is clear evidence of the presence of a micro-endolithic fauna within the speleothemic calcite. Note the elongate boring (white arrow) and the profusion of small spherical (fungal) bodies, in the lower left of the micrograph (black arrow). Scanning electron micrograph (Sample EEQ 728). Scale bar = 50 µm.

(D) Enlarged view of plate C, showing cross section of some microborings that do not exceed 10 µm in diameter. Scanning electron micrograph (Sample EEQ 728). Scale bar = 10 µm.

(E) Calcite raft fragment trapped in a pore throat has become encrusted in many generations of calcite cement. The central core of the raft (F) is encrusted with microspar (1), followed by an organic rich internal sediment (2), and an isopachous pore filling cement (3). Photomicrograph, plane polarized light. Scale bar = 250 µm.

(F) Early or penecontemporaneous calcification of an algal filament ?, is demonstrated by the fractured algal filament being surrounded by later calcite growth. Photomicrograph, plane polarized light. Scale bar = 50 µm.

(G) Transverse section of a Rotoliinid Foraminifera, which is found in a cavity in the speleothemic calcite. Photomicrograph, plane polarized light (Sample CIQ 1252). Scale bar = 150 µm.

(H) Medial section of a Rotoliinid Foraminifera, also discovered in a cavity fill in speleothemic calcite. Photomicrograph, plane polarized light (Sample CIQ 1252). Scale bar = 200 µm.

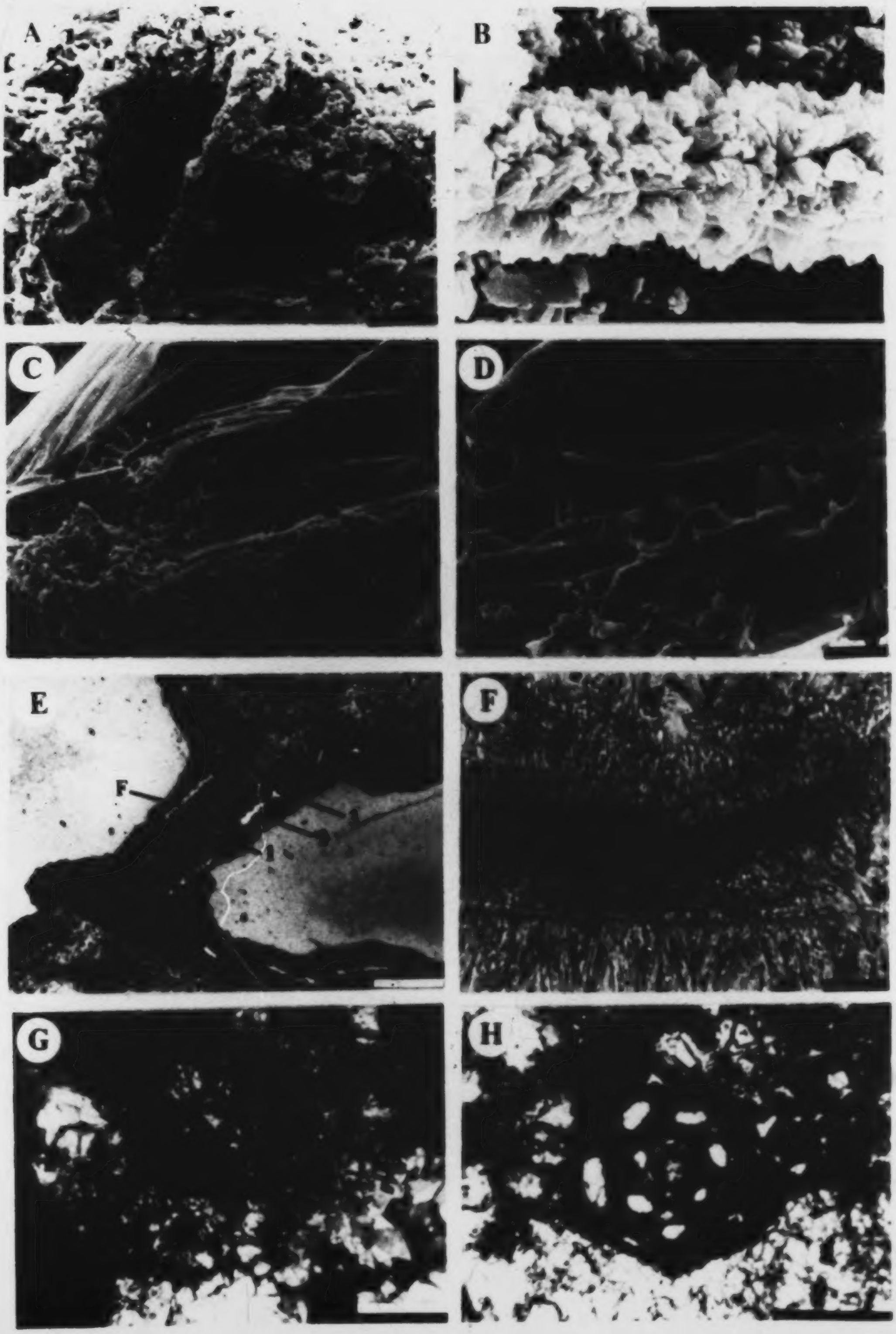
A
B
C
D
E
F
F
G
H

PLATE 17

(A) A polished slab from sample 728, from which numerous sequential micro samples were extracted for stable isotope geochemical studies (arrow = example of a microsample area). Scale bar = 1.5 cm.

(B) A polished slab from sample 1252, showing the complexity of some of the structures developed in the speleothems. Geopetal fills containing marine organisms (arrow) are found in numerous samples. Scale bar = 3 cm.

(C) A polished slab from sample 1250, with unusual accumulations of micro crystalline calcite (MC) between layers of botryoidal columnar calcite (BC). Note the abundance of terra rosa (arrow) contained in small cavities in the speleothemic calcite. Scale bar = 2.5 cm.

(D) Enlarged view of a polished slab from sample 726, shows a zone of 'rafted' algal filaments (large arrow). Above this, a zone of botryoidal calcite showing small euhedral trigonal crystals (small arrow) developed in a 'ponded' fluid. Scale bar = 1 cm.

(E) Pronounced wave cut notch (Wn), developed approximately 6 m above present day sea level (Queens' road). Scale bar = 1.5 m.

(F) Area of the Bluff Formation where there is no soil zone, and Vegetation must root directly into the bed rock (Queen's Road). Photograph courtesy Suzanne Pleydell. Scale bar = 50 cm.

(G) Section in the Bluff Formation showing terra rosa filling a cavity or joint planes (Pedro Castle Quarry). Scale bar = 1 m.

(H) Sedimentary dyke (arrow) consists of terra rosa filling a fissure in the Bluff Formation. Scale bar = 10 cm.

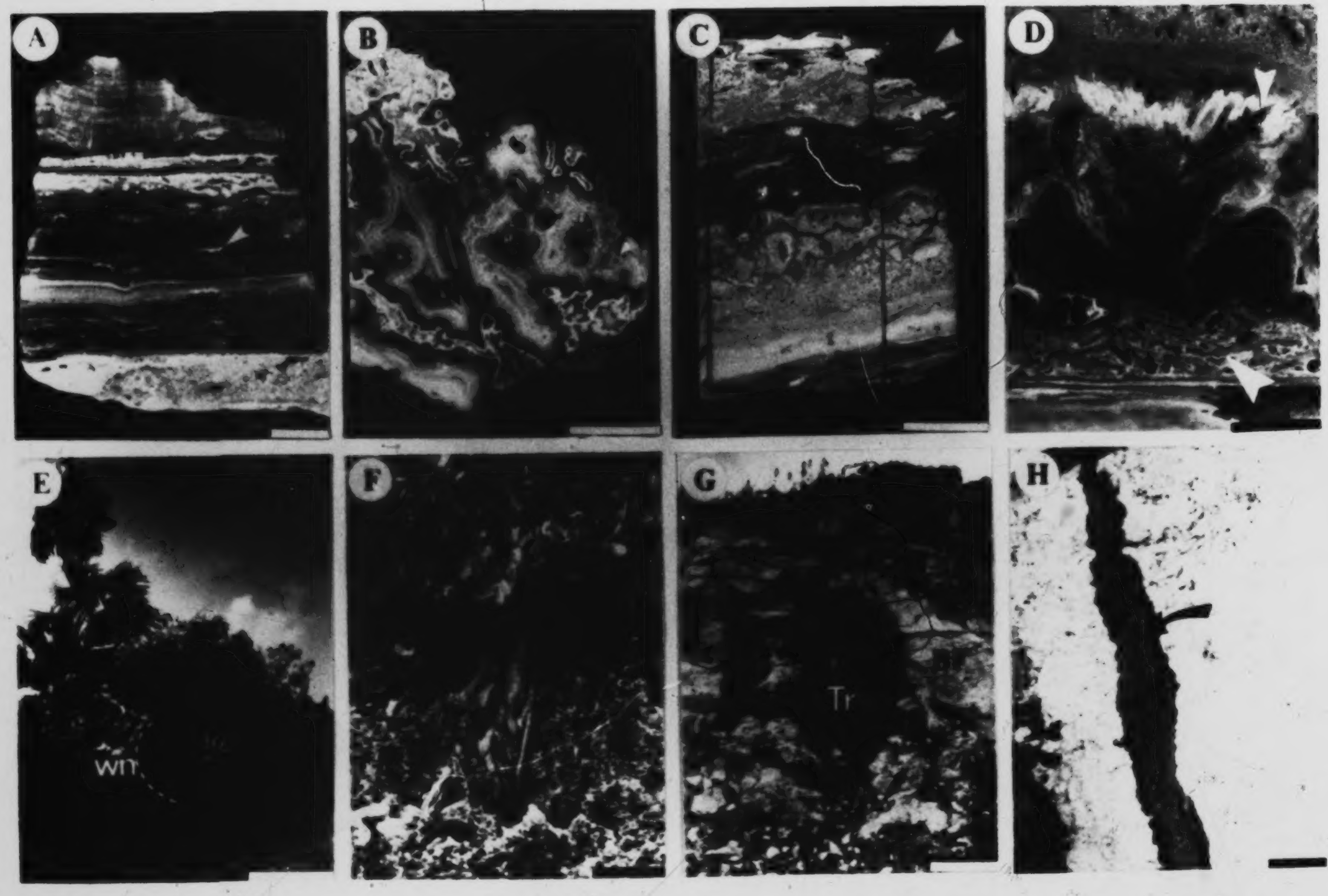
A
B
C
D
E
wn
F
G
Tr
H

PLATE 18

(A) Large elongate pore (P) with an isopachous rim cement (Rc). Large opaque organic (bacterial) clumps comprise most of the section, with numerous small pores occluded by spar cement. Photomicrograph, plane polarized light (Sample CIQ 1251a). Scale bar = 500 µm.

(B) Same view as plate A, showing the bright orange luminescent zones in the isopachous rim cement. Note the dull red/orange luminescence of the organic clumps (O). Two very similar and closely spaced occluded pores are shown, one which displays bright orange luminescence (Lp) and another which is non-luminescent (NLp). Notice that from the pore margin (Pm), in towards the centre, the luminescence is generally increasing from a dull non-descript luminescence (NL), to a bright orange banded luminescence. Cathodoluminescent photomicrograph (Sample CIQ 1251a). Scale bar = 500 µm.

(C) A marked contrast in luminescent properties exists between the speleothemic columnar calcite (Cc) and the porosity occluding cement (Po). The original pore space, with a partial fill of peloids (Pe), has now been occluded with luminescent calcite. This photomicrograph was exposed under electron excitation and transmitted light (Sample CIQ 1251b). Scale bar = 250 µm.

(D) Same view as plate C, showing a highly complex pattern of dull and bright orange luminescent zones. Note how the calcite precipitated in the centre of the pore, presumably the latest cement phase, is distinctly non-luminescent. Cathodoluminescent photomicrograph (Sample CIQ 1251b). Scale bar = 250 µm.

THE QUALITY OF THIS MICROFICHE IS HEAVILY DEPENDENT UPON THE QUALITY OF THE THESIS SUBMITTED FOR MICROFILMING.

UNFORTUNATELY THE COLOURED ILLUSTRATIONS OF THIS THESIS CAN ONLY YIELD DIFFERENT TONES OF GREY.

LA QUALITE DE CETTE MICROFICHE DEPEND GRANDEMENT DE LA QUALITE DE LA THESES SOUMISE AU MICROFILMAGE.

MALHEUREUSEMENT, LES DIFFERENTES ILLUSTRATIONS EN COULEURS DE CETTE THESES NE PEUVENT DONNER QUE DES TEINTES DE GRIS.

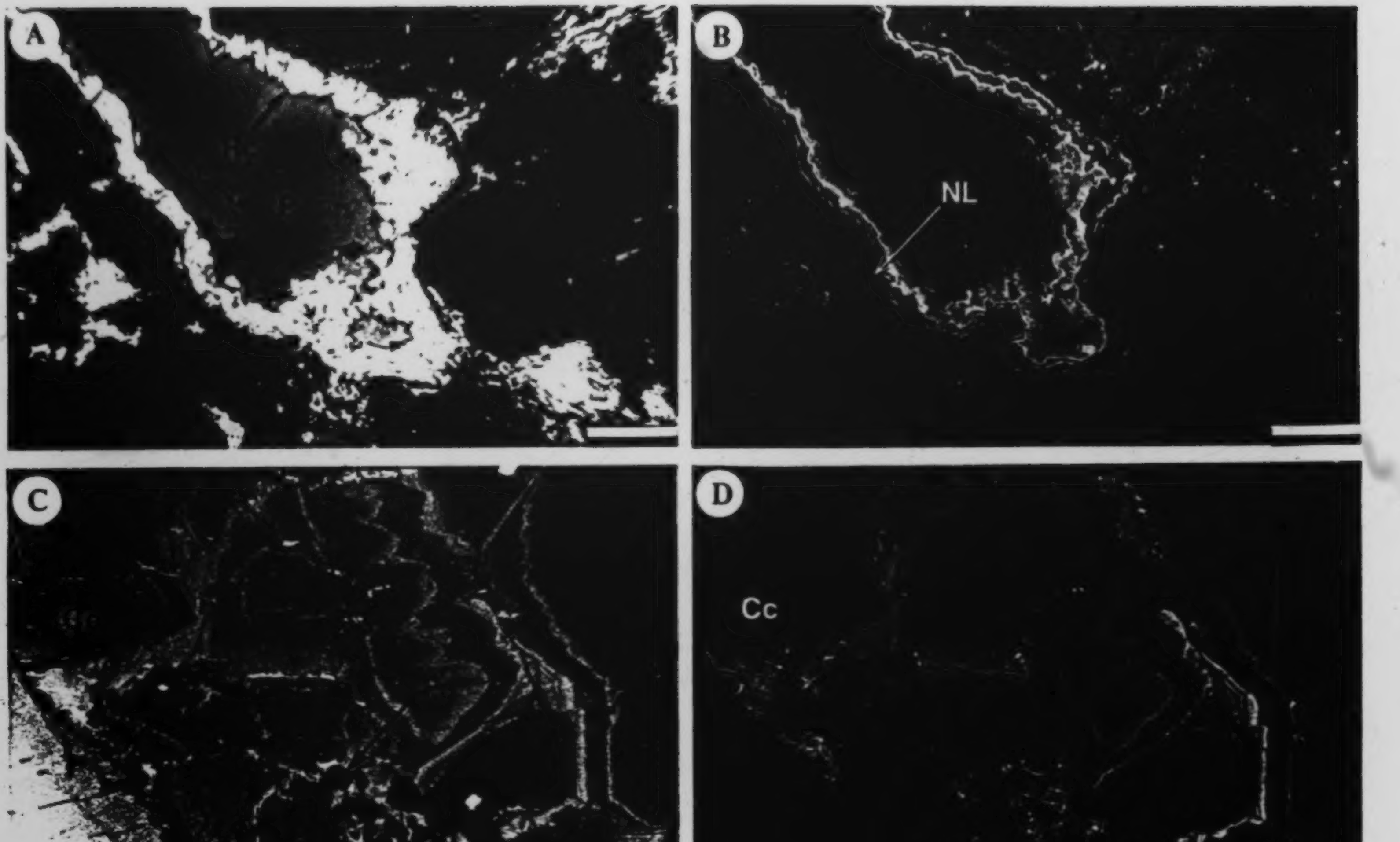
A
B
NL
C
D
Cc

PLATE 19

(A) Sharply defined, bright orange "hairline" luminescence, which reflects the spatial distribution of the impurity ions throughout the ontogeny of the crystals. Cathodoluminescent photomicrograph (Sample EEQ 1219). Scale bar = 300 µm.

(B) Speleothemic calcite (non-luminescent) has precipitated on a clast of the Bluff dolostone. The dolostone shows a rather inhomogeneous pattern of cathodoluminescent colour and intensity. Overall, the Bluff dolostone gives a dull to moderate, orange/red luminescence . Cathodoluminescent photomicrograph (Sample EEQ 726). Scale bar = 1 mm.

(C) Sample of flowstone, with a succession of well formed organic rich growth bands, which follow a relatively organic free calcite zone. Arrow marks a common point with plate D. Photomicrograph, plane polarized light (Sample 727). Scale bar = 250 µm.

(D) Same view as plate C. Note how the bright orange luminescent zones mimic the morphology of the organic rich growth bands, although they never appear to correspond directly to one another. Furthermore, the lower organic free calcite, clearly displays a series of bright orange luminescent zones, which indicates that organics are not a prerequisite for luminescence. Arrow marks a common point with plate C. Cathodoluminescent photomicrograph (Sample 727). Scale bar = 250 µm.

(E) Inclusion rich calcite which possesses a great deal of opaque organic material. A thick layer of internal sediment has truncated the crystal growth at some point in time. Photomicrograph, plane polarized light (Sample 726b). Scale bar = 150 µm.

(F) Same view as plate E. Note how the luminescence appears to be controlled by the pattern of inclusions, producing markedly elongate zones of luminescence. Arrow is a common point with plate E. Cathodoluminescent photomicrograph (Sample EEQ 726b). Scale bar = 150 µm.

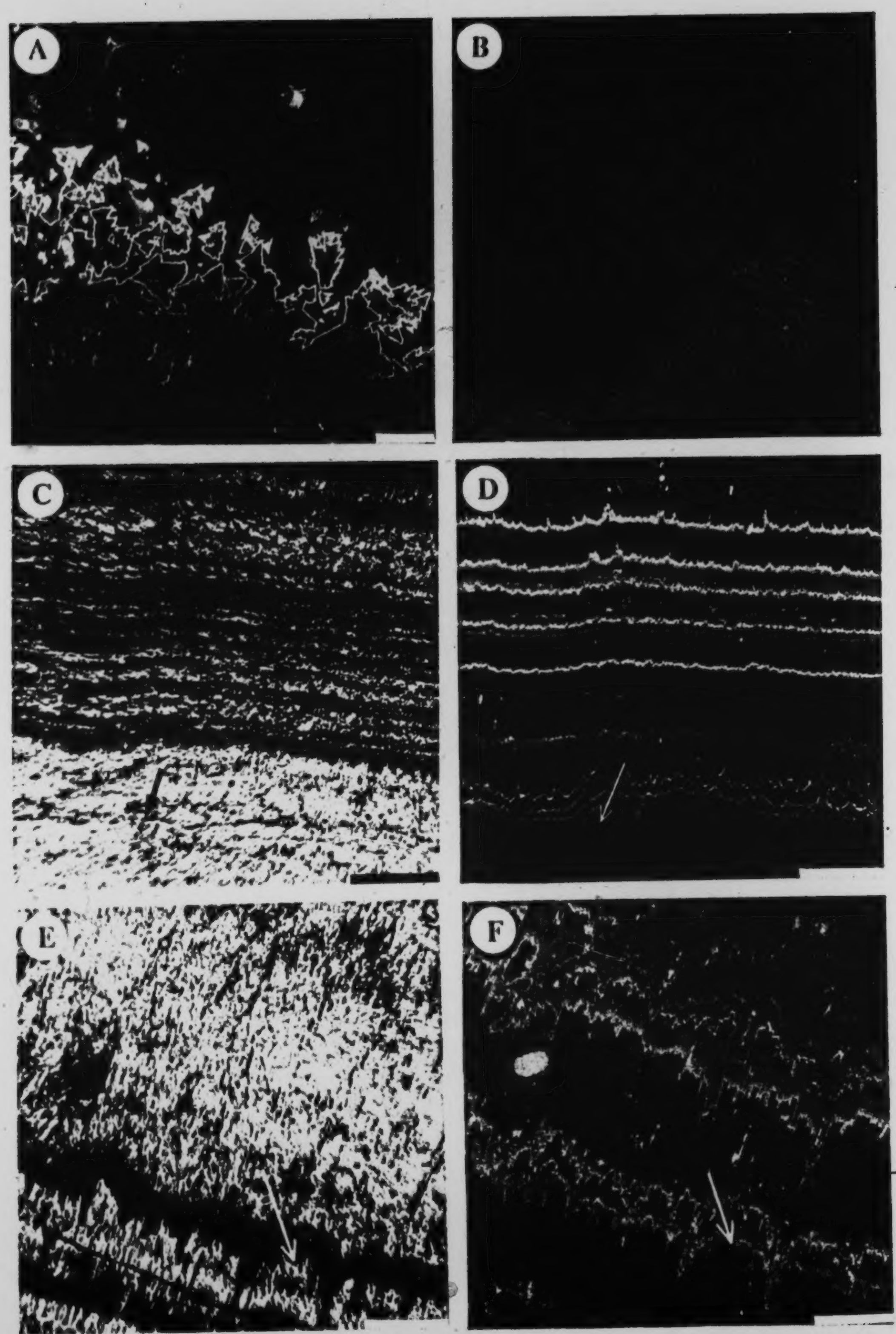
A
B
C
D
E
F

PLATE 20

(A) Prominent zone of perched organic material (O) on well defined crystal terminations. The calcite in the upper right of the photomicrograph, is a radial arrangement of columnar crystals. The central area marks a prominent morphology change (Mc) to an end on view of a stalactite soda straw. A prominent inclusion zone (Ir) has formed in the lower left of the photomicrograph. Photomicrograph, plane polarized light (Sample PCQ 1241). Scale bar = 500 µm.

(B) Same view as plate A. Note the zone of hairline luminescence (HL) which is found in the zone of radial columnar calcite, no organics define this zone of luminescence. The pore water chemistry obviously differed in the soda straw, giving rise to complex luminescent zoning. Notice how the luminescence, which defines former crystal faces, apparently occurs prior to the organics (O), suggesting the two may not be related. (Lz) is a broad luminescent zone, the presence of which is defined by inclusion rich calcite. Cathodoluminescent photomicrograph (Sample PCQ 1241). Scale bar = 500 µm.

(C) Enlarged view of the luminescent zone shown in plate 20 (A). Notice how the narrow band of inclusion rich calcite (Ir) corresponds to the luminescent zone in plate 20 (B). Cathodoluminescent photomicrograph (Sample PCQ 1241). Scale bar = 300 µm.

(D) Same view as plate 20 (C). The unusual morphology of this luminescent zone, which does not appear to conform to crystal morphology, is the result of the crystals being cut at an oblique angle to the c-axis. Note how a change in the pore fluid chemistry has resulted in a distinct zone of dull orange luminescence across the whole zone. Cathodoluminescent photomicrograph (Sample PCQ 1241). Scale bar = 300 µm.

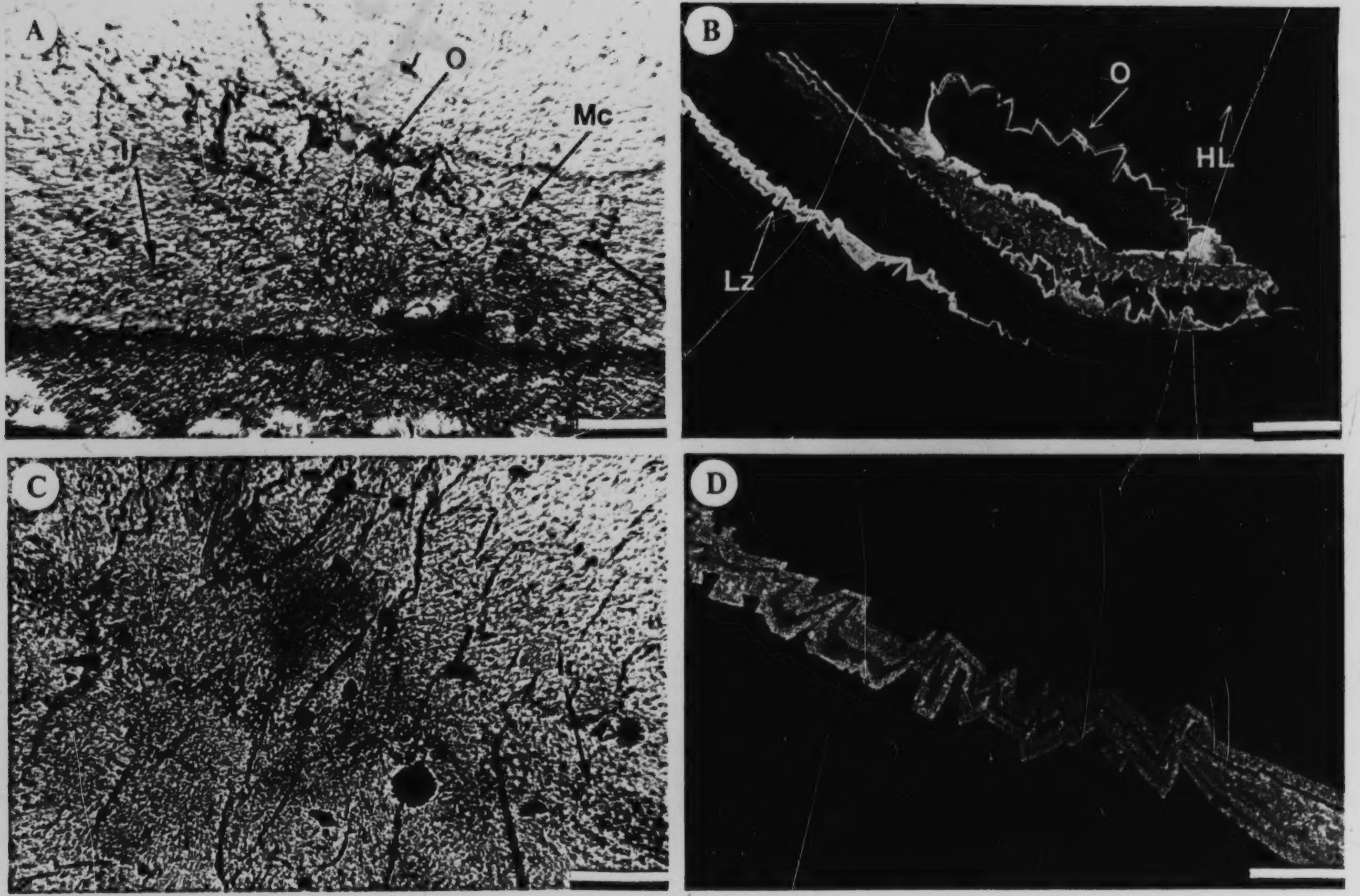
A
O
Mc
B
O
HL
Lz
C
D

XII. REFERENCES

ALLAN, J. R. 1976. Carbon and oxygen isotope criteria for recognizing subaerial diagenesis in limestone: examples from the Pleistocene (Barbados, West Indies) and ancient (Newman limestone, Mississippian, Kentucky). Geological Society of America, abstracts with programs, annual meeting, Denver. pp. 751-752.

——— and MATHEWS, R. K. 1977. Carbon and oxygen isotopes as diagenetic and stratigraphic tools: surface and subsurface data, Barbados, West Indies. Geology, **5**, pp. 16-20.

——— and MATHEWS, R. K. 1982. Isotopic signatures associated with early meteoric diagenesis. Sedimentology, **29**, pp.797-817.

ASSERETO, R., and FOLK, R. L. 1980. Diagenetic fabrics of aragonite, calcite and dolomite in an ancient peritidal-spelean environment: Triassic Calcare Rosso, Lombardia Italy. Journal of Sedimentary Petrology, **50**, pp. 371-394.

ATKINSON, T. C., and SMITH, D. I. 1976. The erosion of limestone. *In* The science of speleology. *Edited by* T. D. Ford and C. H. D. Cullingford, Academic Press, London, pp. 151-177.

BACK, W., and HANSHAW, B. B. 1970. Comparison of chemical hydrology of Florida and Yucatan. Journal of Hydrology, **10**, pp. 330-368.

———, ———, HERMAN, J. S., and VAN DRIEL, J. N. 1986. Differential dissolution of a Pleistocene reef in the ground water mixing zone of coastal Yucatan. Geology, **14**, pp. 137-140.

BAKER, R. J. 1974. Cayman Islands: soil and land use sur[illegible]s No 26. Department of soil science, University of the West Indies, Trinidad. 35 p.

BALASHOV, Y. A., RONOV, A. B., MIGDISOV, A. A., and TURANSKAYA, N. V. 1964. The effect of climate and facies environment on the fractionation of the Rare Earths during sedimentation. Geochemical International, **2**, pp. 951-969.

BATHURST, R. G. C. 1959. The cavernous structure of some Mississippian *Stromatactis* reefs in Lancashire, England. Journal of Geology, **67**, pp. 506-521.

——— 1975. Carbonate sediments and their diagenesis. Developments in sedimentology, No. 12. Second Edition. Elsevier, Amsterdam, 658 p.

BECK, F. B. 1978. Colour differentiation in "fried egg" stalagmites. Journal of Sedimentary Petrology, **48**, pp. 821-824.

BENDER, M. M. 1968. Mass spectrometric studies of carbon-13 variation in corn and other grasses. Radiocarbon, **10**, pp. 468-472.

BERNER, R. A. 1971. Principles of chemical sedimentology. McGraw-Hill, New York, 240 p.

BERNER, R. A. and MORSE, J. W. 1974. Dissolution kinetics of calcium carbonate in sea water IV. Theory of calcite dissolution. American Journal of Science, **274**, pp. 108-134.

BINKLEY, K. W., WILKINSON, B. H, and OWEN, R. M. 1980. Vadose beachrock cementation along a southeastern Michigan marl lake. Journal of Sedimentary Petrology, **50**, pp. 553-962.

BÖGLI, A. 1964. Mischungskorrosion, ein Beitrag zum Verkarstungsproblem. Erdkunde, **18(2)**, pp. 83-92.

——— 1980. Karst hydrology and physical speleology. Springer-Verlag, New York, 284 p.

BOWIN, C. O. 1968. Geophysical study of the Cayman trough. Journal of Geophysical Research, **73**, pp. 5159-5173.

BRAITHWITE, C. J. R. 1979. Crystal textures of recent fluvial pisolites and laminated crystalline crusts in Dyfed, South Wales. Journal of Sedimentary Petrology, **49**, pp. 181-194.

BRAND, U., and VEIZER, J. 1980. Chemical diagenesis of a multicomponent carbonate system - 1: Trace Elements. Journal of Sedimentary Petrology, **50**, pp. 1219-1236.

BRAND, U., and VEIZER, J. 1981. Chemical diagenesis of a multicomponent carbonate system - 2: Stable Isotopes. Journal of Sedimentary Petrology, **51**, pp. 987-997.

BRAVAIS, A. 1886. Etudes Cristallographiques. Guathier-Villars, Paris. 185 p.

BRETZ, J. H. 1942. Vadose and phreatic features of limestone caverns. Journal of Geology, **50**, pp. 675-811.

BRINKMAN, R., MUNNICH, K. O., and VOGEL, J. C. 1959. C^{14} age determination of groundwater. Naturwissenschaft, **46**, pp. 10-12.

BROUGHTON, P. L. 1972. Monohydrocalcite in speleothems: An alternative interpretation. Contributions to Mineralogy and Petrology, **36**, pp.171-174

——— 1977. Crystallite precursors and the genesis of irregular crystal boundaries in radial fibrous carbonate fabrics. Proceedings of the 7th. International Speleological Congress, Sheffield 1977, pp.84-86.

BRUNT, M. A., GIGLIOLI, M. E. C., MATHER, J. D., PIPER, D. J. W., and RICHARDS, H. D. 1973. The Pleistocene rocks of the Cayman Islands. Geological Magazine, **110**, pp. 209-221.

BURTON, W. K., and CABRERA, N. 1949. Crystal growth and surface structure - Part I. Discussions of the Faraday Society, **5**, pp. 33-39.

BUSENBERG, E., and PLUMMER, L. N. 1982. The kinetics of dissolution of dolomite in sea water. IV - Theory of calcite dissolution. American Journal of Science, **274**, pp. 108-134.

CABRERA, N. 1949. Crystal growth and surface structure - Part II. Discussions of the Faraday Society, **5**, pp. 40-47.

CARPENTER, A. B., and OGLESBY, T. W. 1976. A model for the formation of luminescent calcite cements and its complications. Geological Society of America, abstracts with programs, **8**, pp. 469-470.

CAUMARTIN, V. 1963. Review of the microbiolgy of underground environments. Bulletin of the National Speleological Society, **25**, pp.1-14.

CHAFETZ, H.S. 1981. Photographs of bacterial shrubs in travertine, Idaho and Italy. Journal of Sedimentary Petrology, **51**, p.1162.

——— 1986. Marine peloids: a product of bacterially induced precipitation of calcite. Journal of Sedimentary Petrology, **56**, pp.812-817.

——— and BUTLER, J. 1980. Petrology of recent pisolites, and speleothem deposits from central Texas. Sedimentology, **27**, pp.497-518.

——— and FOLK, R. L. 1982. Travertine: significance of bacterially precipitated calcite, constituent morphology and depositional environments. International Sedimentological Congress. I.A.S Abstracts p.11.

——— and FOLK, R. L. 1984. Travertines: depositional morphology and the bacterially constructed constituents. Journal of Sedimentary Petrology, **54**, pp. 289-316.

——— and MEREDITH, J. C. 1982. Recent travertine pisoliths (pisoids) from southeastern Idaho, USA. *In* Coated Grains. *Edited by* T. M. Peryt. Springer-Verlag, New York. pp. 450-455.

——— WILKINSON, B. H., and LOVE, K. M. 1985. Morphology and composition of non-marine carbonate cements in near surface settings. Journal of Sedimentary Petrology, **55**, pp. 337-343.

CHAMP, D. R., GULENS, J. and JACKSON, R. E. 1979. Oxidation-reduction sequences in ground water flow systems. Canadian Journal Of Earth Sciences, **16**, pp. 12-23.

CLAUS, G. 1955. Algae and their mode of life in the Baradla cave at Aggtelek. Acta Academiae Scientiarum Hungaricae, **2**, pp.1-26.

CLAYTON, R. N., and DEGENS, E. T. 1959. Use of carbon isotope analysis of carbonates for differentiating fresh water and marine sediments. American Association of Petroleum Geologists, **43**, pp. 890-897.

COX, G. 1977. A living fossil in the twilight zone: a cave-wall bacteria of unique ultrastructure. *In* Proceedings of the 7th. International Speleological Congress, Sheffield 1977. *Edited by* T. D. Ford, pp. 155-156.

CRAIG, H. 1954. Carbon-13 in plants and the relationship between carbon-13 and carbon-14 variations in nature. Journal of Geology, **62**, pp. 115-149.

——— 1957. Isotopic standards for carbon and oxygen and correction factors for mass spectrometric analysis of carbon dioxide. Geochimica et Cosmochimica Acta, **12**, pp. 133-149.

DANIELLI, H. M. C., and EDINGTON, M. A. 1983. Bacterial calcification in limestone caves. Geomicrobiology, **3**, pp. 1-16.

DANSGAARD, W. 1964. Stable isotopes in precipitation. Tellus, **16**, pp. 436-468.

DAVIS, W. M. 1930. Origin of limestone caverns. Geological Society of America Bulletin, **41**, pp. 475-628.

DONNAY, J. D., and HARKER, D. 1937. A new law of crystal morphology extending the law of Bravais. American Mineralogist, **22**, pp. 446-467.

DORMEUS, R. H. 1958. Precipitation kinetics of ionic salts from solution. Journal of Physical Chemistry, **62**, pp. 1025-1068.

DOWTY, E. 1976. Crystal structure and crystal growth: I - the influence of internal structure on surface morphology. American Mineralogist, **61**, pp. 448-459.

DRAGANOV, S. J. 1977. Taxonomic structure of cave algal flora. *In* Proceedings of the 7th. International Speleological Congress, Sheffield 1977: *Edited by* T. D. Ford, pp. 129-131.

DREVER, J. I. 1982. The geochemistry of natural waters. Prentice-Hall, New Jersey. 388 p.

DREYBRODT, W. 1979. Deposition from thin films of natural calcareous solutions and the growth of speleothems. Chemical Geology, **29**, pp. 89-105.

——— 1981*a*. Kinetics of the dissolution of calcite and its application to karstification. Chemical Geology, **31**, pp. 245-269.

——— 1981*b*. Mixing corrosion in $CaCO_3$ - H_2O systems and its role in the karstification of limestone areas. Chemical Geology, **32**, pp. 231-236.

EDWARDS, B. D., and PERKINS, R. D. 1974. Distributions of microborings within continental sediments of the southeastern United States. Journal of Sedimentary Petrology, **44**, pp. 1122-1135.

EMERY, K. O. 1981. Low marine terraces of Grand Cayman Island. Estuarine, Coastal and Shelf Science, **12**, pp. 569-578.

ERICKSON, A. J., HELSEY, C. E., and SIMMONS, G. 1972. Heat flow and continuous seismic profiles in the Cayman Trough and Yucatan Basin. Geological Society of America Bulletin, **83**, 1241-1260.

ESTEBAN, M. 1982. Comments on 'petrology of recent caliche, pisolites, spherulites and speleothem deposits from central Texas' by Chafetz, H. S. and Butler, J. C. Sedimentology, **29**, pp. 441-445.

EVAMY, B. D. 1969. The precipitational environment and correlation of some calcite cements deduced from artificial staining. Journal of Sedimentary Petrology, **39**, pp. 787-821.

FAIRCHILD, I. J. 1983. Chemical controls of cathodoluminescence of natural dolomites and calcites: new data and review. Sedimentology, **30**, pp. 579-583.

FANTIDIS, J. and EHHALT, D. H. 1970. Variations of the carbon and oxygen isotope composition in stalagmites and stalactites: Evidence of non-equilibrium isotopic fractionation. Earth and Planetary Science Letters, **10**, pp. 136-144.

FOLK, R. L. 1965. Some aspects of recrystallization in ancient limestones. *In* Dolomitization and limestone diagenesis. *Edited by* L. C. Pray and R. C. Murray, Society of Economic Mineralogists and Paleontologists Special Publication, Number 13, pp. 14-48.

——— 1974. The natural history of crystalline calcium carbonate: effect of magnesium content and salinity. Journal of Sedimentary Petrology, **47**, pp. 40-53.

——— ROBERTS, H. H., and MOORE, C. H. 1973. Black phytokarst from Hell, Cayman Islands, British West Indies. Geological Society of America Bulletin, **84**, pp. 2351-2360.

——— and ASSERETO, R. 1976. Comparative fabrics of length slow and length fast calcite and calcitized aragonite in a Holocene speleothem, New Mexico. Journal of Sedimentary Petrology, **46**, pp. 486-496.

——— and CHAFETZ, H. S. 1980. Quaternary travertine of Tivoli (Roma), Italy: Bacterially constructed carbonate rock. Geological Society of America, abstracts with programs, **12**, p. 428.

——— and CHAFETZ, H. S. 1983. Pisoliths (pisoids) in Quaternary travertines of Tivoli, Italy. *In* Coated Grains. *Edited by* T. M. Peryt. Springer-Verlag, New York, pp. 474-787.

——— CHAFETZ, H. S., and TIEZZI, T. A. 1985. Bizzare forms of depositional and diagenetic calcite in hot-springs travertines, central Italy. *In* Carbonate cements. *Edited by* N. Schneiderman and P. M. Harris. Society of Economic Mineralogists and Paleontologists Special Publication Number 36, pp. 349-369.

FRANK, F. C. 1949. The influence of dislocations on crystal growth. Discussions of the Faraday Society, **5**, pp. 48-54.

FRANK, J. R., CARPENTER, A. B., and OGLESBY, T. W. 1982. Cathodoluminescence and composition of calcite cement in the Taum Sauk limestone (Upper Cambrian), southeast Missouri. Journal of Sedimentary Petrology, **52**, pp. 631-638.

FRANKE, H. W. 1963. Formgesetze der Korrosion. Jahresh Karst-Hölenkund, **23**, pp. 207-224.

——— 1965. The theory behind stalagmite shapes. Studies in Speleology, **1**, pp. 89-96

FREEMAN, T. 1971. Morphology and composition of an Ordovician vadose cement. Nature, Physical Sciences, **233**, pp. 133-134.

FREIDEL, G. 1907. Studies on Bravais' law. Bulletin Society Française Mineralogie et Cristalographie, **30**, pp.326-455.

FRIEDMAN, G. M. 1965. Terminology of crystallization textures and fabrics in sedimentary rocks. Journal of Sedimentary Petrology, **35**, pp. 643-655.

FRIEDMAN, I., and O'NEIL, J. R. 1977. Compilation of stable isotope fractionation factors of geochemical interest. *In* Data of geochemistry: (6th edition). *Edited by* M. Fleischer. U.S Geological Survey Professional Paper 440-kk.

GASCOYNE, M. 1977. Trace element geochemistry of speleothems. *In* Proceedings of the 7th. International Speleological Congress, Shefield, England, 1977, British Cave Research Association, pp. 205-208.

——— BENJAMIN, G. J. and SCHWARCZ, H. P. 1979. Sea-level lowering during the Illinoian glaciation: evidence from a Bahama "Blue Hole". Science, **205**, pp. 806-808.

——— SCHARCZ, H. P., and FORD, D. C. 1978. Uranium series dating and stable isotope studies of speleothems: Part I - Theory and Techniques. Transactions of the British Cave Research Association, **5**, pp. 91-111.

GAVISH, E. and FRIEDMAN, G. M. 1973. Quantitative analysis of calcite and Mg-calcite by X-ray diffraction: effect of grinding on peak height and peak area. Sedimentology, **20**, pp. 437-444.

GINES, J., GINES, A., and POMAR, L. 1981. Morphological and mineralogical features of phreatic speleothems occurring in coastal caves of Majorca (Spain). Proceedings of the 8th. International Speleological Congress, Shefield 1977, pp. 529-532.

GIVEN, R. K., and LOHMANN, K. C. 1985. Derivation of the original isotopic composition of Permian marine cements. Journal of Sedimentary Petrology, **55**, pp. 430-439.

——— and ——— 1986. Isotopic evidence for the early meteoric diagenesis of the reef facies, Permian reef complex of West Texas and New Mexico. Journal of Sedimentary Petrology, **56**, pp. 183-193.

——— and WILKINSON, B. 1985. Kinetic control of morphology composition and mineralogy of abiotic sedimentary carbonates. Journal of Sedimentary Petrology, **55**, pp. 109-119.

——— and WILKINSON, B. 1985. Kinetic control of morphology composition and mineralogy of abiotic sedimentary carbonates: A Reply. Journal of Sedimentary Petrology, **55**, pp. 919-934.

GOLDMAN, J. C., PORCELLA, D. B., MIDDLEBROOKS, E. J., and TOERIEN, T. F. 1972. The effect of carbon on algal growth - its relationship to eutrophication. Water Research, **6**, pp. 637-679.

GOLDSMITH, J. R., and GRAF, D. L. 1960. Subsolidus relations in the system $CaCO_3$-$MgCO_3$-$MnCO_3$. Journal of Geology, **68**, pp. 324-335.

GOLUBIC, S. 1973 . The relationship between blue-green algae and carbonate deposits. *In* The biology of blue-green algae. *Edited by* N. G. Carr and B. A. Whitton. Botanical Monographs, **9**, pp.434-472.

GOLUBIC, S., FRIEDMAN, I., and SCHNEIDER, J. 1981. The lithobiontic ecological niche, with special reference to microorganisms. Journal of Sedimentary Petrology, **51**, pp. 475-478.

GRIGOR'EV, D. P. 1965. The ontogeny of minerals. Jerusalem, Isreal program for scientific translations, 250 p.

GROSS, M. G. 1964. Variation in the O18/O16 and C12/C13 ratios of diagenetically altered limestones in the Bermuda Islands. Journal of Geology, **72**, pp. 170-194.

GROVER, G. Jnr. and READ, J. F. 1983. Palaeoaquifer and deep burial related cements defined by regional cathodoluminescence patterns, middle Ordovician carbonates, Virginia. American Association of Petroleum Geologists, **67**, pp. 1275-1303.

HALLAM, A. 1984. Pre-Quaternary sea-level changes. Annual Review of Earth and Planetary Sciences, **12**, pp. 205-243.

HANSHAW, B. B., and BACK, W. 1980*a*. Chemical reactions in the salt-water mixing zone of carbonate aquifers. Geological Society of America, abstracts with programs, **12**, pp. 441-442.

——— and ——— 1980*b*. Chemical mass-wasting of the northern Yucatan peninsula by groundwater dissolution. Geology, **8**, pp. 222-224.

HEM, J. D. 1972. Chemical factors that influence the availability of iron and manganese in aqueous systems. Geological Society of America Bulletin, **83**, pp. 443-450.

HENDY, C. H. 1971. The isotopic geochemistry of speleothems-I. The calculation of the effects of different modes of formation on the isotopic composition of speleothems and their applicability as palaeoclimatic indicators. Geochimica et Cosmochimica Acta, **35**, pp. 801-824.

HONESS, A. P. 1918. On the etching figures of the dihexagonal alternating type. American Journal of Science, **45**, pp. 201-221.

HSÜ, S. A., GIGLIOLI, M. E. C., REITER, P., and DAVIES, J. 1972. Heat and water balance studies on Grand Cayman. Caribbean Journal of Science, **12**, pp. 9-22.

HOLLAND, H. D., KIRSUPI, T. V., HUEBNER, S. J., and OXBURGH, U. M. 1964. On some aspects of the chemical evolution of cave waters. Journal of Geology, **72**, pp. 36-67.

HOWARD, A. D. 1963. The development of karst features. National Speleological Society Bulletin, **25**, pp. 45-65.

HUDSON, J. D. 1975. Carbon isotopes and limestone cements. Geology, **3**, pp. 19-22.

——— 1977*a*. Stable isotopes and limestone lithification. Journal of the Geological Society of London, **133**, pp. 637-660.

——— 1977*b*. Oxygen isotope studies on Cenozoic temperatures, oceans and ice accumulation. Scottish Journal of Geology, **13**, pp. 313-325.

HYDRICK, J. L. 1917. Report on hookworm survey of the Cayman Islands from April 18th. 1917 to June 20th. 1917. The Rockefeller Foundation, International Health Board. 21 p.

IRION, G. and MÜLLER, G. 1968. Mineralogy, petrology and chemical composition of some calcareous tufa from the Schwäbische Alb, Germany. *In* Recent Developments in Carbonate Sedimentology in central Europe. *Edited by* G. Müller and G. M. Friedman. Springer-Verlag, New York. pp. 157-171.

JAMES, N. P. 1972. Holocene and Pleistocene calcareous crust (caliche) profiles: Criteria for subaerial exposure. Journal of Sedimentary Petrology, **42**, pp. 817-836.

——— and CHOQUETTE, P. W. 1985. Diagenesis 9 -. The meteoric diagenetic environment. Geoscience Canada, **11**, pp. 161-194.

JONES, B., LOCKHART, E. B., and SQUAIR, C. 1984. Phreatic and vadose cements in the Tertiary Bluff Formation of Grand Cayman Island, British West Indies. Bulletin of Canadian Petroleum Geology, **32**, pp. 382-397.

——— and KAHLE, C. K. 1985. Lichen and algae: Agent of biodiagenesis in karst breccia from Grand Cayman Island. Bulletin of Canadian Petroleum Geology, **33**, pp. 446-461.

——— and MOTYKA, A. 1987. Biogenic structures and micrite in stalactites from Grand Cayman Island, British West Indies. Canadian Journal of Earth Sciences (In press).

_______ In press. Micro-organisms and diagenetic processes associated with plant roots that penetrate caliche in the Pleistocene Ironshore Formation on Cayman Brac, British West Indies. Bulletin of Canadian Petroleum Geology.

KATZ, L. 1973. The interaction of magnesium with calcium during calcite crystal growth at 25° - 90° and one atmosphere. Geochimica et Cosmochimica Acta, **37**, pp. 1536-1586.

KENDALL, A. C. 1977. Fasicular-optic calcite: A replacement of banded acicular carbonate cements. Journal of Sedimentary Petrology, **47**, pp.1056-1062.

——— 1985. Radiaxial calcite: a reappraisal. *In* Carbonate cements. *Edited by* N. Schneiderman and P. M. Harris. Society of Economic Mineralogists and Paleontologists Special Publication Number 36, pp.59-77.

——— and BROUGHTON, P. L. 1977. Discussion: Calcite and aragonite fabrics, Carlsbad caverns: By R. L. Folk and R. Assereto. Journal of Sedimentary Petrology, **47**, pp.1397-1400.

——— and BROUGHTON, P. L. 1978. Origin of fabrics in speleothems composed of columnar calcite crystals. Journal of Sedimentary Petrology, **48**, pp. 519-538.

——— and TUCKER, M. E. 1973. Radiaxial fibrous calcite: a replacement of bundled acicular carbonate cements. Sedimentology, **20**, pp.365-389.

KLAPPA, C. F. 1979. Calcified filaments in Quaternary calcretes: Organo-mineral interactions in the subaerial vadose environment. Journal of Sedimentary Petrology, **49**, pp. 517-528.

KRAL, Z. 1971. Studie vzniku a barevnosti krápníkovych útvaru. Ceskoslovensky Kras, **23**, pp.7-15.

KRAUSKOPF, K. B. 1967. Introduction to geochemistry. McGraw-Hill, New York, 721 p.

KRUMBEIN, W. E. 1979. Photolithotropic and chemoorganotropic activity of bacteria and algae as related to beachrock formation and degradation (Gulf of Aqaba, Sinai). Geomicrobiology Journal, **1**, pp.16-33.

LADD, J. W. 1976. Relative motion of South America with respect to North America and Caribbean tectonics. Geological Society of America Bulletin, **87**, pp. 969-976.

LAFLEUR, R. G. 1984. Groundwater as a Geomorphic Agent. Rensselaer Polytechnic Institute, Troy, New York. 390 p.

LAHANN, R. W. 1978. A chemical model for calcite crystal growth and morphology control. Journal of Sedimentary Petrology, **48**, pp. 337-344.

LANGMUIR, D. 1971. The geochemistry of carbonate groundwater in central Pennsylvania. Geochimica et Cosmochimica Acta, **35**, pp. 1023-1046.

LEFEVRE, M. and LAPORTE, G. S. 1969. The 'Maladie Verte' of Lascaux; diagnosis and treatment. Studies in Speleology. William Pengelly Cave Studies Trust Limited, **2**, pp.34-44.

LEVERENZ, W. W. 1948. Excitation and emission phenomena in phosphors. *In* Preparation and characteristics of some solid luminescent materials. *Edited by* G. R. Fonda and F. Seitz. Cornell Symposium of the American Physical Society. Chapman and Hall, London. 459 p.

LIGHTY, R. G. 1985. Preservation of internal reef porosity and diagenetic sealing of submerged early Holocene barrier reef, southeast Florida shelf. *In* Carbonate cements. *Edited by* N. Schneiderman and P. M. Harris. Society of Economic Mineralogists and Paleontologists Special Publication Number 36, pp.123-151.

LOCKHART, E. B. 1986. Nature and genesis of caymanite in the Oligocene-Miocene Bluff Formation of Grand Cayman Island, British West Indies. Unpublished M.Sc. thesis, University of Alberta, Edmonton, Alberta. 111 p.

LONGMAN, M. W. 1980. Carbonate diagenetic textures from a nearsurface diagenetic environment. American Association of Petroleum Geologists, **64**, pp. 461-487.

MACDONALD, K. C., and HOLCOMBE, T. L. 1978. Inversion and magnetic anomalies and sea floor spreading in the Cayman Trough. Earth and Planetary Science Letters, **40**, pp. 407-414.

MACINTYRE, I. G. 1985. Submarine cements - the peloidal question. *In* Carbonate cements. *Edited by* N. Schneiderman and P. M. Harris. Society of Economic Mineralogists and Paleontologists Special Publication Number 36, pp. 109-121.

MACHEL, H-G. 1985. Cathodoluminescence in calcite and dolomite and its chemical interpretation. Geoscience Canada, **12**, pp. 139-147.

MALEEV, M. N. 1972. Diagnostic features of spherulites formed by splitting of a single crystal nucleus. Mineralogische und Petrographische Mitteilungen Tschermaks, **18**, pp. 1-16.

MALFAIT, B. T., and DINKLEMAN, M. J. 1972. Circum-Caribbean tectonic and igneous activity and the evolution of the Caribbean plate. Geological Society of America Bulletin, **83**, pp. 251-272.

MARFUNIN, A. S. 1979. Spectroscopy, luminescence, and radiation centers in minerals. Springer-Verlag, New York. 352 p.

MARSHAL, D. J. 1977. Suggested standards for the reporting of cathodoluminescence results. Journal of Sedimentary Petrology, **48**, pp. 651-653.

MASON-WILLIAMS, M. A. 1967. Further investigations into bacterial and algal populations of caves South Wales. Speleology II, pp. 839-395.

MATHER, J. D. 1972. The geology of Grand Cayman and its control over the development of lenses of potable groundwater. VI Conferencia Geologica Del Caribe - Margarita Venuzuela Memorias 1972, pp. 154-157.

MATLEY, C. A. 1926. The geology of the Cayman Islands (British West Indies) and their relation to the Bartlett trough. Quarterly Journal of the Geological Society of London, **82**, pp. 352-387.

MAZZULLO, S. J. 1980. Calcite pseudospar replacive of marine acicular aragonite and implications for aragonite cement diagenesis. Journal of Sedimentary Petrology, **50**, pp. 409-422.

McCREA, J. M. 1950. On the isotopic chemistry of carbonates and a paleotemperature scale. Journal of Chemical Physics, **18**, pp. 849-857.

McNAIRN, W. H. 1904. The growth of etch figures. Transactions of the Royal Canadian Institute, **11**, pp. 231-266.

MEYERS, W. J. 1974. Carbonate cement stratigraphy of the Lake Valley formation (Mississippian) Sacramento mountains, New Mexico. Journal of Sedimentary Petrology, **44**, pp. 837-861.

——— 1978. Carbonate cements, their regional distribution and interpretation in Mississippian limestones of southwestern New Mexico. Sedimentology, **25**, pp. 371-397.

MEYERS, W. J., and JAMES, A. T. 1978. Stable isotopes of cherts and carbonate cements in the Lake Valley formation (Mississippian), Sacramento mountains, New Mexico. Sedimentology, **25**, 105-124.

MOLDOVANYI, E. P. and LOHMANN, K. C. 1984. Isotopic and petrographic record of phreatic diagenesis: Lower Cretaceous Sligo and Cupido Formations. Journal of Sedimentary Petrology, **54**, pp. 972-985.

MOLNAR, P., and SYKES, L. R. 1969. Tectonics of the Caribbean and middle America regions from focal mechanisms and seismicity. Geological Society of America Bulletin, **80**, pp. 1639-1648.

MOORE, G. W. 1952. Speleothem - A new cave term. The National Speleological Society News, **2**, p. 2.

——— 1954. The origin of helictites. National Speleological Society, Occasional Paper, **1**.

——— and NICHOLAS, B. G. 1964. Speleology: The study of caves. Heath and Co., Boston. 120 p.

MUCCI, A., and MORSE, J. W. 1983. The incorporation of Mg^{2+} and Sr^{2+} into calcite overgrowths: influences of growth rates and solution composition. Geochimica et Cosmochimica Acta, **47**, pp. 217-233.

MYLROIE, J. E. 1984. Hydrologic classification of caves and karst. *In* Groundwater as a geomorphic agent. *Edited by* R. G. Lafluer. The 'Binghampton' Symposia in Geomorphology, International series, No. 13. London, George Allen and Unwin, pp.157-172.

NAGGY, J. P. 1965. Preliminary note on the algae of Crystal Cave, Kentucky. Speleology, **1**, pp.479-490.

NICKEL, E. 1978. The present status of cathodoluminescence as a tool in sedimentology. Minerals Science Engineering, **10**, pp. 73-100.

NG, KWOK-CHOI. 1985. Geological aspects of groundwater exploitation in Grand Cayman. United Nations Inter-regional Seminar On Development and Management of Groundwater Resources, Hamilton, Bermuda (2-6 December, 1985), pp. 6.1-6.29.

O'NEIL, J. R., CLAYTON, R. N., and MAYEDA, T. K. 1969. Oxygen isotope fractionation in divalent metal carbonates. Journal of Chemical Physics, **51**, pp. 5547-5558.

PALMER, R. J. 1984. Geomorphic interpretation of karst features. *In* Groundwater as a geomorphic agent. *Edited by* R. G. Lafluer. The 'Binghampton' Symposia in Geomorphology, International series, No. 13. George Allen and Unwin Ltd., London, pp. 173-209.

——— 1986. Hydrology and Speleogenesis beneath Andros Island. Cave Science, Transactions of the British Cave Research Association, **13**, pp. 7-12.

PAREKH, P. P., MOLLER, P., DULSKI, P., and BAUSCH, W. M. 1977. Distribution of trace elements between carbonate and non-carbonate phases in limestone. Earth and Planetary Science Letters, **34**, pp. 39-50.

PERFIT, M. R., and HEEZEN, B. C. 1078. The geology and evolution of the Cayman Trench. Geological Society of America Bulletin, **89**, pp. 1115-1174.

PICKNETT, R. G. 1977. Rejuvenation of aggressiveness in calcium carbonate solutions by means of magnesium carbonate. Proceedings of the 7th. International Speleological Congress, Shefield 1977, pp. 346-348.

PIERSON, B. J. 1981. The control of cathodoluminescence in dolomite by iron and manganese. Sedimentology, **28**, pp. 601-610.

PINGITORE, N. E. 1978. The behaviour of Zn and Mn during carbonate diagenesis: Theory and applications. Journal of Sedimentary Petrology, **48**, pp. 799-814.

PLEYDELL, S. M. 1987. Aspects of diagenesis and ichnology in the Oligocene-Miocene Bluff Formation of Grand Cayman Island, British West Indies. Unpublished M.Sc. thesis, University of Alberta, Edmonton, Alberta., 205 p.

PLUMMER, L. N. 1975. Mixing of seawater with calcium carbonate groundwater, quantitative studies in the geological sciences. Geological Society of America Memoir, **142**, pp. 219-236.

PLUMMER, L. N., VACHER, H. L., MACKENZIE, P. T., BRICKER, O. P., and LAND, L. S. 1976. Hydrogeochemistry of Bermuda: A case history of ground-water diagenesis of biocalcarenites. Geological Society of America Bulletin, **87**, pp. 1301-1316.

PLUMMER, L. N., PARKHURST, D. L., and WIGLEY, T. M. L. 1979. Critical review of the kinetics of calcite dissolution and precipitation. *In* Chemical modeling in aqueous systems. *Edited by* E. A. Jenne. Washington: American Chemical Society, Symposium series 93, pp. 537-573.

PREZBINDOWSKI, D. 1979. Microsampling techniques for stable isotopic analysis of carbonates. Journal of Sedimentary Petrology, **49**, pp.

PROTOR, G. R. 1984. Flora of the Cayman Islands. Kew Bulletin additional series XI. London, HMSO. 834 p.

RICHTER, D. K., and ZINKERNAGEL, U. 1981. Zur Anwendung der Kathodoluminezenz in der Karbonpetrographie. Geologische Rundschau, **70**, pp. 1276-1302.

RIGBY, K. J., and ROBERTS, H. H. 1976. Geology, reefs, and marine communities of Grand Cayman Island, British West Indies. Brigham Young University, Geological Studies, Special Publication, **4**, pp. 1-95.

RODRIGUEZ-CLEMENTE, R. 1982. The crystal morphology as a geological indicator. Estudios Geologicos, **38**, pp. 155-171.

ROYSE, C. F. jr., WADELL, J. S., and PETERSEN, L. 1971. X-ray determination of calcite-dolomite: An evaluation. Journal of Sedimentary Petrology, **41**, pp. 483-488.

RUNNELS, D. D. 1969. Diagenesis, chemical sediments, and the mixing of natural waters. Journal of Sedimentary Petrology, **39**, pp. 1188- 1201.

SALLER, A. H. 1986. Radiaxial calcite in lower Miocene strata, subsurface Enewetak atoll. Journal of Sedimentary Petrology, **56**, pp.743-762.

SAUER, J. D. 1982. Cayman Islands seashore vegetation: a study in comparative biogeography. University of California Publications in Geography, **25**, p. 161.

SAVAGE ENGLISH, T. M. 1912. Some notes on the natural history of Grand Cayman. Handbook of Jamaica for 1912, pp. 23-29.

SCHERER, M., and SEITZ, H. 1980. Rare earth element distribution in Holocene and Pleistocene corals and their redistribution during diagenesis. Chemical Geology, **98**, pp. 279-289.

SCHNEIDER, J. 1977. Carbonate construction and decomposition of epilithic and endolithic microorganisms in salt- and fresh water. *In* Fossil Algae. *Edited by* E. Flügel. Springer-Verlag, New York. pp.248-260.

SCHREIBER, B. C., SMITH, D., and SCHREIBER, E. 1981. Spring peas from New York state: Nucleation and growth of fresh water hollow ooliths and pisoliths. Journal of Sedimentary Petrology, **51**, pp. 1341-1346.

SCHROEDER, J. H. 1972. Calcified filaments of an endolithic alga in recent Bermuda reefs. Neues Jahrbuch für Geologie und Palaeontologie Monatschefte, **3**, pp.16-33.

SCHULMAN, J. H., EVANS, L. W., GINTHER, R. J., and MURATA, K. J. 1947. The sensitized luminescence of manganese-activated calcite. Journal of Applied Physics, **18**, pp. 732-739.

SERGEEV, V. M., KONONOV, O. V., and BARSANOV, G. P. 1974. The yellow coloration of Icelandic spar. Geologiya, **29**, pp.38-41.

SOMMER, S. E. 1972*a*. Cathodoluminescence of carbonates, 1. Characterization of cathodoluminescence from carbonate solid solutions. Chemical Geology, **9**, pp. 257-273.

——— 1972*b*. Cathodoluminescence of carbonates, 2. Geological applications. Chemical Geology, **9**, pp. 275-284.

STUMM, W. and MORGAN, J, J. 1970. Aquatic chemistry, 2nd. Edition. Wiley-Interscience, New York. 780 p.

SUNAGAWA, I. 1977. Natural crystallization. Journal of Crystal Growth, **42**, pp. 214-223.

——— 1981. Characteristics of crystal growth in nature as seen from the morphology of mineral crystals. Bulletin of Mineralogy, **104**, pp. 81-87.

——— 1982. Morphology of crystals in relation to growth conditions. Estudios Geologicos, **38**, pp. 127-134.

SWINNERTON, A. C. 1932. Origin of limestone caves. Geological Society of America Bulletin, **43**, pp. 663-693.

THOMPSON, P., SCHWARCZ, H. P., and FORD, D. C. 1976. Stable isotope geochemistry, geothermometry, and geochronology of speleothems from west Virginia. Geological Society of America Bulletin, **87**, pp. 1730-1738.

THRAILKILL, J. 1968. Chemical and hydrological factors in the excavation of limestone caves. Geological Society of America Bulletin, **79**, pp. 19-46.

——— 1976. Speleothems. *In* Stromatolites. *Edited by* M. R. Walter. Developments in Sedimentology, Number 20, Elsevier, pp. 73-86.

VAIL, P. R., and HARDENBOL, J. 1979. Sea-level changes during the Tertiary. Oceanus, **22**, p. 71-80.

VAUGHAN, T. W. 1926. Species of *Lepidocyclina* and *Carpentaria* from the Cayman Islands and their geological significance. Quarterly Journal of the Geological Society of London, **82**, pp. 388-400.

VOGEL, J. C., GROOTES, P. M., and MOOK, W. G. 1970. Isotopic fractionation between gaseous and dissolved carbon dioxide. Zeitschrift für Physik, **230**, p. 225.

WALTERS, L. J., JR., CLAYPOOL, G. E., and CHOQUETTE, P. W. 1972. Reaction rates and δO^{18} variation for the carbonate-phosphoric acid preparation method. Geochimica et Cosmochimica Acta, **36**, pp. 129-140.

WELLS, A. F. 1948. Crystal habit and internal structure. Philosophical Magazine, series 7, **30**, pp. 217-236.

WHITE, W. B. 1984. Rate processes: chemical kinetics and karst landform development. *In* Groundwater as a geomorphic agent. *Edited by* R. G. Lafluer. The 'Binghampton' Symposia in Geomorphology, International series, No. 13. George Allen and Unwin, London, pp. 227-248.

WHITE, W. B., and VAN GUNDY, J. J. 1974. Reconnaissance geology of Timpanogos Cave, Wasatch county, Utah. National Speleological Society Bulletin, **36**, pp. 5-17.

WICKMAN, F. 1952. Variation in the relative abundance of carbon isotopes in plants. Geochimica et Cosmochimica Acta, **2**, pp. 243-254.

WIGGINS, W. D. 1986. Geochemical signatures in carbonate matrix and their relation to deposition and diagenesis, Pennsylvanian Marble Falls Limestone, central Texas. Journal of Sedimentary Petrology, **56**, pp. 771-783.

WOODROFFE, C. D. 1983. Development of mangrove forests from a geological perspective. *In* Biology and ecology of mangroves. *Edited by* H. J. Teas. Junk T:VS, pp. 1-17.

———, STODDART, D. R., HARMON, R. S., and SPENCER, T. 1983. Coastal morphology and late Quaternary history, Cayman Islands, West Indies. Quaternary Research, **19**, pp. 64-84.

ZIMMERMAN, U., EHALT, D., and MUNNICH, K. O. 1967. Soil water movement and evapotranspiration. Changes in the isotopic composition of the water. Isotopes in Hydrology, Proceedings of the International Symposium. International Atomic Energy Agency, Vienna, 1966. pp. 567-585.